Reactions of CO_2 with Amines:

The search for a sustainable route for isocyanates synthesis

Sandra Filipa Sousa da Silva

Thesis to obtain the Master of Science Degree in

Chemical Engineering

Supervisor: Prof. Ana Margarida Sousa Dias Martins

Examination Committee

Chairperson: Prof. João Carlos Moura Bordado

Supervisor: Prof. Ana Margarida Sousa Dias Martins

Members of the Committee: João Emídio da Silva da Costa Pessoa

November, 2016

This page was intentionally left blank.

Acknowledgments

First, I would like to acknowledge the contribution of Professor Ana Margarida Martins for her guidance, sharing her experience and knowledge, answering all my questions and doubts and for let me do this work in her research group. I also like to acknowledge to Professor João Moura Bordado for the opportunity to do this thesis.

To all the people who work in the laboratory of Organometallic Chemistry and Homogeneous Catalysis for all the patience and guidance, especially to Filipe Madeira, for always helping me during experiences and results interpretations. Their contribution was essential for me to conclude this task with success.

To all my friends and colleagues of Técnico, especially to Tânia, Elisabete and Maria for all the patience, talks and laughs during these last years together. I wish you a very happy and lucky life with lots of fun, good times and love.

To Susana and Vasco, my first colleagues and friends in Técnico for all their friendship and for always been there when I need. I know that I'm not the most present person nowadays but I've never forgotten you.

To all my great friends outside the college, for their friendship, experience sharing and kind of inspiration. You are the best!

To my family for all the support and for always believing in me.

Last but not the least, the huge acknowledgment goes to my parents, Mário and Rosa, and to my brother, Ricardo, and sister-in-law, Ângela, for all the patience, love, and support when I am in difficulties and for always believing in me and in my capacities. Without you and your support, would not have been possible ending this chapter of my life.

This page was intentionally left blank.

Resumo

Os isocianatos são intermediários químicos importantes na produção de poliuretanos. Contudo, os processos de produção existentes à escala industrial implicam a utilização de grandes quantidades de espécies cloradas e a síntese de produtos secundários nocivos.

A importância crescente dada à redução da emissão de gases de estufa, nomeadamente de dióxido de carbono, tem conduzido à procura de formas de utilização deste mesmo composto como reagente para a produção de compostos químicos de alto valor acrescentado.

Estúdios prévios demonstram que a utilização de dióxido de carbono em reacções com aminas é um método pouco eficaz para a síntese e isolamento de isocianatos, devido à grande reactividade do grupo funcional N=C=O. Tentou demonstrar-se, assim, a eficácia destes mesmos métodos na síntese de isocianatos, através da utilização do zwitterião Mitsunobu ($^{i}PrO_2C-N(P^{+}R_3)-N^{-}-$ $^{i}PrO_2C$), bem como através da utilização de complexos metálicos de magnésio ($C_{24}H_{34}N_2(Si(CH_3)_3)_2Mg(THF)_x$; $C_{16}H_{18}N_2(Si(CH_3)_3)_2Mg(THF)_x$; $Cp^{bz}Mg(THF)NSi(CH_3)_3Ph(CH_3)_2$; $BrMg(THF)_2NSi(CH_3)_3Ph(CH_3)_2$; $^{tBu2}C=N-Mg(THF)_2NSi(CH_3)_3Ph(CH_3)_2$) e vanádio ($C_{24}H_{34}Cl_2N_2V_2$). Os compostos foram caracterizados através de espectroscopia de infra-vermelhos e NMR.

Palavras-chave: isocianato, dióxido de carbono, aminas, magnésio.

This page was intentionally left blank.

Abstract

Isocyanates are important chemical intermediates in polyurethanes production. However, the existent production processes used at industrial scale implies the utilization of huge amounts of chlorinated species and the synthesis of harmful byproducts.

The increasing importance given to the reduction of the emission of greenhouse gases, including carbon dioxide, have led to the search for new methods of utilization of this same class of compounds as reagents to produce chemical compounds with high added value.

Previous studies showed that the carbon dioxide with amines cannot be a relatively efficient method for the synthesis of various products including, isocyanates due to high reactivity of N=C=O group. In this project, it was attempted to demonstrate the effectiveness of these methods in the synthesis of isocyanates, using Mitsunobu zwitterion ($^{i}PrO_2C-N(P^+R_3)-N^-$- $^{i}PrO_2C$), as well as using metal complexes of magnesium ($C_{24}H_{34}N_2(Si(CH_3)_3)_2Mg(THF)_x$; $C_{16}H_{18}N_2(Si(CH_3)_3)_2Mg(THF)_x$; $Cp^{bz}Mg(THF)NSi(CH_3)_3Ph(CH_3)_2$; $BrMg(THF)_2NSi(CH_3)_3Ph(CH_3)_2$; $^{tBu2}C=N-Mg(THF)_2NSi(CH_3)_3Ph(CH_3)_2$) and vanadium ($C_{24}H_{34}Cl_2N_2V_2$).

The compounds were characterized by infrared spectroscopy and NMR.

Keywords: isocyanate, carbon dioxide, amines, magnesium.

This page was intentionally left blank.

Table of Contents

This page was intentionally left blank.

List of Figures

This page was intentionally left blank.

List of Tables

This page was intentionally left blank.

Nomenclature

R-N=C=O – isocyanate functional group

HDI – hexamethylene diisocyanate

HMDI – methylene diclohexyl diisocyanate

IPDI – isophorene diisocyanate

UV – ultra violet

PU – polyurethane

MDI – methylene diphenyl diisocyanate

TDI – toluene diisocyanate

Pd – palladium

Ni – Nickel

^{o}C – Celsius degree

$B_{oc2}O$ – ditert-butyl dicarbonate

DMAP – 4-dimethylpyridine

DDQ – 2,3-dichloro-5,6-dicyanobenzoquinone

Br_2 – dibromide

CO_2 – carbon dioxide

Ppm – parts per million

$POCl_3$ – Phosphoryl chloride

DIAD – diisopropylazodicarboxylate

CO – carbon monoxide

NMR – nuclear magnetic resonance

THF – tetrahydrofuran

TMSCl – trimethylsilyl chloride

r.t. – room temperature

o.n. – overnight

tol-d_8 – deuterated toluene

C_6D_6 – deuterated benzene

$CDCl_3$ – deuterated chloroform

$CDCl_2$ – deuterated dichloromethane

EtMgBr – Ethylmagnesium bromide

Ph(CH$_3$)$_2$NHTMS – 2,6-dimethyl-N-trimethylsilylaniline

NaBr – Sodium bromide

Li(N=C^{t}Bu$_2$) – di-t-butylmethylene-amidolithium

LiBr – Lithium Bromide

NaH – Sodium hydride

This page was intentionally left blank.

1 Introduction

1.1 Isocyanates importance

Isocyanates are organic compounds with an R-N=C=O functional group (Fig.1). They have a low molecular weight and they are chemically very reactive.

$$R\!\!-\!\!N\!\!=\!\!C\!\!=\!\!O$$
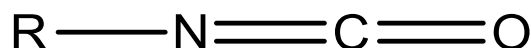
Figure 1. Isocyanate functional group

The first synthesis of this type of compounds occurred in 1848 by Wurtz from the reaction of diethyl sulfate with potassium-cyanide (Fig.2).

$$R_2SO_4 + KNCO \longrightarrow R\text{-}N\text{=}C\text{=}O$$
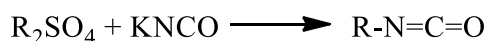
Figure 2. Reaction of Wurtz

The development of this type of compounds begins during the Second World War, in Germany, with the purpose of replacing natural rubber that was becoming scarce. [1-2]

1.2. Market and applications

The market of isocyanates has grown rapidly, both on production rates and applications [2]. Depending if the isocyanate has an aliphatic or an aromatic nature the end use sector can be different. Aliphatic isocyanate, as hexamethylene diisocyanate (HDI), methylene dicyclohexyl diisocyanate (HMDI) and isophorene diisocyanate (IPDI), can produce UV stable, colorless and transparent polyurethane (PU) systems that may be exposed to the environment and/or have very demanding performance requirements [3-5]. Some properties that can define the performance of these type of compounds are related to the equivalent weight of NCO group (grams of a given product which contains one equivalent of isocyanate groups – 42.02 g/mol), the percentage of NCO group (4202/NCO equivalent weight) and the functionality of the isocyanate (number of NCO groups per molecule). The greater the functionality, the greater the crosslinking and thus harder and more resistant chemical and thermally are the systems [6].

Aromatic isocyanates, as methylene diphenyl diisocyanate (MDI) and toluene diisocyanate (TDI), presented in Fig.2, are used when the UV oxidative discoloration is not a problem. The major application of these compounds consists of indoor applications like floor coatings. [3-5]

The most used aromatic isocyanates are TDI and MDI (Fig.3). The first is used essentially to produce soft synthetic rubbers while the major applications of MDI are foams, hard synthetic rubbers, and coatings [3-7].

2,6 - TDI   **4,4 - MDI**
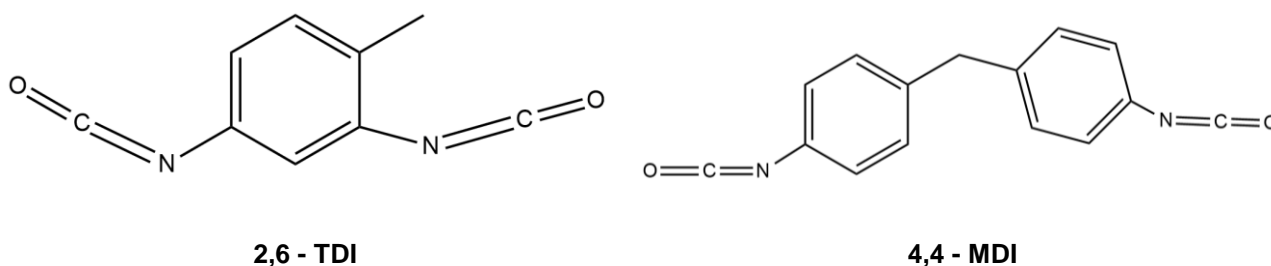
Figure 3. Chemical structures of 2,6 - TDI and 4,4 - MDI [7]

The worldwide production of isocyanates is around 3 million tons [8]. The market for these products is growing around the world at rapid pace in Asia-Pacific. The main reason for this growth is the industrialization activities in countries as China, Japan, and India. It is possible to expect that the market of isocyanates will experience a high growth due to the rising demand for more and new applications that can become significant in the future [9].

1.3 Synthesis processes

1.3.1 Phosgene Route

There are several ways to produce isocyanates. The most common way used to produce isocyanates is known as "the phosgene route". This technique consists in doing a reaction between an amine and phosgene (fig.4) [10-12].
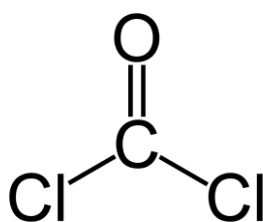
Figure 4. Phosgene chemical structure [12]

Phosgene is a colorless and a highly toxic gas that is used as an intermediate in many organic syntheses. At room temperature, it is a poisoning gas that can be converted into a liquid with cooling and pressure. It was used during World War I as a chocking agent being responsible for a high number of deaths that occurred at that time [10-12].

The first usage of phosgene with arylamines to produce isocyanates was reported in 1884 by Hentschel. Later, Gatterman extended this reaction to aliphatic amines hydrochlorides [1]. The "phosgene route"

involves simple organic reactions. In the first place, a nitro substrate is reduced to the corresponding amine in the presence of a Pd or Ni catalyst with a yield of 98 to 99% [13] (Fig.5).

$$R\!-\!NO_2 \;+\; H_2 \;\xrightarrow{Pd/Ni}\; R\!-\!NH_2$$
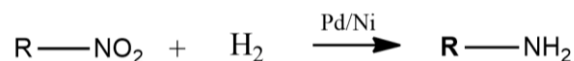
Figure 5. Hydrogenation step [13]

The next step is the treatment of the produced amine with phosgene, in an inert solvent as chloro or dichlorobenzene to control mixing and the reaction temperature [1;13]. If the reaction is carried under pressure, phosgene in a liquid state can be used as diluent because a slurry of carbamoyl chloride and amine hydrochloride is formed at the initial state. To prevent the formation of by-products, it is necessary a good stirring [1]. Then, this slurry can be heated above 50ºC to dissociate the carbamoyl chlorides. The phosgenated reaction of amine hydrochlorides occurs above 100ºC at a good rate. In a way to minimize the possible side reactions, this process is carried with a high dilution (20%) and in the presence of phosgene excess (50 to 200%) [13]. The reactions occurring are shown in the next figure [1]:

$$R\!-\!NH_2 \;+\; COCl_2 \;\longrightarrow\; RNHCOCl + RNH_2.HCl$$

$$RNH_2.HCl + COCl_2 \;\longrightarrow\; RNCO + 3\,HCl$$

$$RNHCOCl \;\longrightarrow\; RNCO + HCl$$

$$\rule{10cm}{0.4pt}$$

$$RNH_2 + COCl_2 \;\longrightarrow\; RNCO + 2\,HCl$$
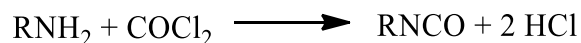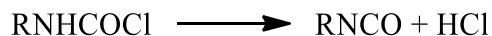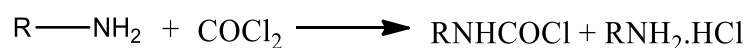
Figure 6. Phosgene route [1]

There are four major drawbacks related to the utilization of phosgene. The first is related to the extreme toxicity and flammability of phosgene and isocyanates that make these compounds difficult to handle in bulk quantities. In second place and by the analysis of the reactions scheme presented in figure 6, it is possible to affirm that for one mole of amine group there are formed two moles of hydrochloric acid. The existence of this acid allows the occurrence of parallel reactions and the degradation of reactors. The third aspect is related to high dilution that is needed to perform reactions of this type. Ideally, concentrations should be high and volumes as low as possible to avoid recycling and concentration costs. For last, it is impossible not to include compounds that not contain chloride groups in the final product which can be detrimental to further processing of isocyanate [13].

To avoid the usage of poisoning phosgene gas, derivatives with similar properties as diphosgene (liquid) and triphosgene (solid), shown in Fig.7, are used for easily handling in the laboratory [14].
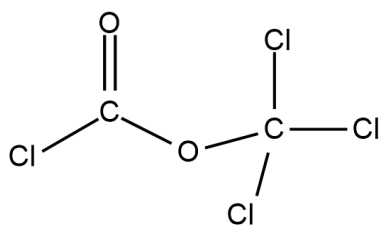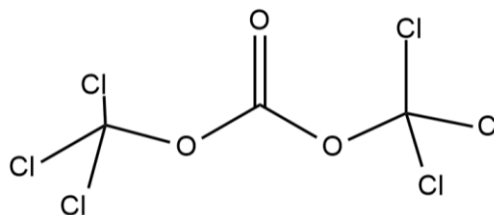
Diphosgene   **Triphosgene**

Figure 7. Diphosgene and triphosgene chemical structures [14]

The utilization of phosgene or its derivatives brings huge environment and health problems. The huge amounts of chloro-based compounds used during the syntheses of isocyanates can cause corrosion of the equipment and the repeated exposure to phosgene can cause chronic bronchitis and emphysema. Furthermore, the availability of petrochemicals and their depletion leads to discovering of new sustainable methods of production of this type of products [15].
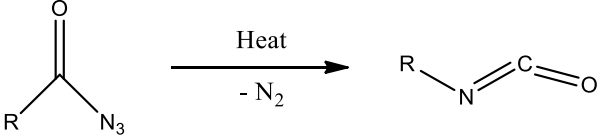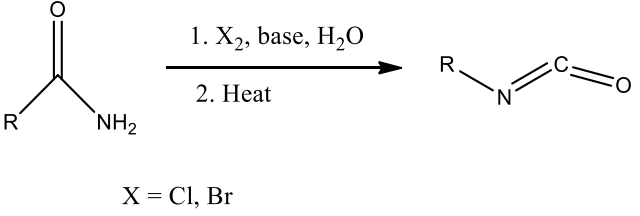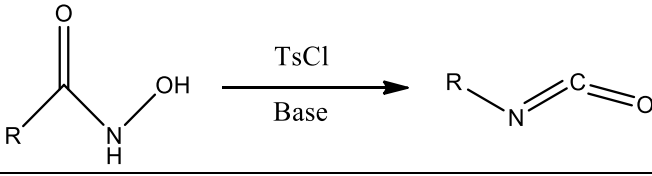
1.3.2 Other synthesis processes

Along the time, other methods were described and used to produce isocyanates. Table 1 summarizes the most important researches and the relative drawbacks.

Due to the limitations and disadvantages of all the processes described before, it is possible to conclude that a sustainable route for isocyanates' production is highly desirable. The growing value of polyurethane into the global market and the importance of isocyanates as PU precursor led to the search for more sustainable and ecological routes for their synthesis to avoid phosgene and hazardous procedures [16].

Table 1. Other synthesis processes of isocyanates

Author	Reaction Scheme	Explanation	Yield	Drawbacks	Reference
Knölker *et al.*	$R-NH_2$ + t-Bu—O–CO–O–CO–O—t-Bu (1.4 eq.) / DMAP (1.0 eq.) → $R-N=C=O$	Use di-*tert*-butyl dicarbonate (Boc$_2$O) with stoichiometric amounts of 4-dimethylaminopyridine (DMAP)	Good yields in laboratory scale	Boc$_2$O is toxic and a derivative of phosgene; Excess of B$_{oc2}$O and stoichiometric quantity of DMAP produce huge quantities of waste	16
Wurtz; Hofmann; Slotta; Lorenz	$R-X$ + $\overset{\oplus}{M}\overset{\ominus}{NCO}$ $\xrightarrow[\overset{\oplus}{M}\ \overset{\ominus}{X}]{S_N2}$ $R-N=C=O$ X = OTs, OMs, OTf, Cl, Br, I	Nucleophilic substitution (S$_N$2 reaction) of alkyl halides, tosylates, mesylates or triflates with metal cyanates	Low yields	Side reactions and polymerizations were described	
Akhlaghinia	$R-Y$ $\xrightarrow[Me_3CN]{Ph_3P/DDQ/Bu_4NOCN}$ $R-N=C=O$ Y = OH, SH, OSiMe$_3$ R = 1°, 2°, 3° alkyl	Use of alcohols, thiols or trimethylsilyl ethers with a mixture of triphenylphosphine, 2,3-dichloro-5,6-dicyanobenzoquinone (DDQ) and tetrabutylammonium cyanate	High yields	Chloro containing materials and reaction time (0 to 42 hours)	16;17

Author	Reaction Scheme	Explanation	Yield	Drawbacks	Reference
Curtis	Heat, - N_2	Rearrangement of acyl azides by thermal decomposition, under non-aqueous conditions and inert solvents	High yields	High toxicity and explosive properties of azides	16
Hofmann	1. X_2, base, H_2O 2. Heat X = Cl, Br	Rearrangement of amidos		Produce isocyanates as an intermediate that, are directly degradated to primary amines or can be trapped with alcohols to the corresponding carbamates. Use stoichometric amounts of toxic and corrosive agents and acetic anhydride or acetyl chloride.Produces high amounts of waste.	
Lossen	TsCl, Base	Rearrangement of hydroxamic acids	Low yields		16;19-20

Author	Reaction Scheme	Explanation	Yield	Drawbacks	Reference
Minisci et al.	R–NH–C(=O)–CO$_2$H + (NH$_4$)$_2$S$_2$O$_8$ $\xrightarrow[\substack{-\,CO_2 \\ -\,2\,HSO_4^-}]{\substack{cat. \\ Ag^I \text{ and } Cu^{II}}}$ R–N=C=O	Reaction of monoamidos with an excess of ammonium persulfate in the presence of catalytic amounts of silver (I) and copper (II) salts forms carbamoyl radicals. The following decarboxylation of such radicals leads to isocyanates formation.	Good yields	Limited small scale procedure and the synthesis of oxalic acids monoamido is extensive and the use of excess of ammonium persulfate makes this process unsustainable.	16
Lesiak and Seyda	R–NH–C(=O)–H $\xrightarrow[\text{Heat}]{\substack{Br_2/DABCO \\ benzene}}$ R–N=C=O	Heating formamidos with an excess of bromine in benzene in the presence of 1,4-diazabyciclo[2,2,2]-octane (BABCO).	Good yields	Harsh conditions are limited to non-sensitive formamidos and used halogens are not suitable for a sustainable procedure.	

Author	Reaction Scheme	Explanation	Yield	Drawbacks	Reference
Greger *et al.*; **Chong** *et al.*; **Gastaldi** *et al.*	R^1–NH–C(=O)–OR^2 $\xrightarrow[\text{NEt}_3 \text{ / Heat}]{\text{SiR}^3_n\text{Cl}_{4-n} \text{ or } \text{SiH}_2\text{I}_2}$ R^1–N=C=O	Silane-induced cleavage of carbamates	Good yields under mild conditions	Limited to laboratory scale; High price of silanes and toxicity of boron halogenides; many side reactions; limited to N-aryl carbamates	16
Valli *et al*; **Buttler** *et al.*	R^1–NH–C(=O)–OR^2 $\xrightarrow[\text{NEt}_3 \text{ / Heat}]{\text{BCl}_3}$ R^1–N=C=O	Boron trichloride-induced cleavage of carbamates			

1.3.3 Carbon dioxide utilization

To achieve a new safer and cleaner process, phosgene has been replaced by new eco-friendly technologies using carbon dioxide and amines as starting materials [21].

There are four methods to transform CO_2 into useful chemicals [22]:

i.   Using high energy starting materials such as hydrogen, unsaturated compounds, small membered ring compounds and organometallics;
ii. To choose oxidized low energy synthetic targets such as organic carbonates;
iii. To shift the equilibrium to the product side by removing a particular compound;
iv. To supply physical energy such as light or electricity.

Carbon dioxide is an easily renewable carbon source with the advantages of being non-toxic, economical and abundant, although it is only used as starting material in few industrial processes (Fig.8) [23].
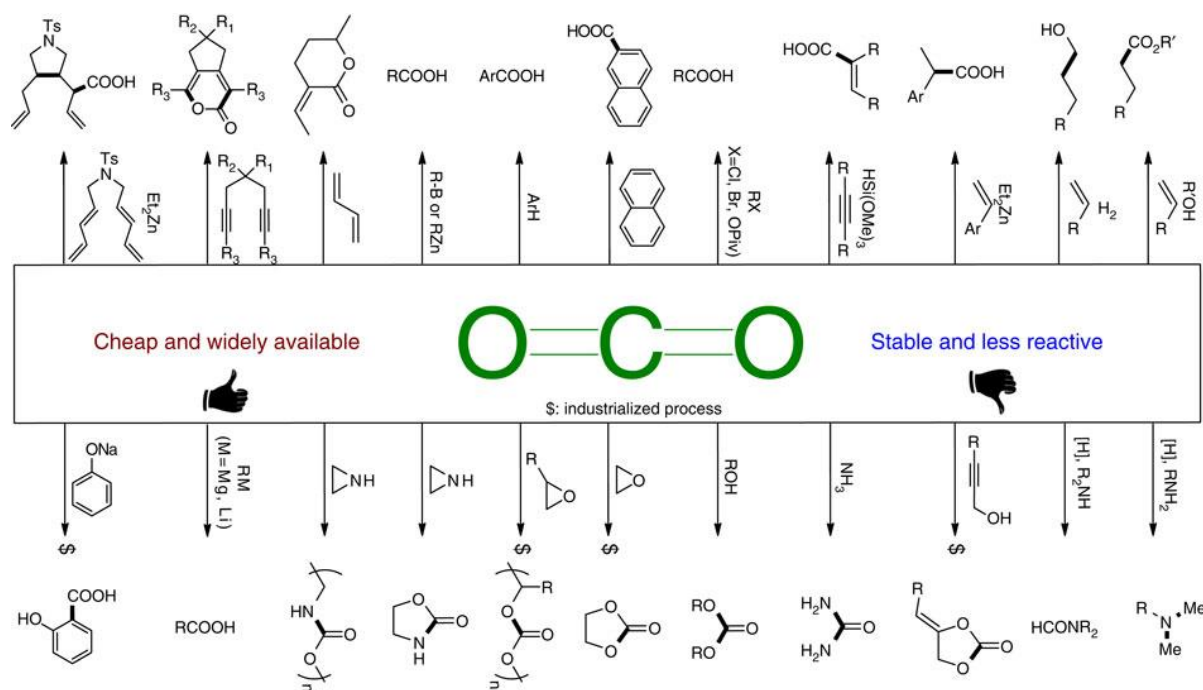
Figure 8. CO_2 as carbon resource [24]

Carbon dioxide concentration in the atmosphere is increasing over the time. The actual concentration of CO_2 is around of 386 ppm, which is much higher from the pre-industrial levels of 280 ppm [25]. In the next figure, it is possible to see the increasing of global emission from 1995 to 2012 (Fig. 9) [26].

Global CO$_2$ emissions from 1995 to 2012
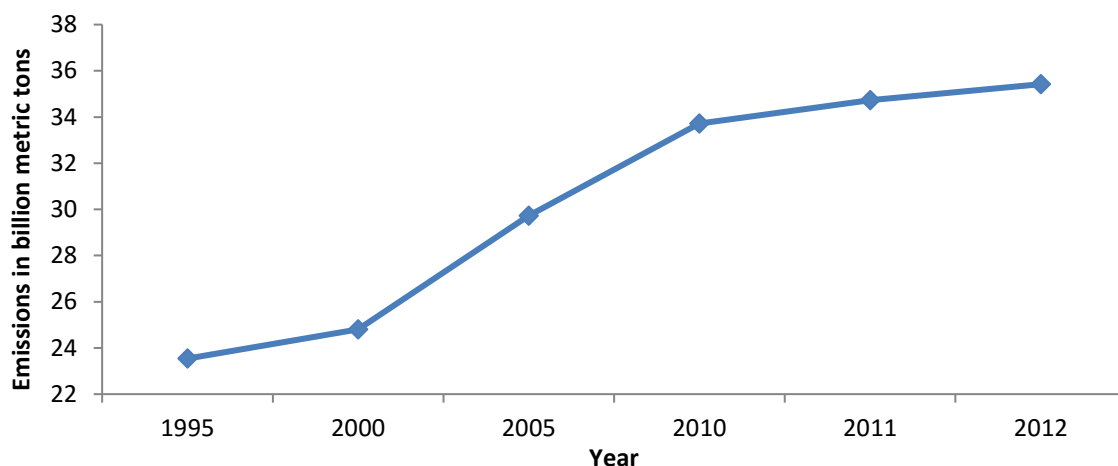
Figure 9. Global CO$_2$ emission from 1995 to 2012 [26]

The replacement of phosgene by CO$_2$ strives many obstacles related to the catalytic activation of CO$_2$ due to its thermodynamic stability and inert kinetics, and so it's potential is not totally explored. The electronic deficiency of carbonyl carbons leads to a strong affinity for nucleophiles and electron-donating reagents [22]. Grignard compounds react with CO$_2$ even at low temperatures. The reaction of CO$_2$ with water, alkoxides and amines produce compounds with carboxyl and carboxylate groups. Furthermore, the reactions of carbon dioxide with low valent metal complexes as, for example, nickel (0) and palladium (0) and unsaturated compounds can form metallalactones (Fig. 10). [22]
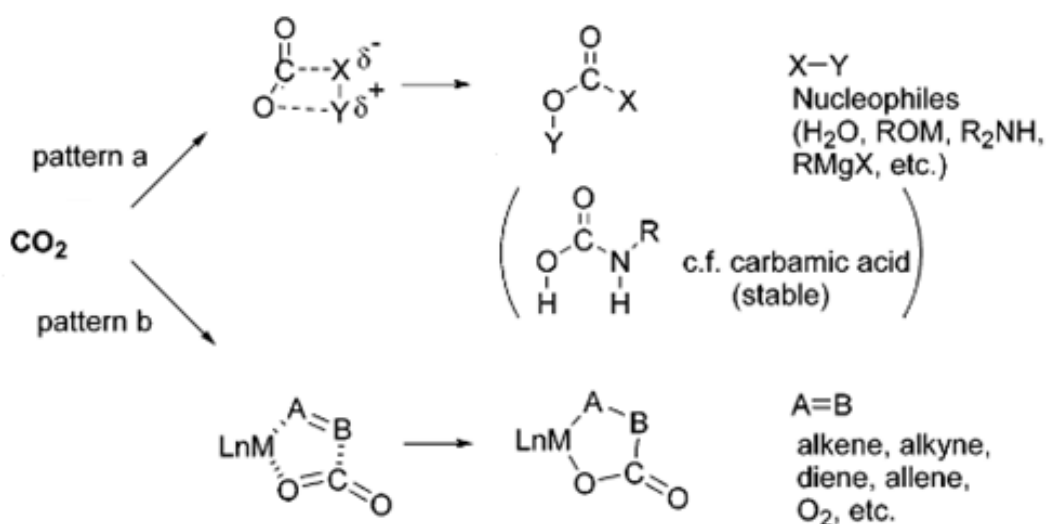
Figure 10. Typical transformations of carbon dioxide [22]

The main difficulty for using carbon dioxide is how is possible to achieve a new clean and selective route to produce high value-added products. [22]

1.3.4. New Processes development

There is a considerable amount of research aiming at the development of new commercial and environmental routes to produce isocyanates. Two of these strategies are a target of attention: one involves the carbonylation of nitroarenes in the presence of an alcohol [27]; the second involves the carbonylation of amines in the presence of an alcohol and an oxidizing agent [28]. In both processes, carbamate esters are formed. The pyrolyses of carbamate esters at temperatures greater than 300°C in the presence of additives give in general low yields of isocyanates. Nevertheless, the elimination of methanol from the carbamate methyl esters with a mixture of chlorocatecholborane and trimethylamine to give isocyanates can achieve high yields. The second approach corresponds to a reaction of an amine with carbon dioxide and dehydration of the resulting carbamate salt [29].

The reaction of amines with CO_2 is described by the following equilibrium (Fig.11):

$$2\ RNH_2 + CO_2 \rightleftharpoons \left[RNHCO_2^{\oplus}RNH_3^{\ominus} \right] \rightleftharpoons RNHCO_2 + RNH_2$$

Figure 11. Amines and CO_2 equilibrium reaction [29]

A procedure that has been investigated for alkyl and hindered aryl isocyanate synthesis is Mitsunobu technology [21]. This system involves the reaction of primary aliphatic or hindered aromatic amines, under mild conditions. In the first step occurs the reaction of the amines in dichloromethane with CO_2 at -5° to -10°C to form the carbamate salts. Then, the solution is treated with $POCl_3$ to form the carbamic acid species [21] (Fig.12).

$$2\ R'NH + CO_2 \xrightarrow{\text{Base}} \left[R'NHCO_2^{\oplus}R'NH_3^{\ominus} \right] \xrightarrow{POCl_3} R'NHCO_2H + R'NH_2$$

Figure 12. Formation of carbamic acids [21]

Lastly, the Mitsunobu zwitterion, which is obtained by diisopropylazodicarboxylate (DIAD) with a solution of tri-*n*-butyl phosphine or triphenylphosphine in dichloromethane, is added to the reaction system, forming the isocyanate in the sequential dehydration process [21] (Fig.13).

$$R'NHCO_2H \quad + \quad {}^iPrO_2C-N-\overset{\ominus}{N}-CO_2{}^iPr \quad \rightleftharpoons \quad R'NCO \quad + \quad {}^iPrO_2C-\overset{H}{N}-\overset{H}{N}-CO_2{}^iPr \quad + \quad R_3PO$$
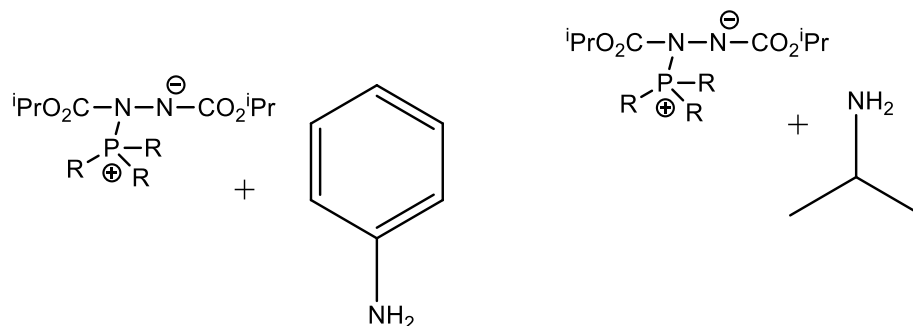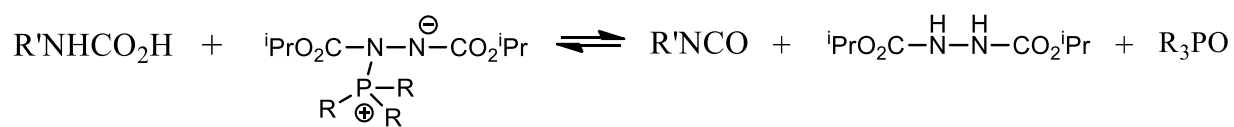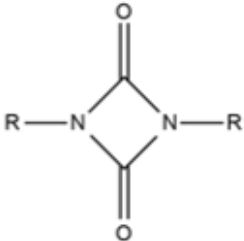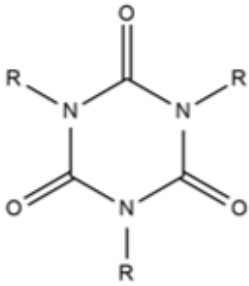
Figure 13. Mitsunobu zwitterion formation [21]

1.3.5. Difficulties in the implementation of new processes: isocyanates organic reactions

The main difficulties in the implementation of new methods are related to the chemistry of isocyanates which are very reactive compounds. Isocyanates can react with any active protic compound [30]. The next table summarizes the side reactions of isocyanates.

Table 2. Side reactions of isocyanates

Reaction	Scheme Reaction	Comments
Urethanes Formation		Isocyanates can react with alcohols or phenols; The rate of reaction decreases according to the following order: Primary alcohols > Secondary alcohols > 2-alkoxyethanols > 1-alkoxy-2-propanols > Tertiary alcohols. However, the reactivity of the products follows the inverse order being the urethanes resulting from tertiary alcohols the most unstable compounds [30].
Allophanates Formation		Isocyanates can also react with urethanes to form allophanates. One atom of H-bonded to a nitrogen of a urethane group can react with an isocyanate group to form an allophanate [31]. This reaction is slower than the reaction with alcohols [30].
Ureas Formation		Another possible organic reaction of isocyanates is the reaction with primary or secondary amines to form ureas [30]. The rate of this reaction is much higher than the rate of the reaction of isocyanates with alcohol groups.
Biurets Formation		The –NCO group can react with the ureas to form biurets [30]. In this reaction, one hydrogen atom of a disubstituted urea can react with an isocyanate group to form a biuret [31].

Reaction	Scheme Reaction	Comments
Carbamic Acids Formation	$R-N=C=O + H_2O \longrightarrow \left[R-\overset{H}{N}-\overset{\overset{O}{\|}}{C}-O-H \right] \longrightarrow R-NH_2$	Reactions of isocyanates with water form unstable carbamic acids that can dissociate in amine and carbon dioxide [30]. As the resulting amine group is much more reactive than water, it can react with another isocyanate group to form ureas [30].
Amidos and CO₂ formation	$R-N=C=O + R'-\overset{\overset{O}{\|}}{C}-O-H \longrightarrow \left[R-\overset{H}{N}-\overset{\overset{O}{\|}}{C}-O-\overset{\overset{O}{\|}}{C}-R' \right]$ $\left[R-\overset{H}{N}-\overset{\overset{O}{\|}}{C}-O-\overset{\overset{O}{\|}}{C}-R' \right] \xrightarrow{-CO_2} R-\overset{H}{N}-\overset{\overset{O}{\|}}{C}-R'$	Reaction of the isocyanate with carboxylic acids to form amidos wih loss of carbon dioxide [30].
Uretdione and Isocyanurate formation	Uretidione Isocyanurate	Isocyanates can dimerize to form uretidones and trimerize to form isocyanurates [30]. The first type is catalyzed by phosphines; the second type can be divided in aliphatic isocyanurates, which are catalyzed by quaternary ammonium compounds, and aromatic isocyanurates, which are catalyzed by tertiary amines [30].

1.3.6. Organometallics catalysis

Due to the thermodynamic stability of CO_2, the process of its fixation and activation to produce high-value products is a field of investigation. The most important research in the activation of carbon dioxide is centered in transition metals systems, however, main group metal complexes have been studied already [32].

It is possible to admit two paths [32]:

   i.   Using a reduced metal (Fig.14);

$$\text{Base} + \text{R}\text{—}\text{NH}_2 + \text{CO}_2 \xrightarrow{\text{M}_{\text{Red}}} \text{R}\text{—}\text{N}\text{=}\text{C}\text{=}\text{O} + 2\,\text{H}^+\text{Base}$$
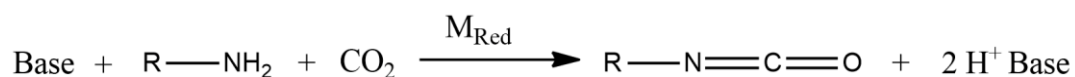
Figure 14. Isocyanate synthesis using a reducing metal [32]

   ii. Heteroatom metathesis (Fig.15).
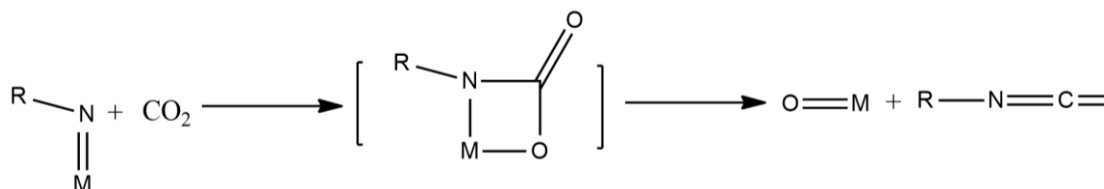
Figure 15. Isocyanate synthesis by heteroatom metathesis [32]

In heteroatom metatheis, it is necessary to choose the right transition metal for the preparation of the coordination compound [32]. Some characteristics are needed:

   i.   Facile formation of imido and oxo bonds with metal center;
   ii. The metal heteroatom double bond must undergo [2+2] cycloaddition with cumulated double bonds;
   iii. Selective cycloaddition with carbon dioxide in the presence of isocyanates.

Other aspects can be:

   iv. Stability of the complex towards air and moisture;
   v.   Compatibility of the metal complex with the reagents.

An example of metal transition complex utilization is described by [33]. It was proven that the use of metal catalysts coupled with reducing agents was an effective way to reduce carbon dioxide and had resulted in activation and incorporation of CO_2 into larger molecules yielding functionalized products. The metals with a low valence of *d*-block are especially interesting for carbon dioxide reduction and activation because they are highly reducing oxophilic metals that can mediate redox processes with one electron or more [33].

 One of the first indications that uranium can be used to activate carbon dioxide is reported in the mid-1980, with the exposure of carbonyl sulfide, SCO. Exposure of trivalent uranium metallocene [η^5-

$(C_5H_4Me)_3U(THF)]$ to an excess of SCO had produced the bridging sulfide species $[\{\eta^5-C_5H_4Me)_3U\}_2(\mu-S)]$ and loss of CO [33]. Other similar reductions of CO_2 were observed with low valent uranium complexes supported by a macrocyclic polyamine chelator [33]. The uranium (III) complex, more specifically, *tert*-butyl-derivatized aryloxide-functionalized triazacyclononane uranium (III) complex $[((^{tBu}ArO)_3tacn)U]$, can reduce carbon dioxide by two electrons to release carbon monoxide and produce a dinuclear U (IV/IV) bridging μ-oxo species $[\{((^{tBu}ArO)_3tacn)U\}_2(\mu-O)]$, as can be seen in figure 16 [33].
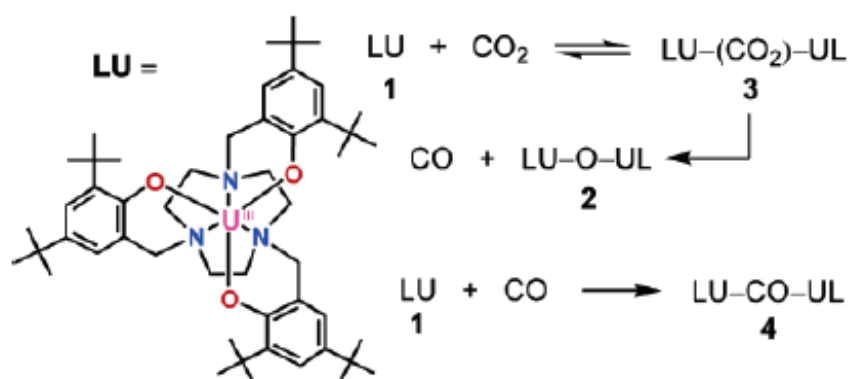
Figure 16. Unsaturated tris-aryloxide uranium (III) complex (LU) reactions with CO_2 to yield $[\{(L)U\}_2(\mu-O)]$ (2) by an intermediate (3) and the reaction of the same complex with CO to give $[\{(L)U\}_2-(\mu-CO)]\cdot3C_6H_6$ (4) [33]

Exchanging the ortho *tert*-butyl substituent on the previous complexes for adamantly groups to achieve $[(((^{Ad}ArO)_3tacn)U]$ the reactivity with CO_2 changes. This reaction of this functionalized complex produces an unknown complex η^1-OCO uranium complex, $[((^{Ad}ArO)_3tacn)U(\eta^1-OCO)]$ where the carbon dioxide ligand is bound to η^1 end-on through one of the oxygen atoms (Fig.17) [33].
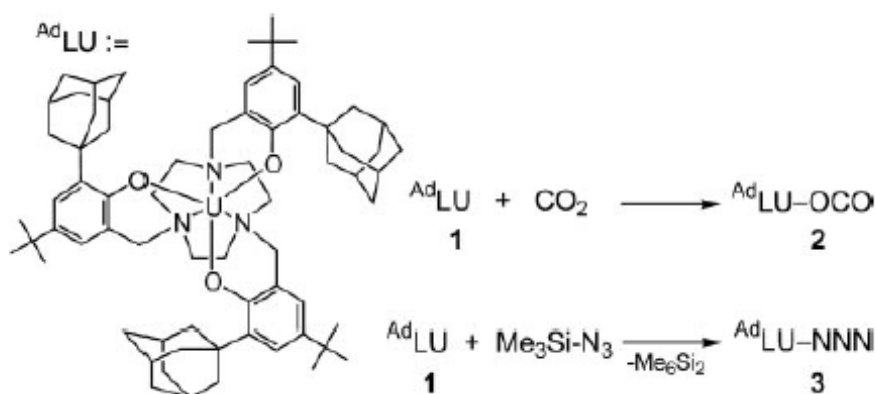
Figure 17. Synthesis of complexes [33]

Evans reported that carbon dioxide addition to $[(C_5Me_5)_2Sm(THF)_2]$ resulted in reductive dimerization of CO_2 to yield the oxalate complex, $[[(C_5Me_5)_2Sm]_2(\mu-\eta^2:\eta^2-O_2CCO_2)]$ [33;34]. The samarium center coordinates and reduces CO_2 to generate a radical species, $[CO_2]^-$, which another equivalent to yield the observed dimer (Fig.18) [34].
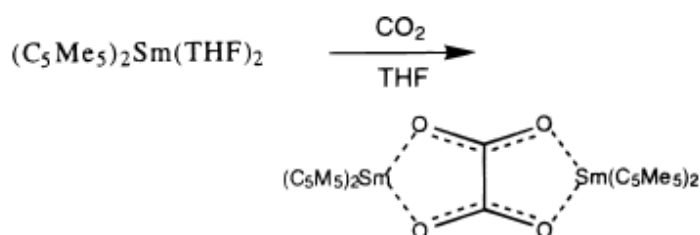
Figure 18. Reaction of [(C₅Me₅)₂Sm(THF)₂] with CO₂ [34]

Later, it was demonstrated that addition of carbon dioxide to a family of trivalent metallocene complexes $[(\eta^5\text{-}C_5Me_4H)_3M]$ (where M can be lanthanum (La), cerium (Ce), praseodymium (Pr), neodymium (Nd) or samarium (Sm)) resulted in CO_2 insertion into one of the M-C bonds of the coordinated Cp derivative to result in $\{[\eta^5\text{-}C_5Me_4H)_2M](\mu\text{-}\eta^1:\eta^1\text{-}O_2CC_5Me_4H)\}_2$, as demonstrated in figure 19 [35].

Ln = La, Ce, Pr, Nd, Sm
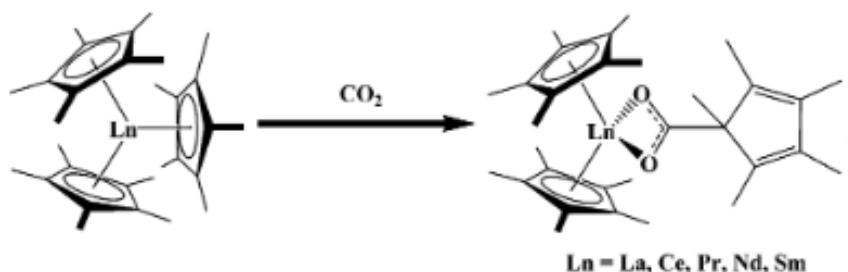
Figure 19. Reaction of trivalent metallocene complexes with CO₂ [35]

The first crystallographically characterized complexes, was the obtained through the insertion of CO_2 into Sm-S and Sm-Se bonds of $[(\eta^5\text{-}C_5Me_5)_2Sm(\mu\text{-}EPh)]_2$ (E = S, Se) featuring an $(O_2CEPh)^{1-}$ ligand, more specifically $[(\eta_5\text{-}C_5Me_5)_2Sm(\mu\text{-}O_2CEPh)]_2$ (Fig.20) [36].

E = S, 1; Se, 2
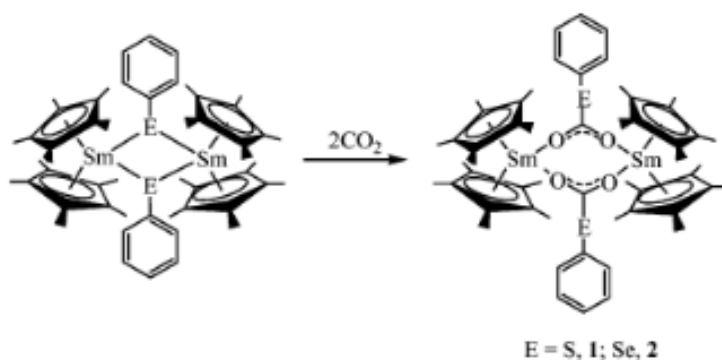
Figure 20. Synthesis of (O₂CEPh)¹⁻ ligands (E = Se, S) by CO₂ insertion into lanthanide chalcogen bonds [36]

Similar results of carbon dioxide insertion into uranium chalcogenide bonds were observed for the reaction of uranium (IV) dithiolate complex $[(\eta^5\text{-}C_5Me_5)_2U(O_2\text{-}CS^iBu)_2]$ [37]. Extrusion of carbon dioxide was achieved by thermolysis of this complex (Fig.21) [37].
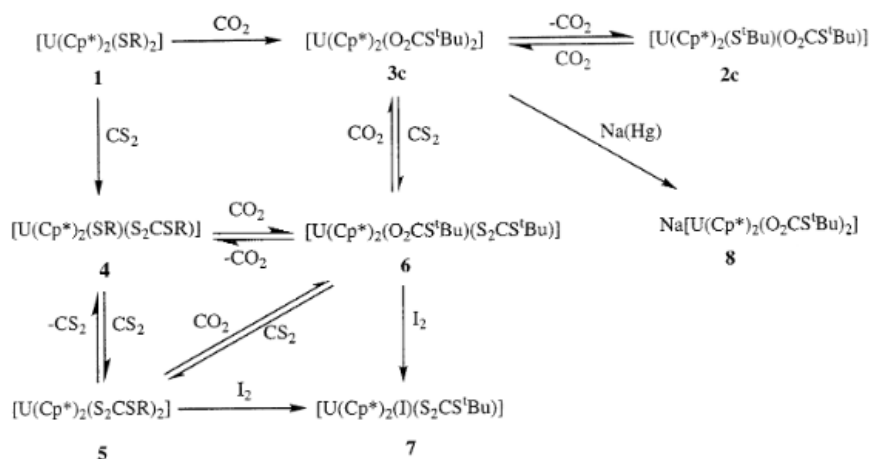
Figure 21. Formation and reactions of the CO₂ and CS₂ insertion compounds [37]

In [33], it was studied the activation and functionalization of CO_2 by aryloxide-substituted triazacyclononane uranium complexes, mid- and high valent uranium amido and imido derivatives U–NHR and U=R (Fig.22).
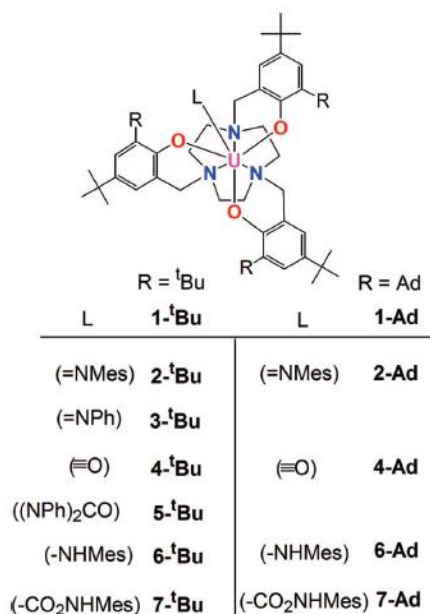
Figure 22. Compounds studied in [33]

To synthesize uranium (V) imido and oxo complexes, mesityl azide was added to red-brown pentane solutions of uranium (III) complexes [33]. The imido fragment of 2-ᵗBu can react with π-acids as carbon monoxide and methyl isocyanide to produce the U (IV) isocyanate and carbodiimide compounds [33]. Conversely, the linear imido ligand (2-Ad) is unreactive toward these π-acids [33]. Toluene solutions of both uranium (V) mesityl imido species were stirred under an atmosphere of CO_2, according to figure 23 [33]. Removal of the solvent under reduced pressure and further analysis by IR spectroscopy, in nujol, of the yielded material revealed the existence of a band at 2286 cm⁻¹ consistent with the formation

of free mesityl isocyanate [33]. This by-product was removed by washing the yielded residue with pentane [33].
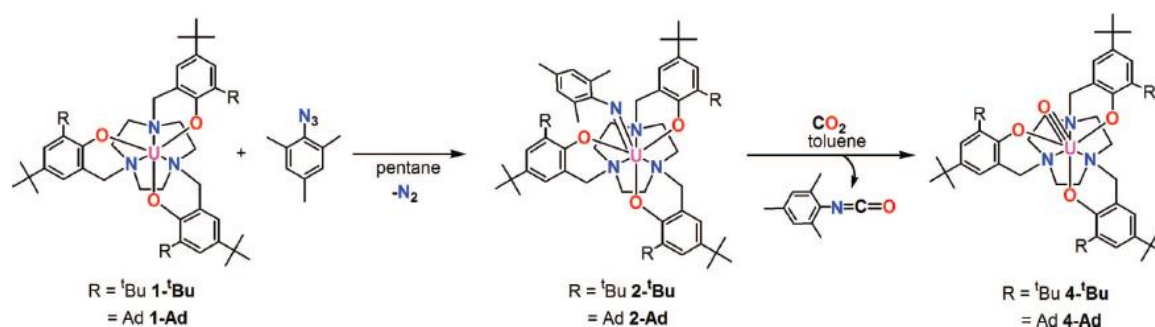
Figure 23. Synthesis of uranium (V) imido complexes and uranium (V) oxo complexes [33]

The driving force for multiple bond metathesis (Fig.24) in order to obtain the stable terminal oxo species from the metal imido compound can be the formation and release of isocyanate [33]. These oxo species indicates that this ligand system can support uranium centers with very reactive terminal functionalities [33].
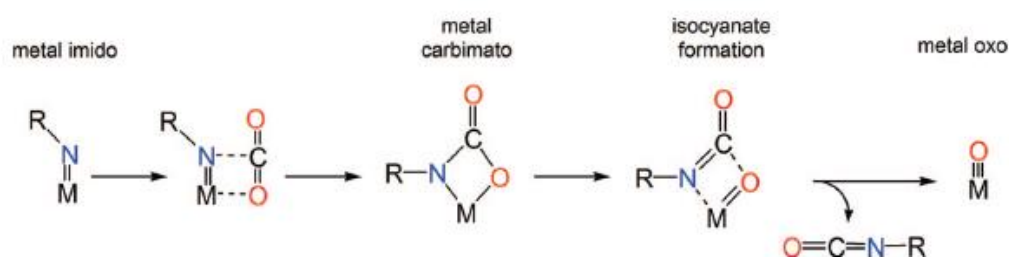
Figure 24. Mechanistic possibility for formation of metal carbimato species via [2+2] cycloaddition [33]

Treating uranium (III) precursor complexes with a standard O-atom transfer, as CO_2, leads to the formation of dinuclear U (IV/V) μ-oxo bridged compounds, as a result of the low quantity of uranium (III) starting material in solution [33].

To observe the intermediate uranium (V) carbimate species, the influence of steric pressure on the multiple bonds was studied [33]. That was predicted that decreasing the steric bulk will decrease the loss of isocyanate [33]. Following this, it was synthesized a uranium complex with the less bulky, unsubstituted phenyl imido ligand, through the addition of phenyl azide to the sterically less encumbered uranium (III) complex, 1-^{t}Bu, yielding the corresponding phenyl imido complex (3-^{t}Bu) [33]. Carbon dioxide was added to a toluene solution of 3-^{t}Bu producing a dark insoluble solid that was isolated by vacuum filtration [33]. Dissolving this solid in THF and the following filtration yielded an orange product on the filter assigned as oxo complex 4-^{t}Bu [33]. The existence of some dark crystals and X-ray analysis revealed the diphenyl urea derivative (5-^{t}Bu) [33] (Fig.25). The formation of this product leads to the conclusion that the previous mechanism of metathesis reaction with carbon dioxide is right [33].
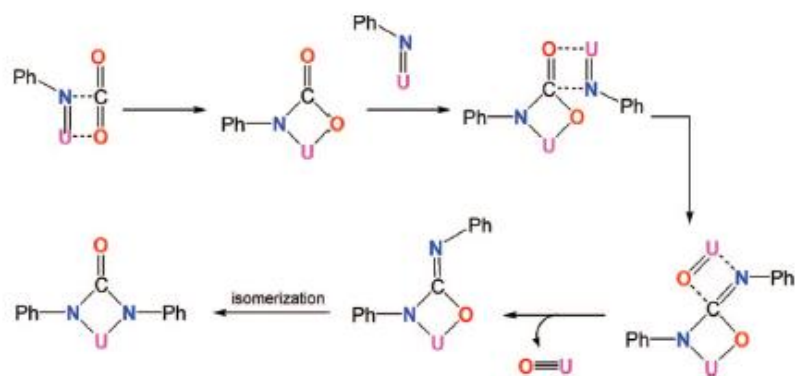
Figure 25. Possible mechanism for formation of diphenyl urea derivative (5-ᵗBu) [33]

The carbimate intermediate is stable to isocyanate loss but is very reactive and can do a second [2+2] cycloaddition with another equivalent of uranium (V) phenyl imido species present in the solution to form the N,O-diphenyl ureate [33]. Isomerization of this coordinate specie leads to the observed N,N-diphenyl ureate derivative 5-ᵗBu [33]. According to [38], the N,N-bound ureate derivative has lower energy. As the N,O-ureate derivative was never observed, this difference in energy accounts for the isomerization to the isolated N,N-bound derivative. The presence of $[(($ᵗBu$ArO)_3tacn)U(k^2$-N,N-(NPh$)_2CO]$, resulted from two consecutives multiple bond metatheses supports the presence of uranium (V) carbimate intermediate [33]. Still, this species could be formed by the reaction of the imido complex with PhNCO produced in the reaction [33].

In [33], studies also have been made to investigate and understand the reactivity of carbon dioxide with U-N bonds, more specifically, between uranium (IV) amido complexes and carbon dioxide. The additional hydrogen atom present in this type of compounds does not allow the isocyanate formation and extrusion and may allow the retention of the seventh ligand [33]. The uranium (IV) mesityl amido species, $[(($ᴿ$ArO)_3tacn)$-U(NHMes)] (R = ᵗBu (6-ᵗBu), Ad (6-Ad)), were synthetizes by heating 2,4,6-trimethylaniline and uranium (III) $[(($ᴿ$ArO)_3tacn)U]$ compounds to 100ºC, according to Fig.40 [33].

Exposition of a toluene solution of 6-ᵗBu (orange) to an atmosphere of carbon dioxide, results in an intermediate color change to light green [33]. Removing the solvent in vacuum, the yielded residue was triturated with pentane and a light pink precipitate (7-ᵗBu) was isolated by vacuum filtration (Fig. 26) [33].
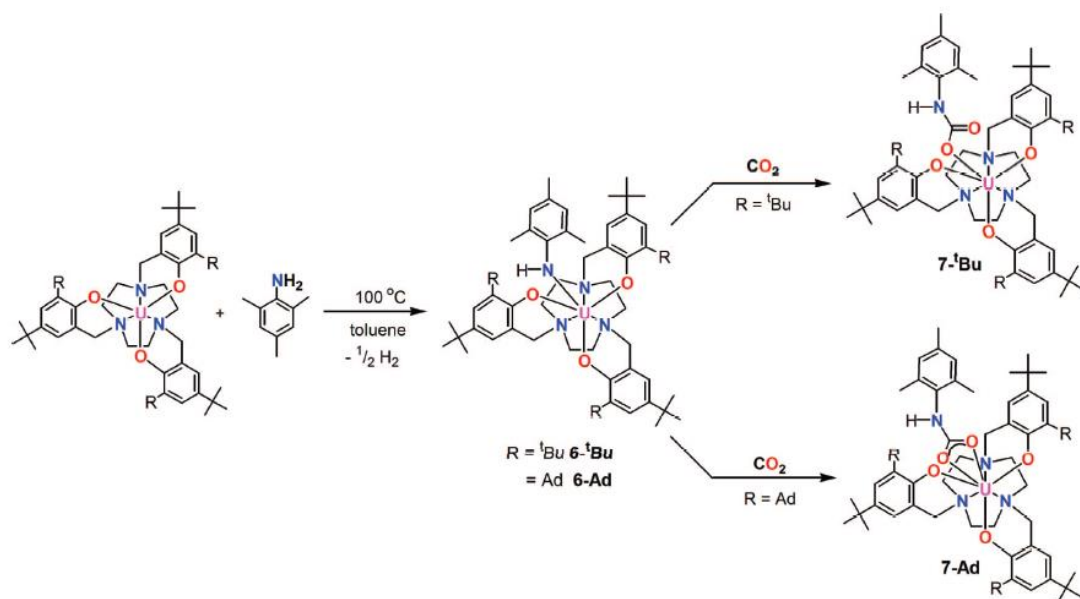
Figure 26. Synthesis of Uranium (IV) amido complexes (6-^{t}Bu, 6-Ad) and Uranium (IV) carbamate species (7-^{t}Bu, 7-Ad) [33]

IR analysis shown an ν(N-H) absorption band centered at 3438 cm^{-1} and an additional strong band at 1651 cm^{-1}, assigned as the C=O stretch of an η^1-O bound, monodentate carbamato ligand, η^1-OC(O)N(H)Mes [33]. Crystals of 7-^{t}Bu were grown from diffusion of pentane into a saturated solution of that compound in diethyl ether. Analysis of these crystals confirmed the carbon dioxide insertion into the U-N (amido) bond, forming uranium (IV) carbamato species, [((^{t}BuArO)$_3$tacn)U(η^1-OC(O)N(H)Mes)] [33]. The uranium is seven-coordinate and only one of the C-O groups of the carbamate ligand is coordinated to the uranium center [33].

Exposure of an orange solution of 6-Ad to carbon dioxide produces a color change to light green. Removal of the solvent in vacuum origins a green residue, assigned to the carbamate complex, [((^{Ad}ArO)$_3$tacnU(OC(O)N(H)Mes)], 7-Ad [33]. IR spectroscopic analysis was made and comparing the obtained results with the previous compound, it is possible to conclude that were not present carbonyl stretches in the expected region. Crystals of 7-Ad were grown from a benzene/acetonitrile solution were analyzed and it confirmed the insertion of carbon dioxide into the U-N bond with a different coordination mode. Both oxygen atoms of the carbimate ligand are coordinated to the uranium center in a bidentate k^2-O$_2$CN(H)Mes compound, resulting in the eight coordinate uranium carbamate species, [((^{Ad}ArO)$_3$tacn)U(k^2-O$_2$CN(H)Mes)] [33].

In conclusion, these studies demonstrated that mid- and high-valent uranium centers can activate an inert molecule as carbon dioxide. Oxidation state of uranium center and molecular disposure have a strong influence on the mechanism of activation as well as the yielded products [33].

Usage of main group metals for reactions with carbon dioxide are described by [39]. The majority of previous studies are related to the use of transition metals. However, some studies on the interaction of carbon dioxide with main group compounds has also been investigated. Main group elements are more available and inexpensive relative to most transition metals.

Sita's group observed that carbon dioxide insertion into divalent systems, $E[N(SiMe_3)_2]_2$, where E can be tin (Sn) or germanium (Ge), gives mixtures of isocyanates and bis(silyl)carbodiimides as ultimate organic compounds (Fig. 27) [40]. This reaction occurs at room temperature, requiring hours of reaction time and high pressures of CO_2.
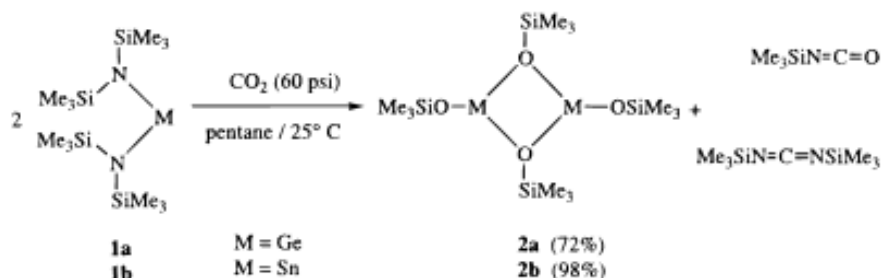
Figure 27. Metathetical exchange between carbon dioxide and the divalent group 14 bisamidos $M[N(SiMe_3)_2]_2$ [40]

Follow up work explored with more details the scope of this reaction. The formation of strong Si-O bonds as the metal siloxide by-product is formed from the starting metal amidos is the appointed driving force of the reaction [39]. Formation of $Me_3SiN=C=O$ and rear reinsertion of $Me_3SiN=C=O$ into the starting metal complex may product $Me_3SiN=C=NSiMe_3$ as a product in addition to the isocyanate, as shown in figure 27 [39-40].

Wannagat used univalent $Na[N(SiMe_3)_2]$ species and reacted them with carbon dioxide. The obtained products were similar to the obtained in Sita's work [39].

Sita described in [40]] that the Sn^{II} reactions with CO_2 are faster than the reactions made with Ge^{II}. Following this idea, it was hypothesized that divalent metals that are more electropositive than Sn^{II} or Ge^{II} can react more readily with carbon dioxide.

Synthesis of bis(silylamidos) of group II metals may follow to types of preparation: alkane elimination or salt metathesis, shown schematically in the next figure [39].
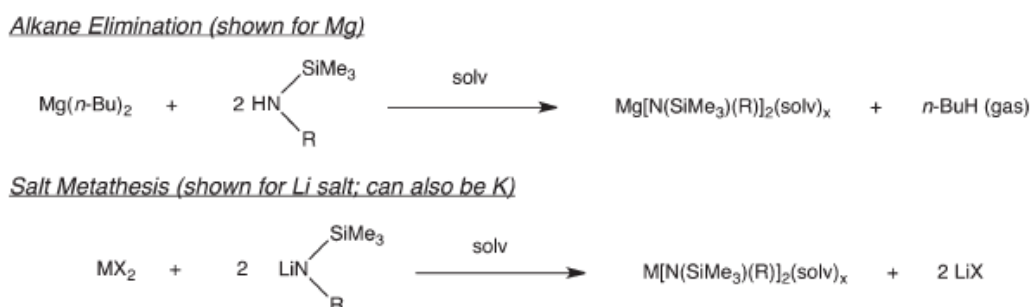
Figure 28. Synthetic routes to prepare group 2 bis(silylamidos) [39]

The initial experiments were conducted under milder conditions than the conditions used in Sita's work [39]. The reactions were performed in a Fischer-Porter reactor capable of adding CO_2 under several atmospheres of elevated pressures or bubbling CO_2 at atmospheric pressure. Carbon dioxide was

bubbled through a hexane or toluene solution of group 2 bis(silylamidos) which react instantaneously (Fig. 29) [39].
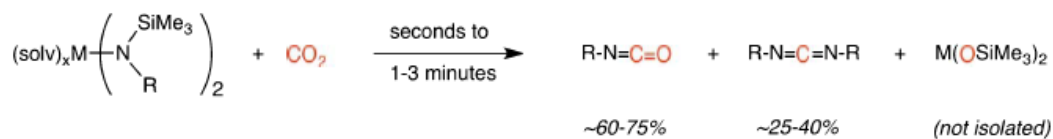
Figure 29. Reaction of group 2 bis(silylamidos) with carbon dioxide [39]

The evidence that reaction occurred is associated with the obtained clouding solution and formation of a precipitate over several minutes. A color change from colorless to light yellow can be observed sometimes upon addition of more gas. The reactions seem to be completed after 1 to 3 minutes, however, stirring was maintained for 10 minutes at room temperature to ensure complete reaction before analysis. Organic products R-N=C=O and R-N=C=N-R were analyzed quantitatively by GC/MS spectroscopy [39].

One point of interest is the ratio of the formed products being 60-75% assigned as the isocyanate and 25-40% being the carbodiimide. In all cases, is the R- group bonded to amido the group that migrates to form the isocyanate or bis(R)carbodiimide and not the –SiMe$_3$ moiety. This conclusion validates the hypothesis that the driving force for this reaction is the migration of the –SiMe$_3$ group to oxygen, yielding a strong Si-O bond. Only, when it is used the –N(SiMe$_3$)$_2$ ligand does either Me$_3$Si-N=C=O or Me$_3$Si-N=C=N-SiMe$_3$ form as products as the –SiMe$_3$ migrates to O. Another conclusion is related to the no change made to the sterics of the ligands, coordination number at the metal nor the change of metals resulted in significant differences in the rate of reaction and ratio distribution of the isocyanate/carbodiimide products [39].

Given the high reactivity of group 2 bis(silylamidos) in solution, it was also studied the direct solid-gas reaction of magnesium bis(silylamidos) with carbon dioxide. It was prepared a cyclic, "tied-back" version in which two methyl groups are linked as the cyclic –[N(SiMe$_2$CH$_2$)$_2$] ligand in order to conclude about the differences in reactivity, represented in the next figure [39].
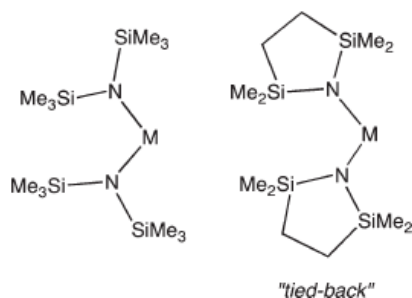
"tied-back"

Figure 30. Comparison of the -N(SiMe$_3$)$_2$ ligand with -[N(SiMe$_2$CH$_2$)$_2$] tied-back version [39]

Crystals of Mg[N(SiMe$_3$)$_2$]$_2$(THF)$_2$ react with carbon dioxide at atmospheric pressure overnight and the progress of this reaction was monitored by NMR. No reaction has occurred. In order to increase the reaction pressure, crystals of this magnesium compound were put into a vial or NMR tube and forward

this vial or NMR tube was put inside of a high-pressure metal reactor. This reactor was attached to a CO_2 cylinder with a headspace pressure of approximately 680 psig (~47 bar). The system was allowed to react for 5-12 hours at room temperature. After that time, the reactor was depressurized and the starting material crystals were converted to a clear and viscous liquid. Comparing the weight of this obtained material with the weight of the starting material it was possible to conclude that were added two moles of CO_2 per Mg. The liquid solidified in a vial over several hours to a transparent, colorless solid comparable with Lexan® polymer. After solidifying, comparing this weight with the weight of the liquid it is possible to conclude that the difference is equal to a loss of two THF molecules. Relatively, to the solubility of this material it was insoluble in any solvent tried and was not water-sensitive. The IR spectroscopy of the solid analysis indicates the presence of a strong band at 2206 cm^{-1}, characteristic of the presence of isocyanate functional group. Analysis of the viscous liquid by GC/MS indicates the presence of Me$_3$Si-N=C=O, Me$_3$Si-N=C=N and (Me$_3$Si)$_2$O as volatile organic compounds. The mechanistic route for the formation of (Me$_3$Si)$_2$O is shown in figure 31 [39]:
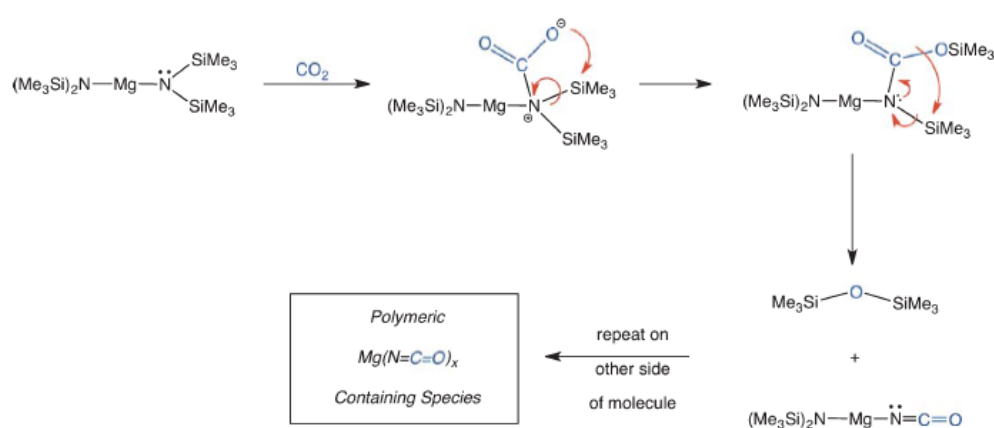
Figure 31. Possible route to generate silyl ether via direct gas-solid reaction [39]

It was hypothesized that (Me$_3$Si)$_2$O is formed by the addition of the amido to the carbon dioxide electrophilic center, forming a carboxylate that can attack –SiMe$_3$ group to achieve a silyl ester intermediate. The rearrange and following formation of a strong Si-O bond by the attack on the other –SiMe$_3$ group can eliminate (Me$_3$Si)$_2$O and form "Mg(N=C=O)$_x$" species, according to [41]. This conclusion led to believe that the yielded clear solid was a form of high polymeric species as "Mg(N=C=O)$_x$". Silyl ether formation can also be explained as result of the reaction of Me$_3$Si-N=C=O and Mg(OSiMe$_3$)$_2$, according to the scheme presented in the next figure [39]:
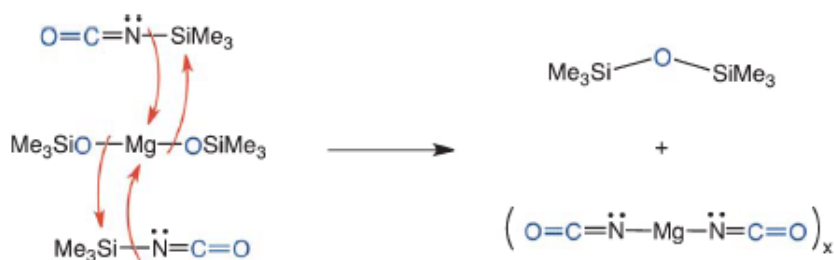
Figure 32. Possible metathesis route to generate silyl ether via direct gas-solid reaction [39]

Another hypothesis is that "Mg(N=C=O)$_x$" species can be an intermediate to produce a poly(magnesiumcarbodiimde), which will better described the obtained solid. The next figure illustrates a schematic route to form a poly(magnesiumcarbodiimde) or magnesium-containing polyurea. The results from IR spectra for ureas are less consistent with the obtained for the yielded solid [39].
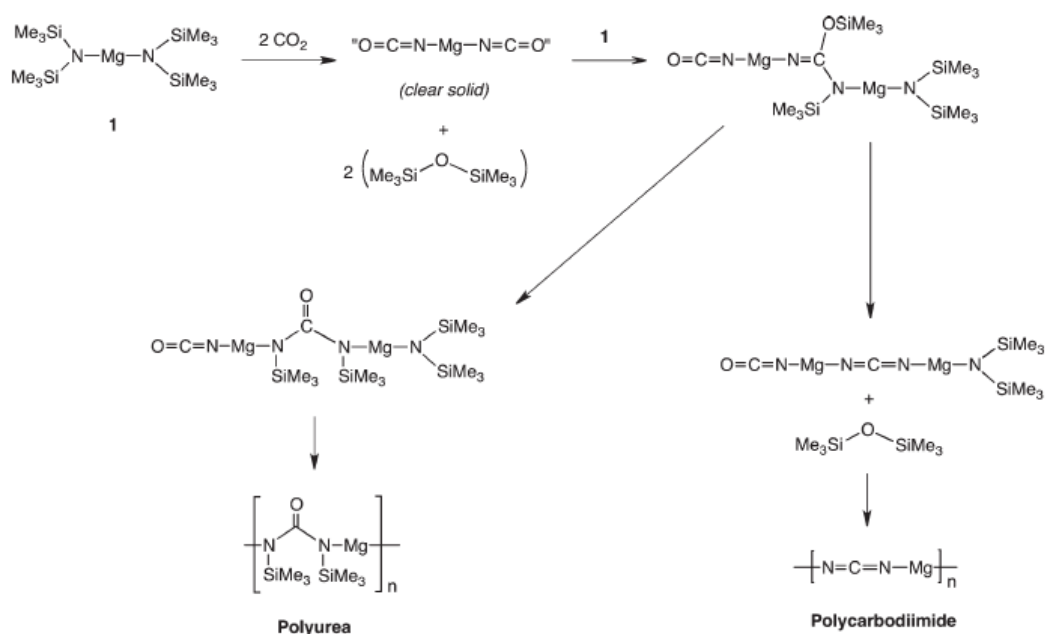
Figure 33. Speculative routes to form poly(magnesiumcarbodiimide) or magnesium-containing polyurea [39]

The reactivity of the "tied-back" ligand was tested with Mg[N(SiMe$_2$CH$_2$)$_2$]$_2$(Et$_2$O)$_2$. This compound was prepared by treating MgBr$_2$ with the lithiated salt of the "tied-back" ligand, in Et$_2$O, for 12 hours at room temperature. The solvent was removed and the product was redissoluted in toluene and filtered in order to remove LiBr. Cooling the toluene solution, it was obtained crystals of Mg[N(SiMe$_2$CH$_2$)$_2$]$_2$(Et$_2$O)$_2$ [39].

Subjecting crystals of Mg[N(SiMe$_2$CH$_2$)$_2$]$_2$(Et$_2$O)$_2$ to identical conditions of Mg[N(SiMe$_3$)$_2$]$_2$(THF)$_2$ no Me$_3$Si-N=C=O and Me$_3$Si-N=C=N-SiMe$_3$ were formed. However, cyclic ether (CH$_2$SiMe$_2$)$_2$O and a white solid were present. This white solid remained solid during the entire reaction time (5-12 hours). The IR analysis indicates that a solid-gas reaction occurred, by the presence of new absorbances in the C-O stretching region (1529 and 1614 cm^{-1}). The metathesis process shown in figure 46 cannot occur using

this cyclic ligand. Contrary to the solid obtained in the previous experiment, the new solid is soluble in pyridine, producing suitable crystals for IR and X-Ray analysis. The results showed the existence of significate absorbances at 2227 and 2199 cm^{-1} and the existence of a –N=C=O fragment. The compound found to be $(pyr)_4Mg(N=C=O)_2$, an unknown compound [39].

The selectivity to produce isocyanates or carbodiimides was also studied using Zn complexes [39]. A series of Zn complexes containing the –N[(SiMe3)(R)]2 were prepared according to [42].

These Zn complexes reacted in a Fisher-Porter bottle system with carbon dioxide at 60 psig (~4 bar) for 30 minutes. In the next figure, are presented the results for each reaction [39].

R Group	% Alkyl/Aryl isocyanate	% Alkyl/Aryl carbodiimide	Comments
$-SiMe_3$	100	0	Quantitative
$-SiPh_2t$-Bu	0	0	No reaction
t-Bu	0	100	Quantitative
c-Hex	0 (trace)	~100	Moderate yield (~50%)
adam	0	100	Quantitative (Exothermic)
Ph-	0	0	No reaction (Heated to 50°C)
$2,6$-$Me_2C_6H_3-$	0	0	No reaction (Heated to 50°C)
$2,4,6$-$Me_3C_6H_2-$	0	0	No reaction (Heated to 50°C)
$(BDI)ZnN(SiMe_3)_2$ *(Coates)* [34]	100	0	

Figure 34. CO_2 reactions with Zn[N(SiMe₃)(R)]₂ [39]

Some conclusions can be taken by the analysis of the previous figure. First of all, Zn complexes with aromatic substituents as the R group do not react with carbon dioxide, even with additional heating. When R is an alkyl group, the opposite selectivity occurs (~100% selectivity). Similarly, to previous studies, a "tied-back" ligand complex, $Zn[N(SiMe_2CH_2)_2]_2$, was used (Fig.35). This complex was allowed to react with CO_2 in a Fischer-Porter reactor system at 60 psig (~4 bar) for 30 minutes in hexane. The reaction was exothermic. The solvent was removed under reduced pressure and the volatile organics were examined – it was only present hexane. The yielded white solid was redissolved in THF and cooled to -20ºC for 24 hours to obtain colorless suitable crystals. Analysis by ^1H and ^{13}C NMR indicates that the cyclic ligand fragment was intact. X-Ray structure analysis leads to revealing that the product is $[Zn_4O][O_2C$-c-$N(SiMe_2CH_2)_2]_6(THF)_2$ [39].
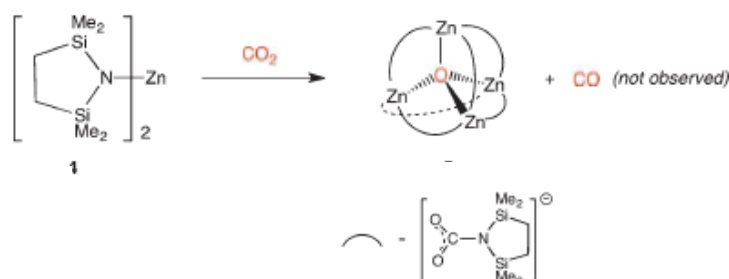
Figure 35. Reaction of Zn "tied-back" complex with CO_2 [39]

The tied-back Zn complex react with carbon dioxide to produce a $[Zn_4O]^{6+}$ core. Carbon dioxide insertion occurs into six Zn-N bonds of the complex forming the carbamate anion $[O_2CN(SiMe_2CH_2)_2]^-$, balancing the positive charge of $[Zn_4O]^{6+}$ core [39].

The most important conclusion of these studies are related to the capability of more electropositive group 2 complexes have to react with carbon dioxide under mild conditions of room temperature and atmospheric pressure and the differences and the differences in products obtained when is used a cyclic ligand $Mg[N(SiMe_2CH_2)_2]_2(Et_2O)_2$ instead $Mg[N(SiMe_3)_2](THF)_2$. Some Zn complexes can be synthetized in order to achieve silyl isocyanate or the bis(alkyl)carbodiimide in near quantitative conversion with ~100% selectivity, instead aromatic substituents which gave no reaction. Lastly, it was shown that the tied-back Zn complex reacts with carbon dioxide at room temperatures and 4 bar, cleaving the gas to achieve a stable containing $[Zn_4O]^{6+}$ core [39].

1.4 Aim of the project

The aim of this project is the search for a sustainable route for the synthesis of aryl isocyanates starting with CO_2 and amines.

Many conventional industrial and laboratory processes are not environmentally friendly or atom efficient. One of the major advantages of using organometallic compounds as catalysts or reagents in organic synthesis is their high reactivity. Some typical reactions that not occur with the usual organic reaction can be easily done using a variety of organometallics. Another advantage is related to the high reaction selectivity obtained by using organometallics catalysts. The stability and the capacity to recover pure metals are other advantages of using organometallics compounds.

Developing new methods based on the mentioned properties of organometallic compounds can lead to a change in organic synthesis: new efficient and environmental safer processes producing fewer by-products can discard other methods used until now [43-44].

2 Results

One of the primary objectives of this work was to study the reactivity of carbon dioxide with several magnesium amido compounds and the yielded products of these reactions. Concurrently with the analysis of these products, a plausible mechanism for the reaction will be suggested. Moreover, isocyanates synthesis with the generated compounds and carbon dioxide will be explored.

2.1. Preliminary Work

2.1.1 Synthesis of Mo (V) complex

A first approach to dry-oxygen-free nitrogen atmosphere reactions in shlenck and glovebox techniques, was performed with a synthesis of a molybdenum (V) complex by the reaction of the $(Me_2NCH_2N(CH_2$-2-HO-3,5-$^tBu_2C_6H_2)_2$ ligand and a solution of $Mo(O)Cl_3(THF)_2$.

The ligand $(Me_2NCH_2N(CH_2$-2-HO-3,5-$^tBu_2C_6H_2)_2$ or briefly $H_2N_2O_2^{t-bu}$ used in the synthesis of molybdenum complex was previously prepared according to [45]. Its preparation consists in refluxing of a solution of 3,4-dimethylphenol, N,N-dimethylethylenodiamine and formaldehyde in methanol for two days according to following scheme (Fig. 36):
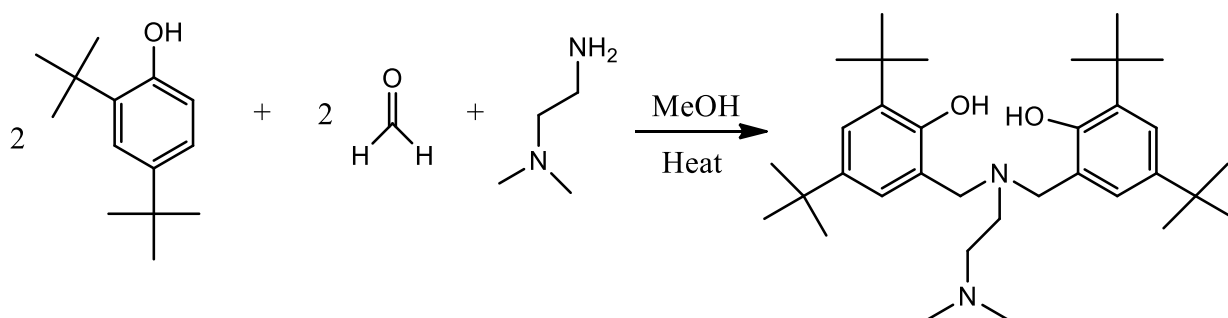
Figure 36. Diamine (bis)phenolate ligand synthesis scheme

The ligand is obtained through Mannich reaction between the amine and the formaldehyde forming the iminium cation that easily follows nucleophilic attack from the aromatic phenol, obtaining the final product. This compound was characterized by NMR spectrum depicted in figure 37:
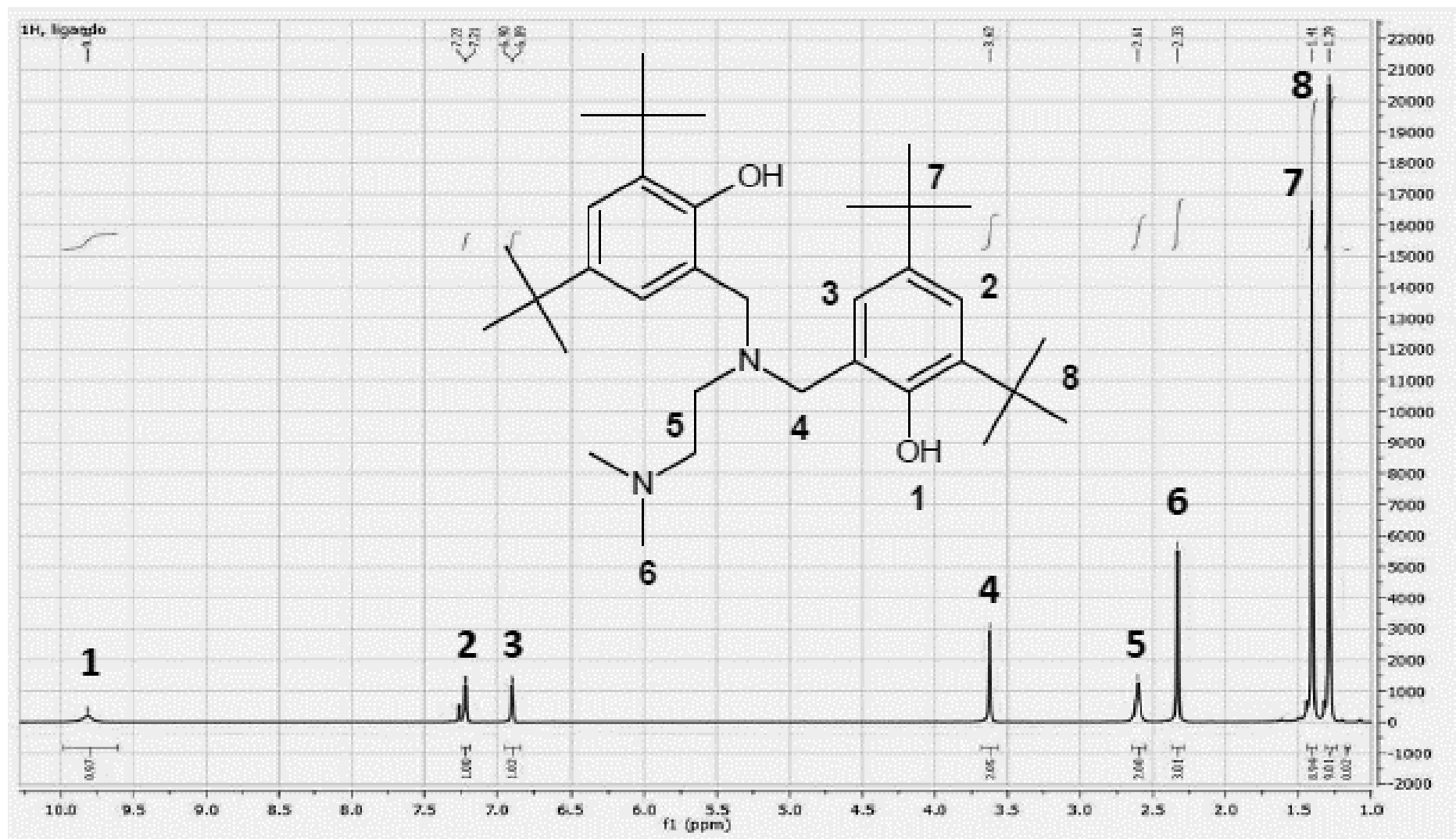
Figure 37. ^{1}H NMR spectrum of bis(phenolate) ligand [45]

The Mo (V) complex synthesis was divided into two steps. First, the ligand is deprotonated with an excess (10%) of NaH to yield sodium diamine bis(phenolate), $NaN_2O_2^{t-Bu}$ (Fig.38).
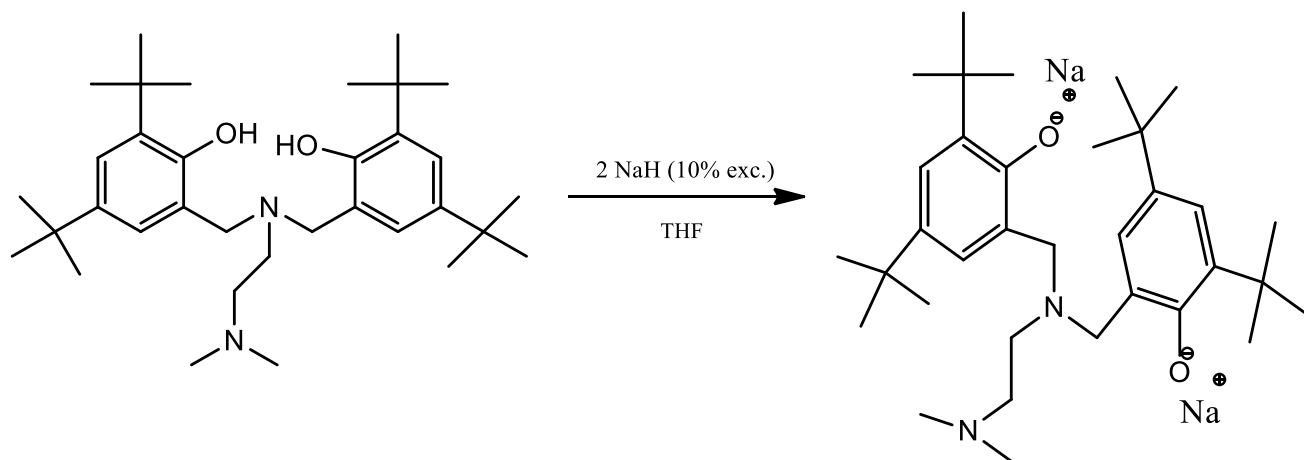
Figure 38. Ligand deprotonation

Foward, to this salt solution in THF is added a cold solution of $Mo(O)Cl_3(THF)_2$ in the same solvent, resulting in the Mo (V) complex as a brown solid (Fig.39).
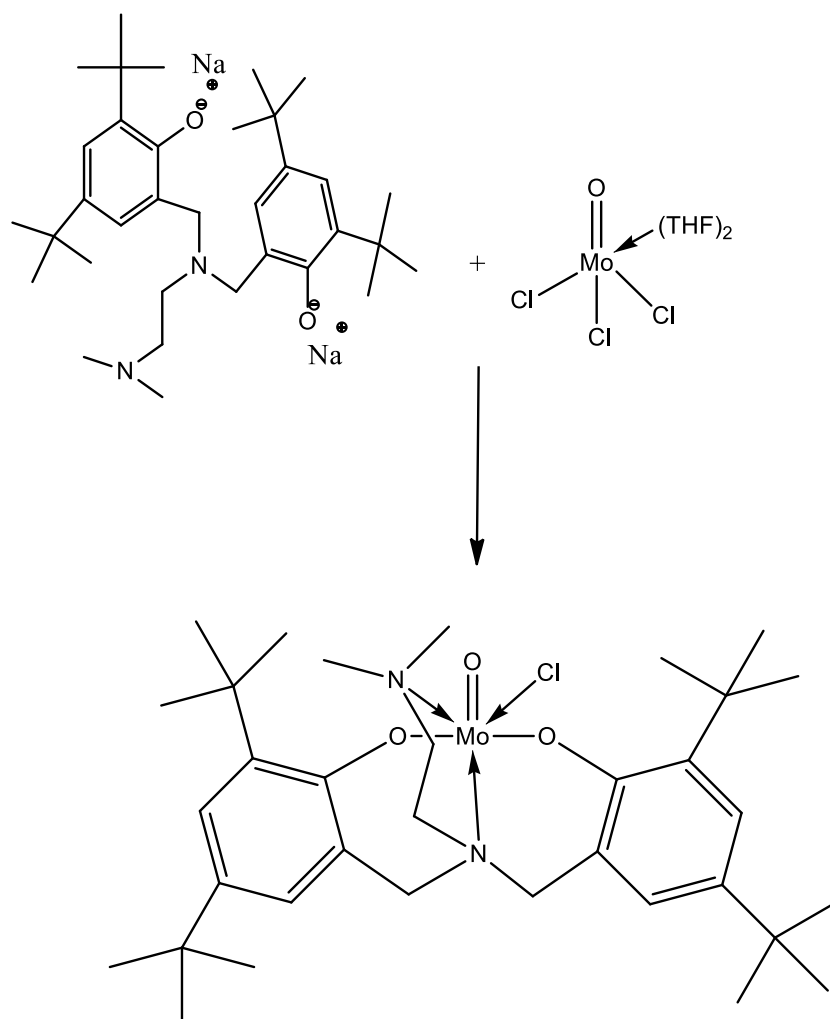
Figure 39. Mo (V) complex synthesis

Due to electronic configuration of Mo, which has an unpaired electron, the characterization of the obtained product was made by IR and elemental analysis instead NMR techniques. In the next figure, it is presented the IR spectrum for the yielded compound and a table with the most important peak values (table 3).
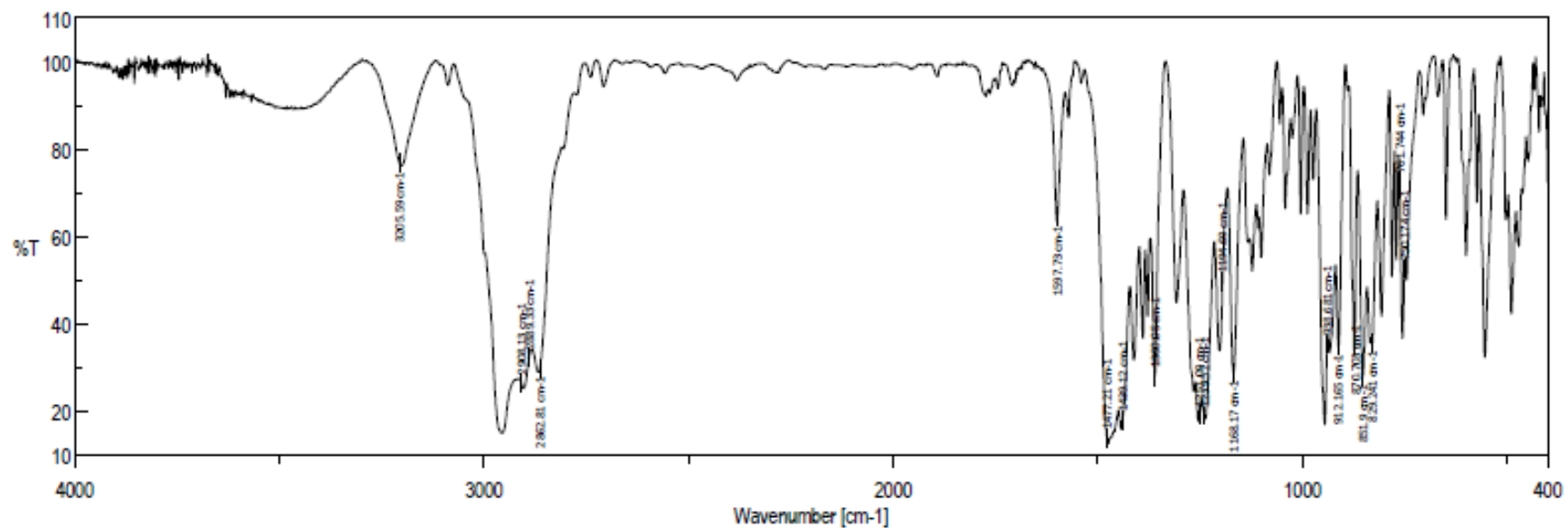
Figure 40. Mo (V) IR spectrum

(a)
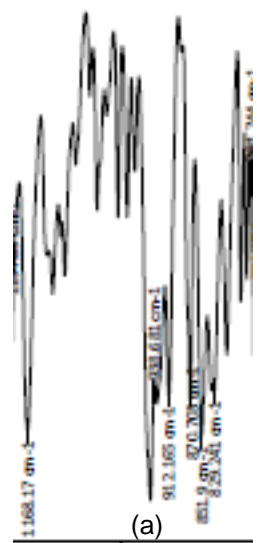
**Figure 41. Mo (V) IR spectrum
amplified in region of Mo=O stretch**

**Table 3. Most important peaks in the region of Mo=O stretch
of Mo (V) IR spectrum**

Position (cm⁻¹)	% Transmittance
944.949 (a)	16.9
1473.83 (b)	12.5

The results of elemental analysis were compared with the predicted values obtained with *ChemDraw Ultra 12.0* software, for the complex structure with and without the presence of oxygen. The relative error between the experimental values and the values obtained from *ChemDraw Ultra 12.0* for the first situation were calculated according to:

$$Percentage\ Error = \frac{|Experimental\ Value - Theoretical\ Value|}{Theoretical\ Value} \times 100\ (1)$$

The results of the elemental analysis are presented in the next table:

Table 4. Results for elemental analysis

Element	Experimental Value (%)	Predicted Value without O_2 (%)	Percentage Error (%)	Predicted Value with O_2 (%)	Percentage Error (%)
Nitrogen	3.36 – 3.42	4.69	27.72	3.51	3.42
Carbon	53.72 – 54.24	66.33	18.62	51.16	5.51
Hydrogen	6.92	9.45	26.77	6.82	1.47

2.2. Synthesis

2.2.1. Synthesis of 2,6-diisopropylphenyl vanadium chloride

Due to the existence of evidence of the utilization of transition metals, like vanadium, for isocyanates production it was hypothesized the following mechanisms (Fig.42):
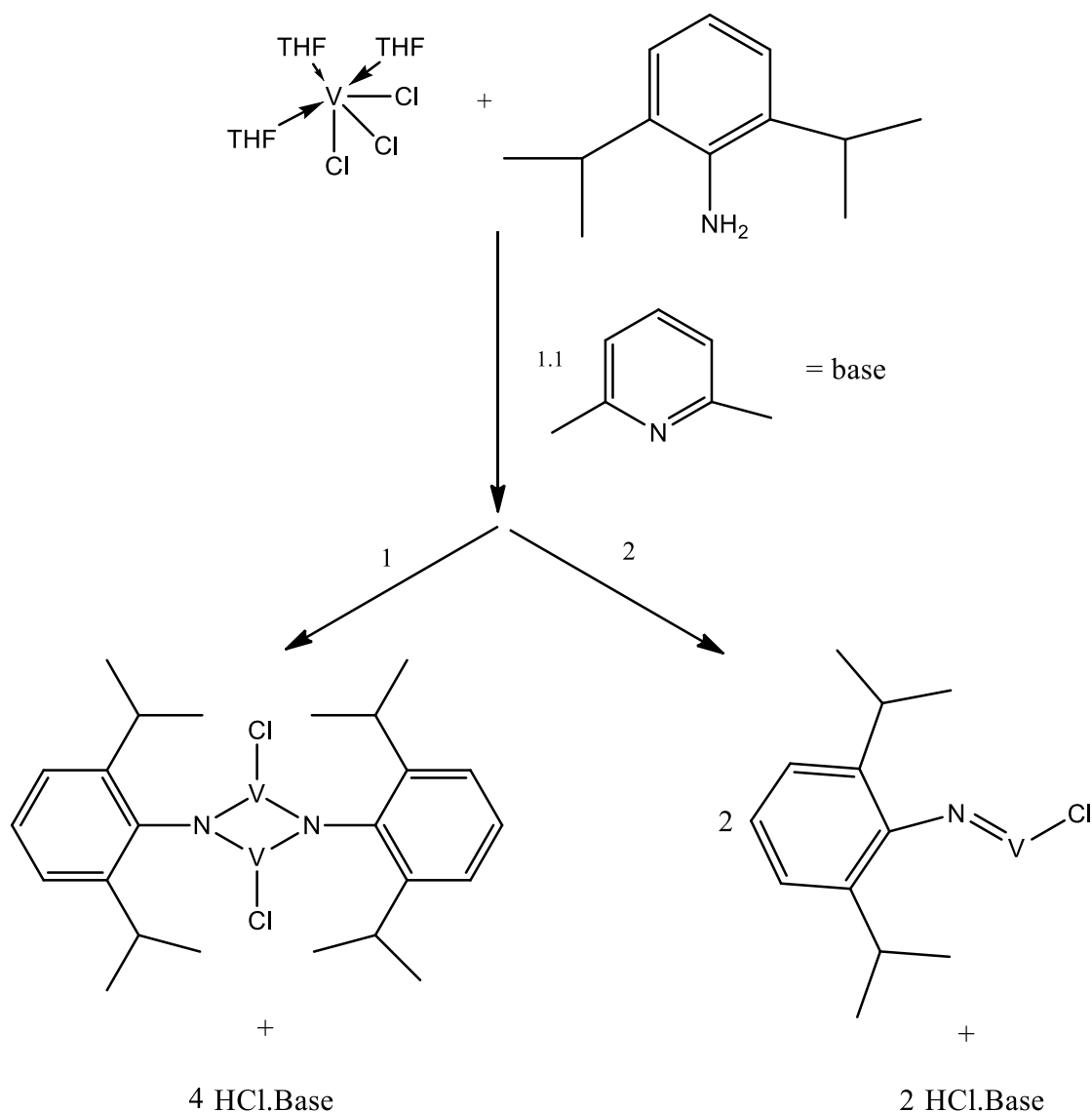
Figure 42. Vanadium complex formation

To a stirred solution of $VCl_3(THF)_3$ in THF was added dropwise a solution of 2,6-diisopropylaniline and lutidine in the same solvent resulting in a violet solution and a white solid. The reaction mixture was allowed to react at room temperature for two hours. In figure 43 it is presented the IR spectrum of the yielded crude solution.
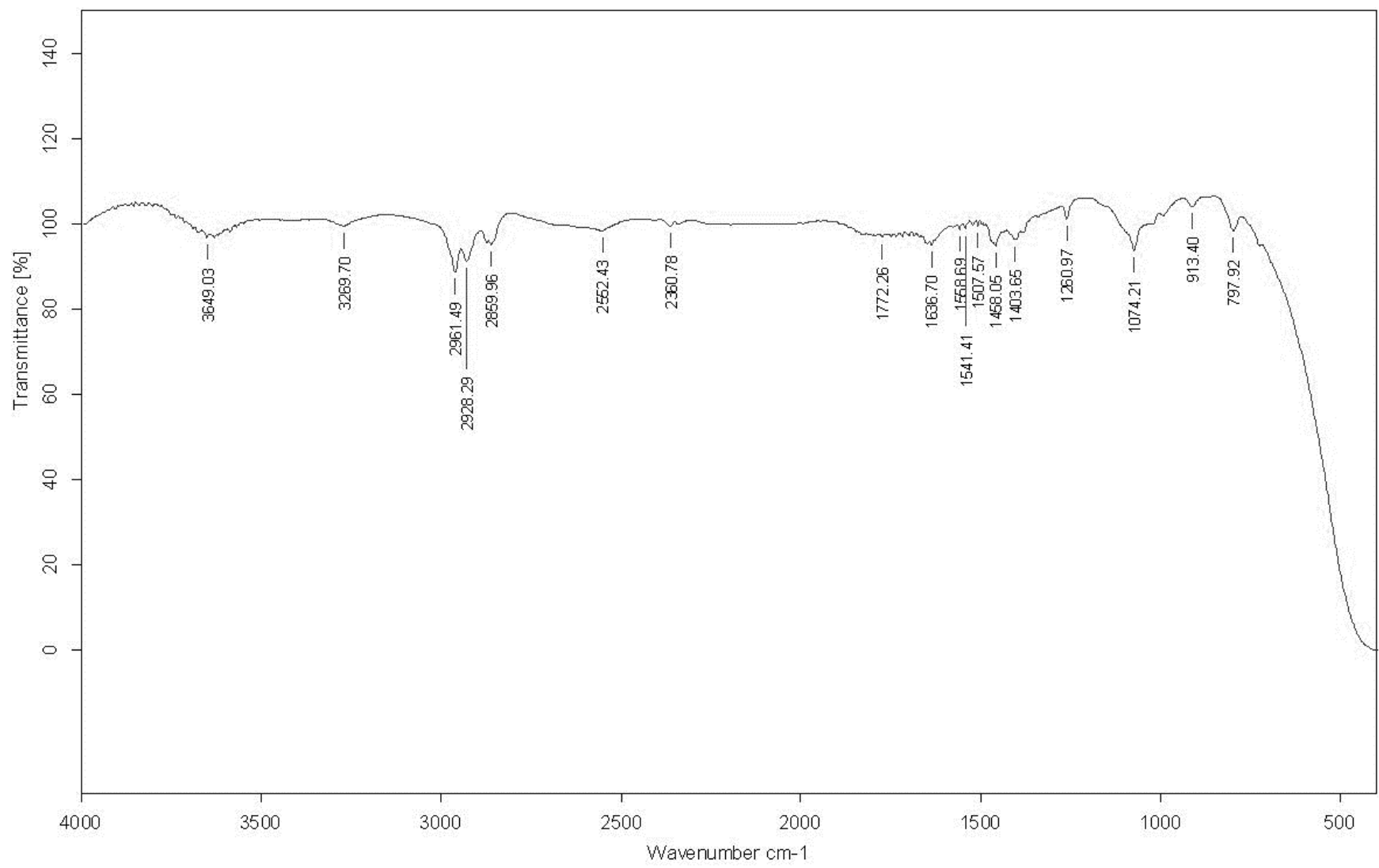
Figure 43. IR spectrum of the crude solution

2.1.2 Synthesis of 2,6-diisopropylphenyl-N-silyl magnesium amido

Recently, main group complexes have been studied in carbon dioxide activation and transformation. These elements are more available and inexpensive that transition metals. Besides that, these types of elements have *s* and *p* orbitals available to react given that carbon dioxide tends to be inert under most conditions. One studied reaction for carbon dioxide activation is the insertion of this gas into a M-N bonds of main group amido complexes (fig.44) [39].
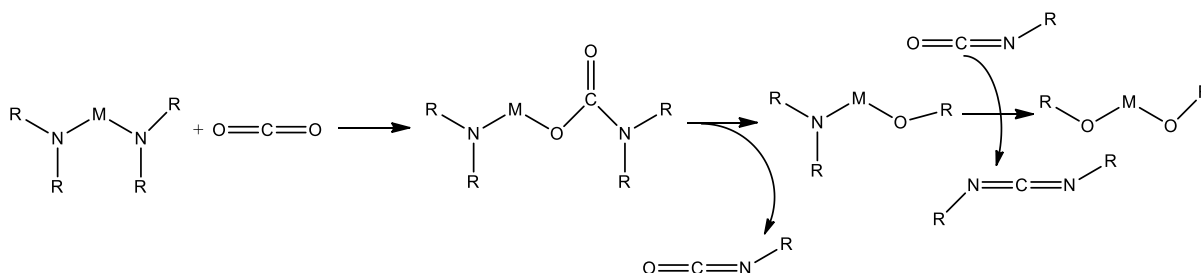
Figure 44. General reaction of divalent main-group amido complexes with CO_2 [39]

It was demonstrated that when R = alkyl or aryl, simple insertion occurs forming a carbamate. On the other hand, if one or both substituents were a silyl group, occurs an elimination of isocyanate driven by the formation of a strong Si-O bond. The remaining compound can react with the isocyanate or with another carbon dioxide molecule to yield more isocyanate or to form a carbodiimide [39].

Taking this into account, it was proposed the synthesis of some magnesium amido compounds to study its reactivity with carbon dioxide and in latter case the production of isocyanate.

The synthesis of 2,6-diisopropylphenyl-N-silyl magnesium amido can be divided into three steps. First, to a stirred solution of 2,6-diisopropylaniline in THF was added dropwise a solution of *n*-butyl lithium in the same solvent (Fig.45). The reaction mixture was stirred for 2 hours at 50°C, yielding a pale-yellow solution.
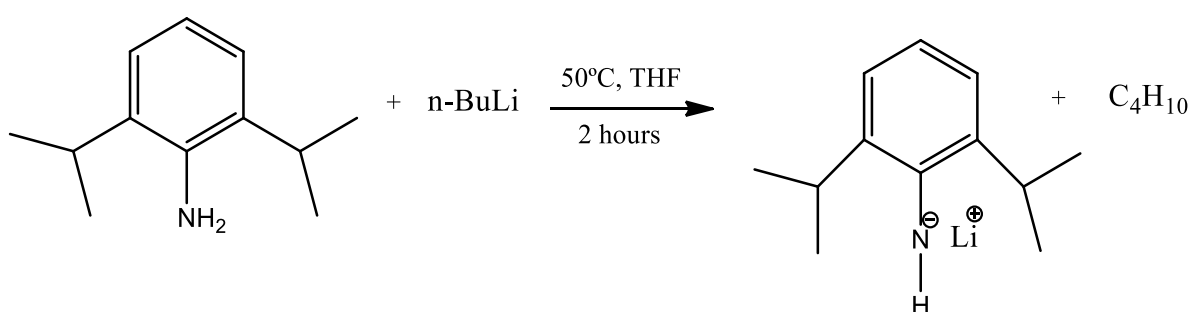
Figure 45. Aniline deprotonation

After that time, trimethylsilyl chloride (TMSCl) was added to the crude product and the resulting solution was stirred overnight (Fig.46).
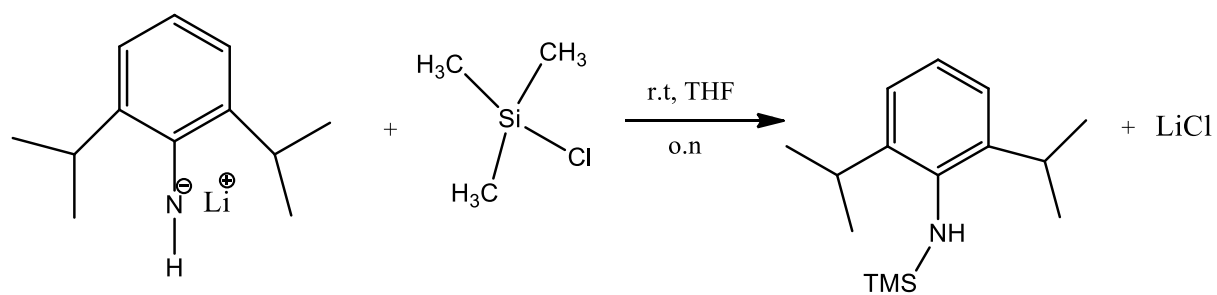
Figure 46. Trimethylsilyl chloride attack

In figure 47 is illustrated the ^{1}H NMR spectrum of the yielded silyl aniline. Figure 48 illustrates the ^{1}H NMR spectrum of 2,6-diisopropylaniline. This spectrum was made to compare it with the results of the aniline silylation shown in the previous figure.
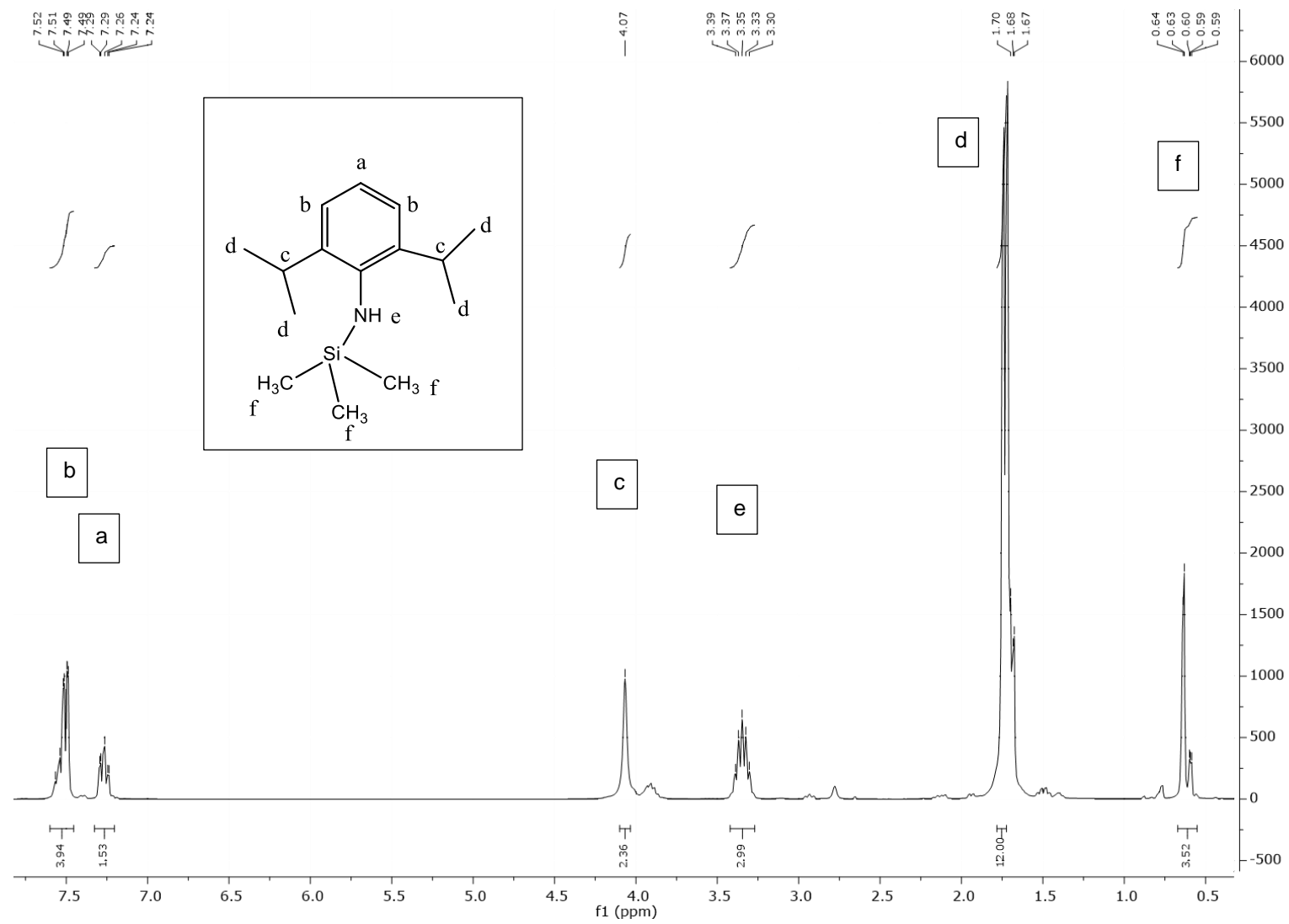
Figure 47. ¹H NMR spectrum of 2,6-diisopropylsilylaniline recorded in CDCl₃
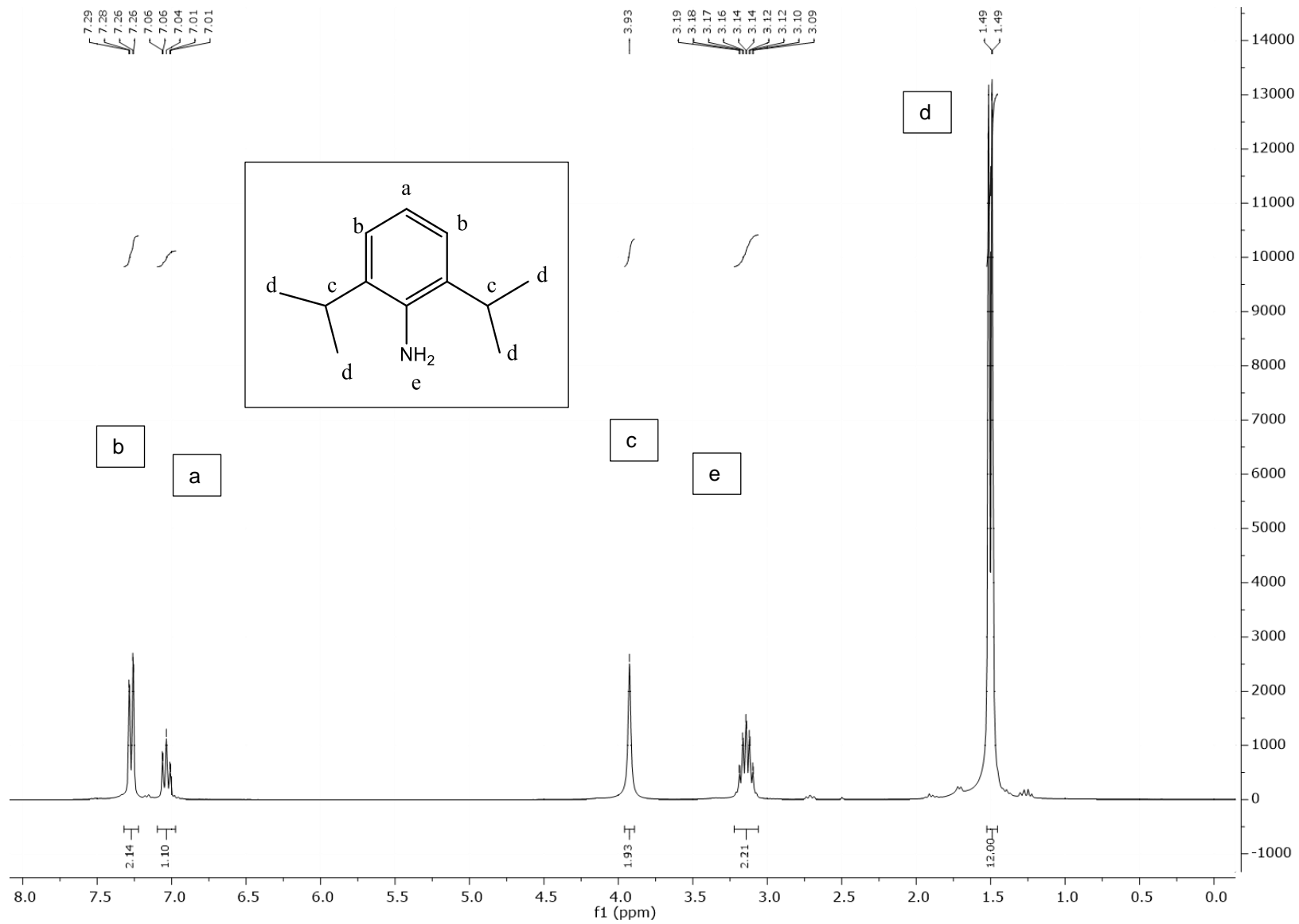
Figure 48. ^{1}H NMR spectrum of 2,6-diisopropylaniline recorded in CDCl$_3$

Afterwards, *n*-dibutyl magnesium was added to the previous cold solution obtaining a transparent solution and the mixture was allowed to react overnight. The resulting solution has a yellow color. The reaction mechanism can be described by (Fig.49):
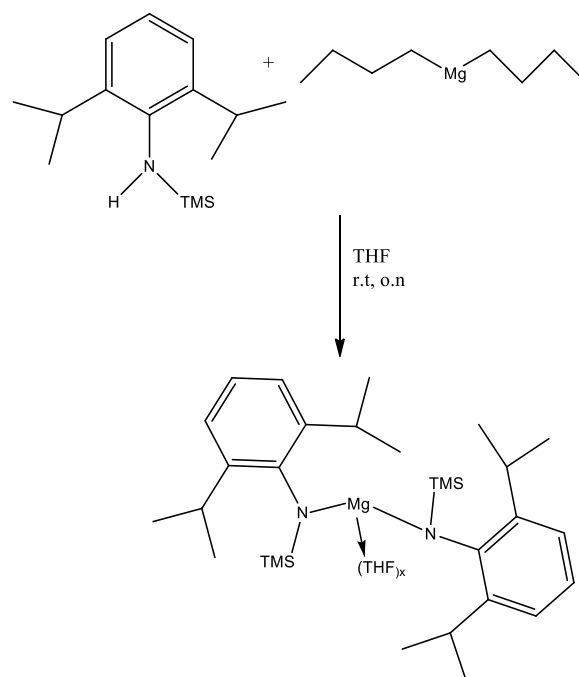
Figure 49. Synthesis of 2,6-diisopropylphenyl-N-silyl-magnesium amido

2.1.3. Synthesis of 2,6-dimethylphenyl-N-trimethylsilyl-magnesium amido

To a stirred solution of 2,6-dimethyl-N-trimethylsilylaniline in THF was added dropwise a solution of *n*-dibutyl magnesium in the same solvent yielding a pale-yellow solution (Fig.50). The reaction mixture was stirred overnight at room temperature.
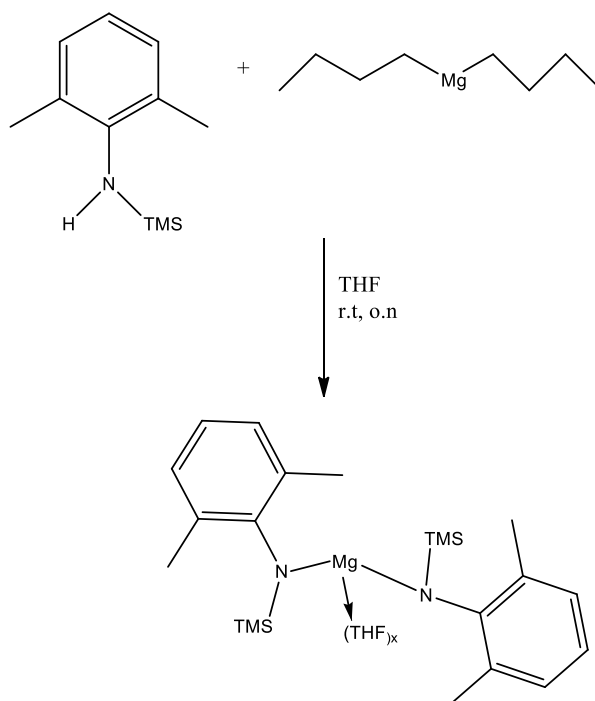
Figure 50. Synthesis of 2,6-dimethylphneyl-N-trimethylsilyl-magnesium amido

2.1.4. Synthesis of 2,6-dimethylphenyl-N-trimethylsilyl-bromomagnesium amido

A nucleophile is a specie that can donate a pair of electrons to another specie (electrophile). Bromide is considered a good nucleophile specie, because there exists a higher charge density in its position [47,48].

To a stirred cold solution of ethyl magnesium bromide (EtMgBr) in THF was added dropwise 2,6-dimethyl-N-trimethylsilylaniline (Ph(CH$_3$)$_2$NHTMS) (Fig.51). The reaction mixture was stirred overnight allowing warming up to room temperature. The solvent was removed under reduced pressure and the resulting solid was dried under vacuum.
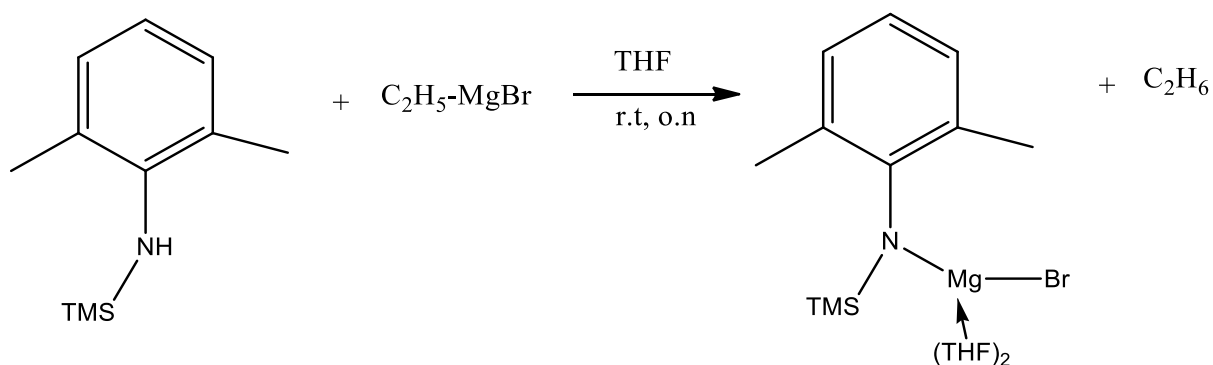
Figure 51. Mechanism for Ph(CH$_3$)$_2$N(TMS)Mg(THF)$_2$Br synthesis

The next figure illustrates the ^{1}H NMR spectrum of the desired product. ^{13}C NMR (fig.53) is further used at this stage to confirm ^{1}H NMR spectrum. IR spectrum was recorded in a potassium bromide (KBr) support is presented in figure 54.
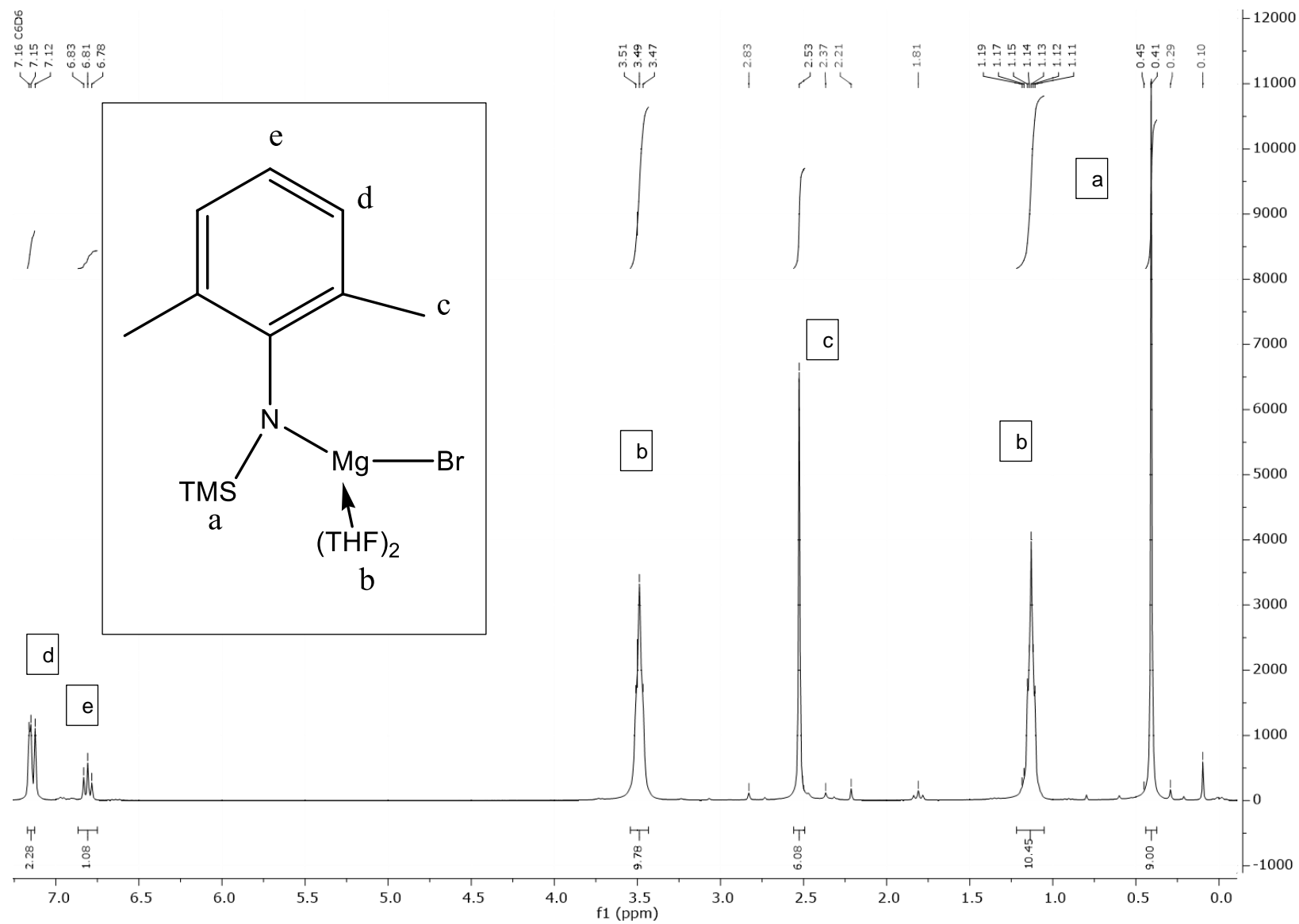
Figure 52. ^1H NMR spectrum of $(THF)_2.MgBrNPh(CH_3)_2TMS$ recorded in C_6D_6
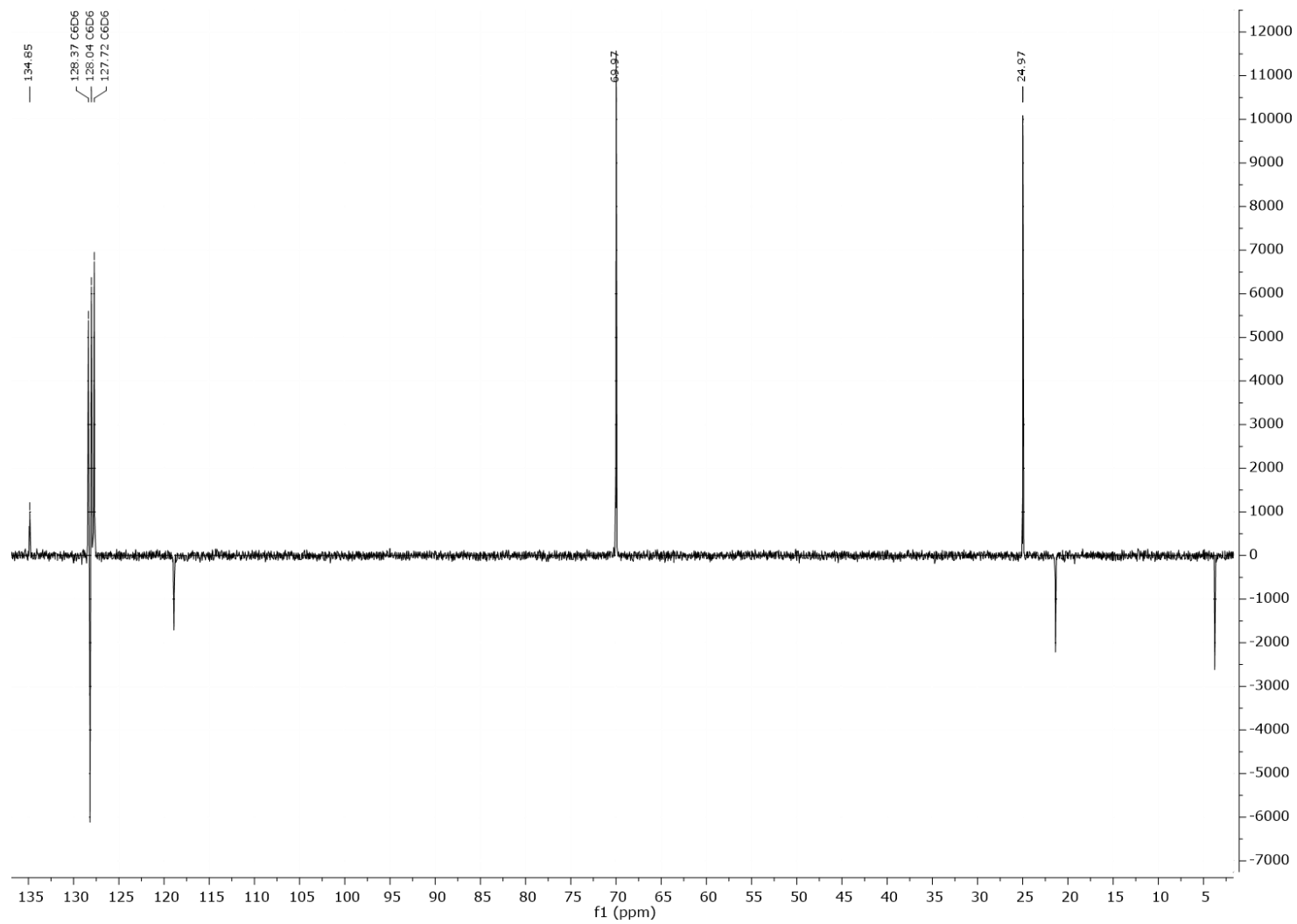
Figure 53. ^{13}C NMR spectrum of recorded $(THF)_2.MgBrNPh(CH_3)_2TMS$ recorded in C_6D_6
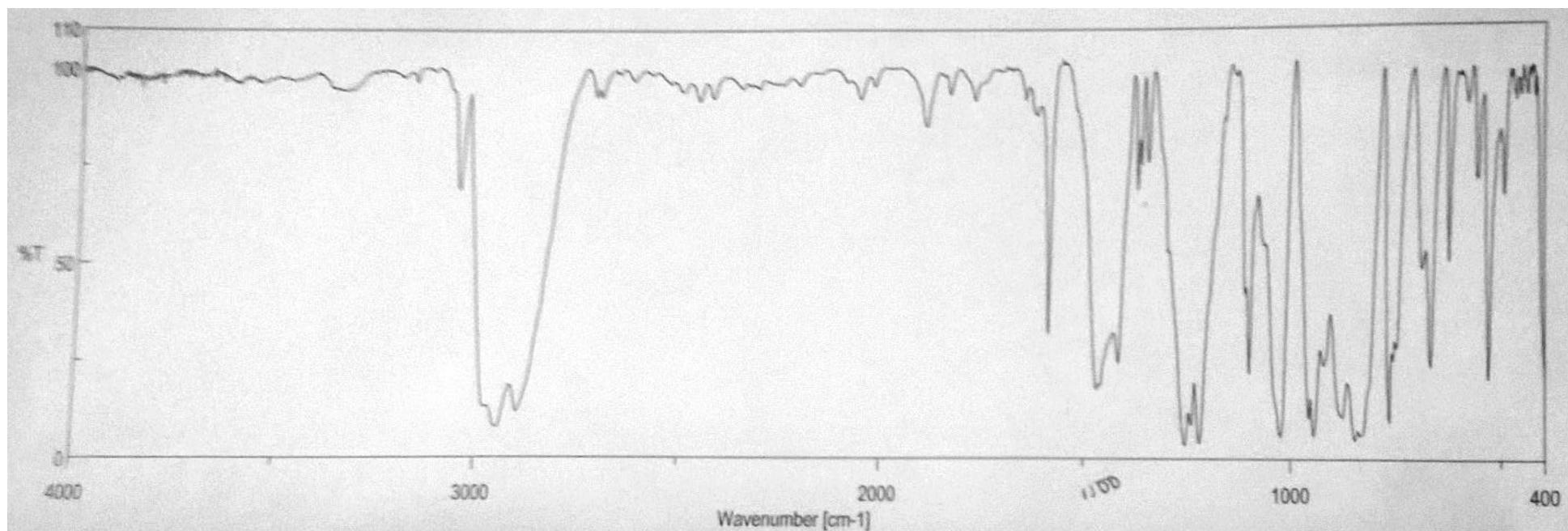
Figure 54. IR spectrum for (THF)$_2$.MgBrNPh(CH$_3$)$_2$TMS recorded in KBr support

2.1.5. Synthesis of 2,6-dimethylphenyl-ciclopentadienyl-N-trimethylsilyl-magnesium amido

Cyclopentadienyl (*Cp*, C_5H_5) ligand is used in organometallic chemistry. *Cp* can remain inert to nucleophiles and electrophiles and can stabilize organometallic complexes: metal bind to all five carbons of the ring. This ligand is an electron rich, aromatic where the existent electrons can create a stable, strong metal-Cp bond with five equal metal-carbon distances. [49-51]

The synthesis of 2,6-dimethylphenyl-ciclopentadienyl-N-trimethylsilyl-magnesium amido was performed in two ways: in a first place, by reaction of $Cp^{bz}MgEt(THF)$ and 2,6-dimethyl-N-trimethylsilylaniline and in second place by reaction of $NaCp^{bz}(THF)_{2.5}$ and 2,6-dimethylphenyl-N-trimethylsilyl-bromomagnesium amido.

In an NMR tube, ethyl-cyclopentadienyl magnesium amido ($Cp^{bz}MgEt(THF)$) was dissolved in deuterated toluene. Forward, 2,6-dimethyl-N-trimethylsilylaniline was added to the previous mixture and let to react at room temperature (Fig. 55).
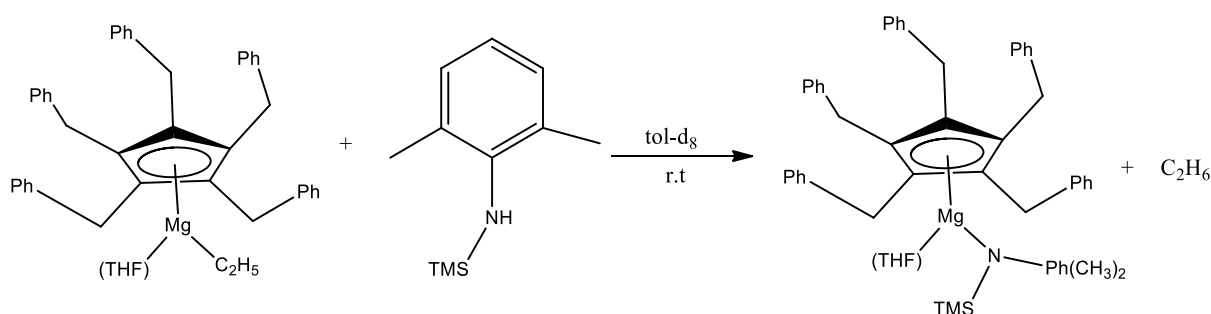
Figure 55. Synthesis of $Cp^{bz}Mg(THF)_2NPh(CH_3)_2TMS$

Figures 56 and 57 shows the ^{1}H NMR and ^{13}C NMR spectrum of 2,6-dimethyl-N-trimethylsilylaniline, recorded in deuterated toluene. Figures 58 to 60 presents the evolution of ^{1}H NMR spectrum during the time reaction for the yielded product and figure 61 shows the resultant ^{13}C NMR spectrum for the same product. All these spectra was recorded in deuterated toluene.
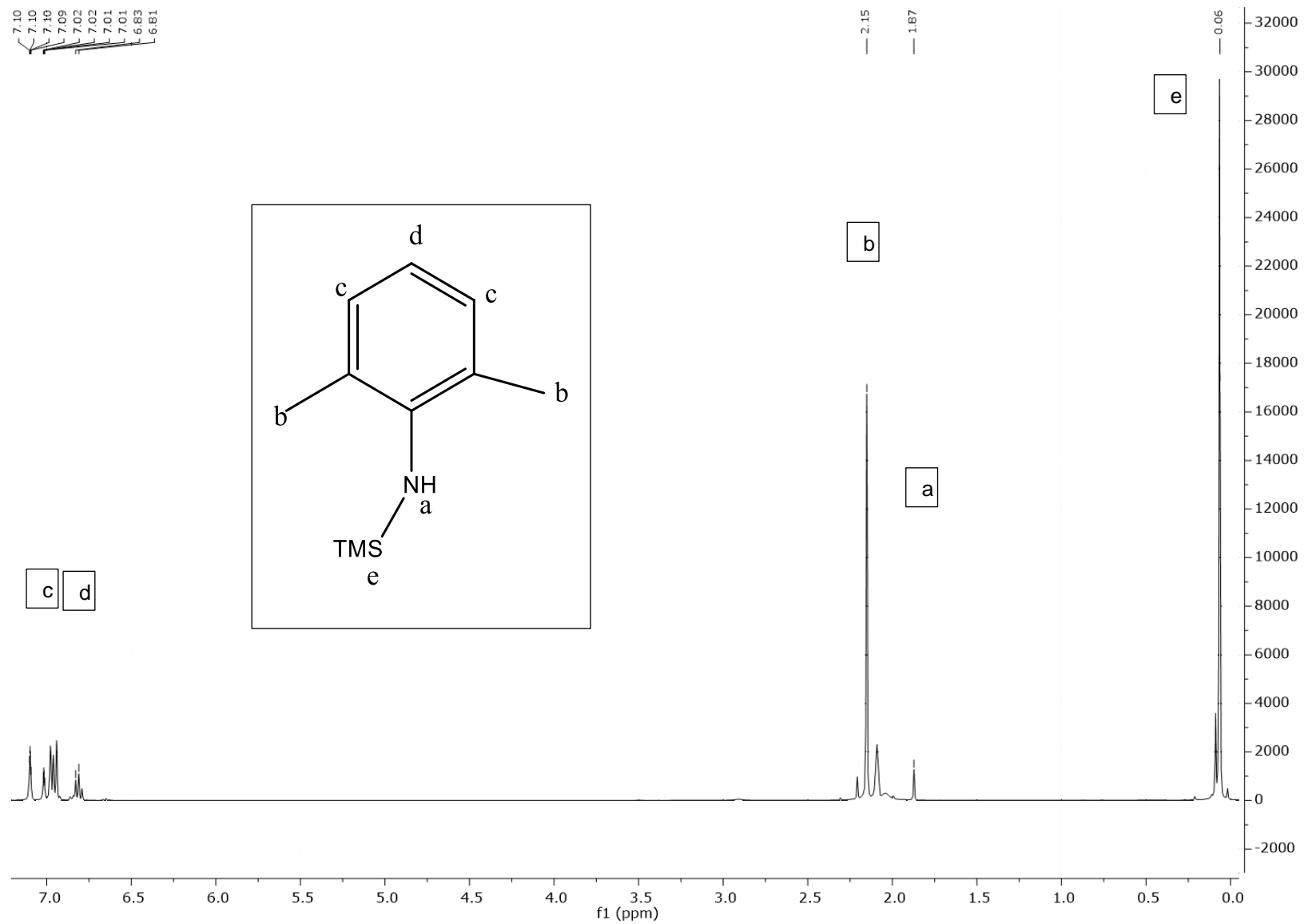
Figure 56. ^{1}H NMR spectrum of 2,6-dimethyl-N-trimethylsilylaniline recorded in tol-d$_8$
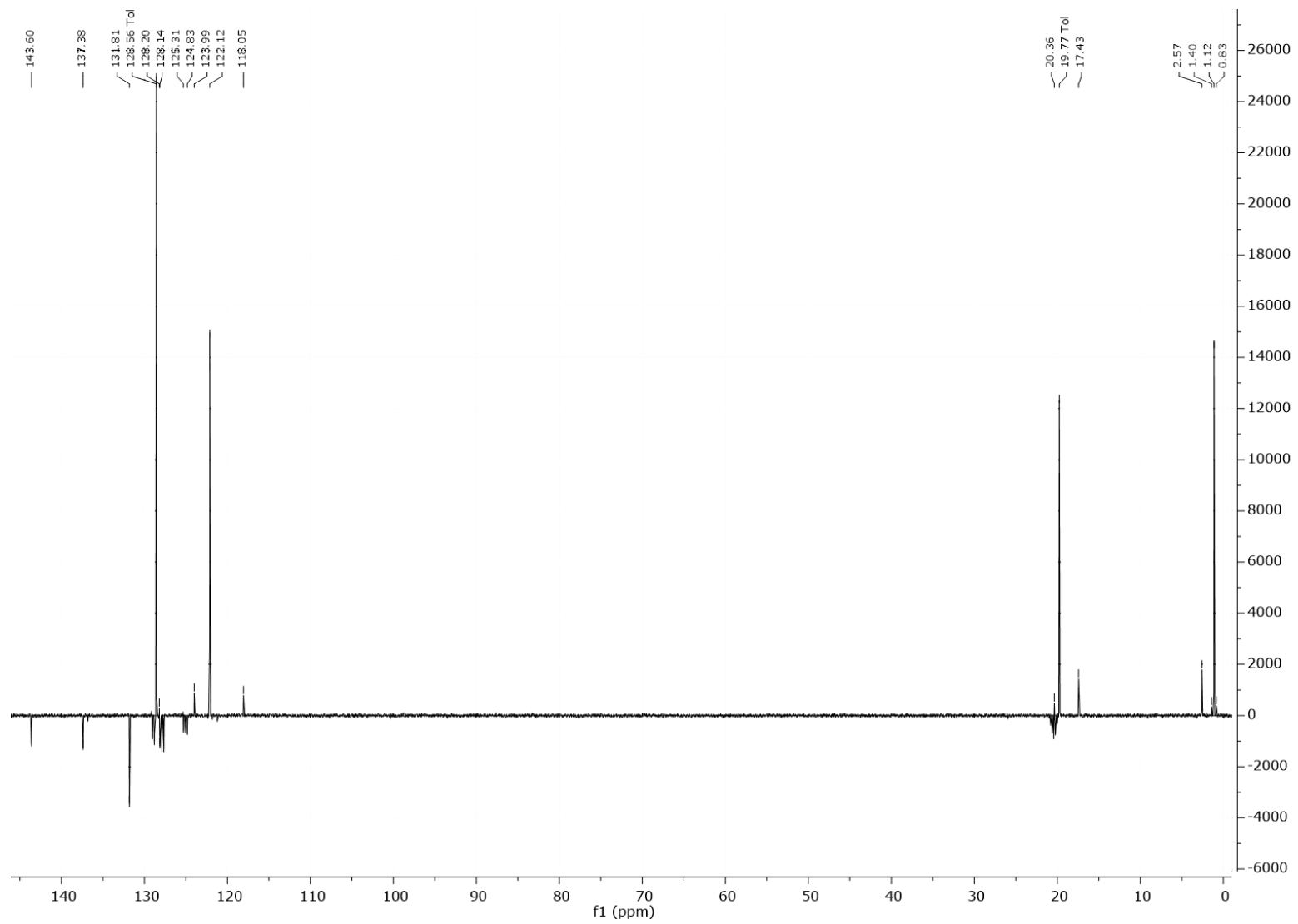
Figure 57. ^{13}C NMR spectrum of 2,6-dimethyl-N-trimethylsilylaniline recorded in tol-d$_8$
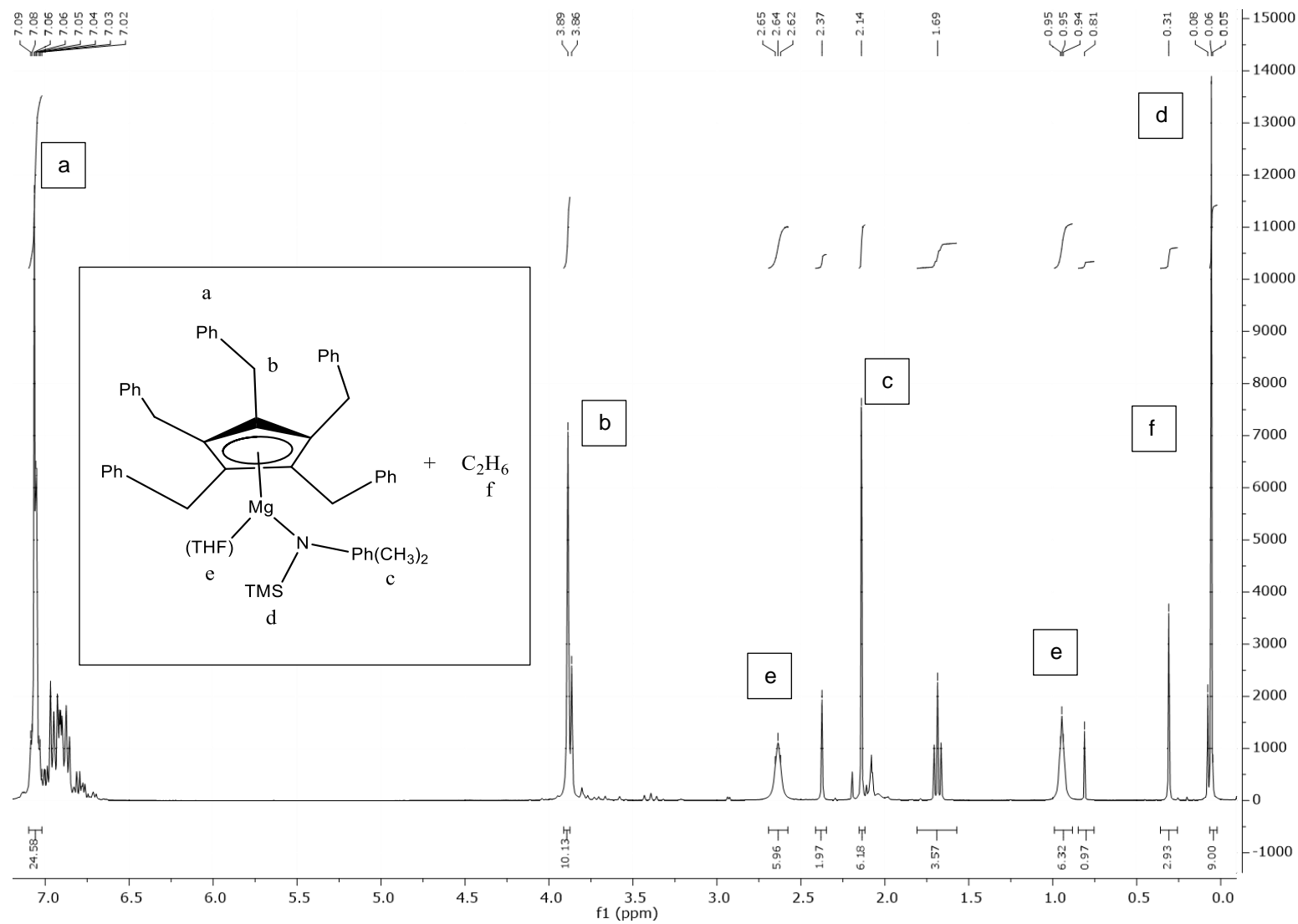
Figure 58. ^{1}H NMR spectrum of $Cp^{bz}Mg(THF)NPh(CH_3)_2Si(CH_3)_3$ recorded in tol-d$_8$

48
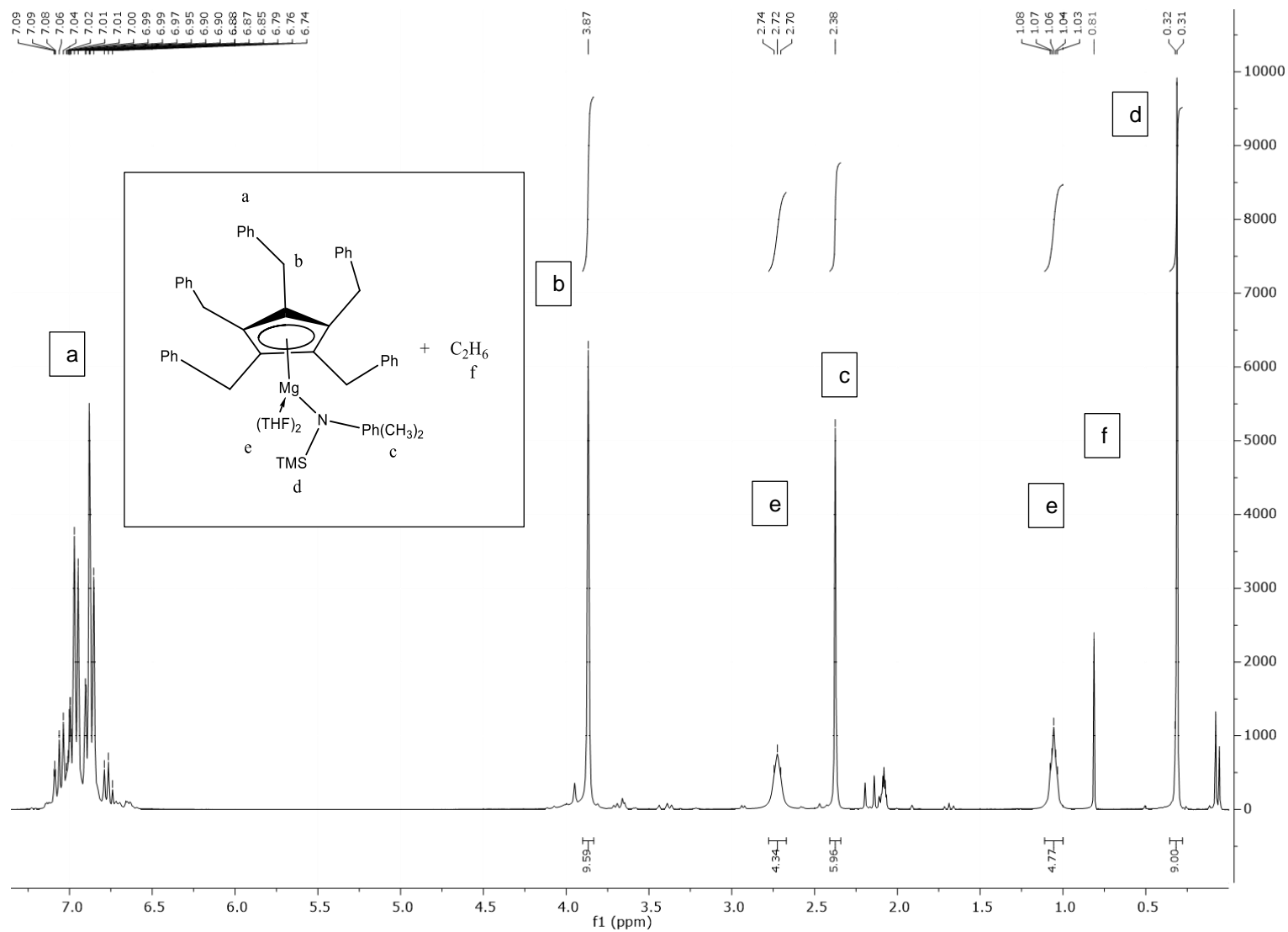
Figure 59. ^{1}H NMR spectrum of Cp^{bz}Mg(THF)NPh(CH$_3$)$_2$TMS recorded in tol-d$_8$ after heated at 50°C overnight
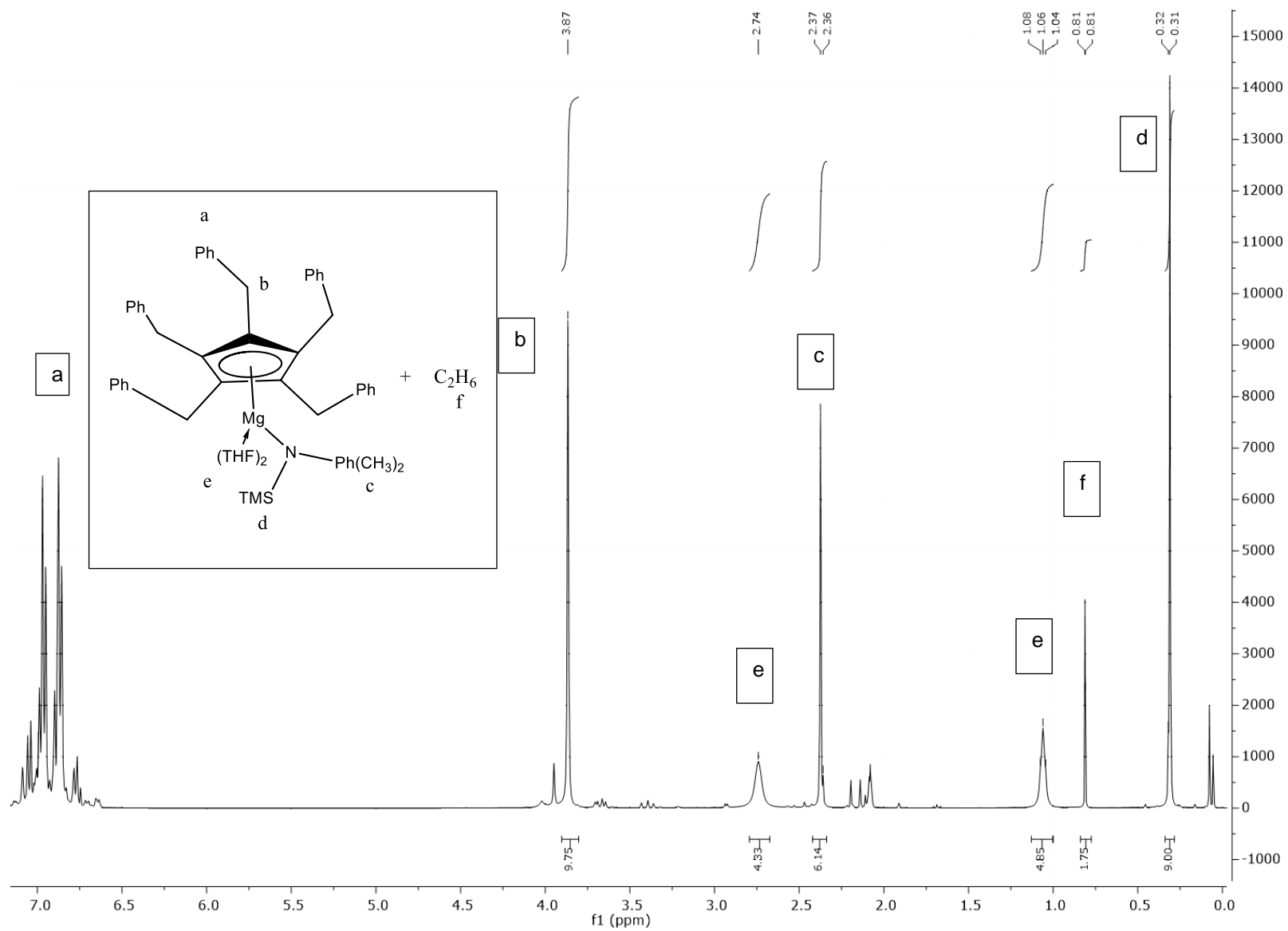
Figure 60. ^{1}H NMR spectrum of $Cp^{bz}Mg(THF)NPh(CH_3)_2TMS$ recorded in tol-d_8 after 16 hours
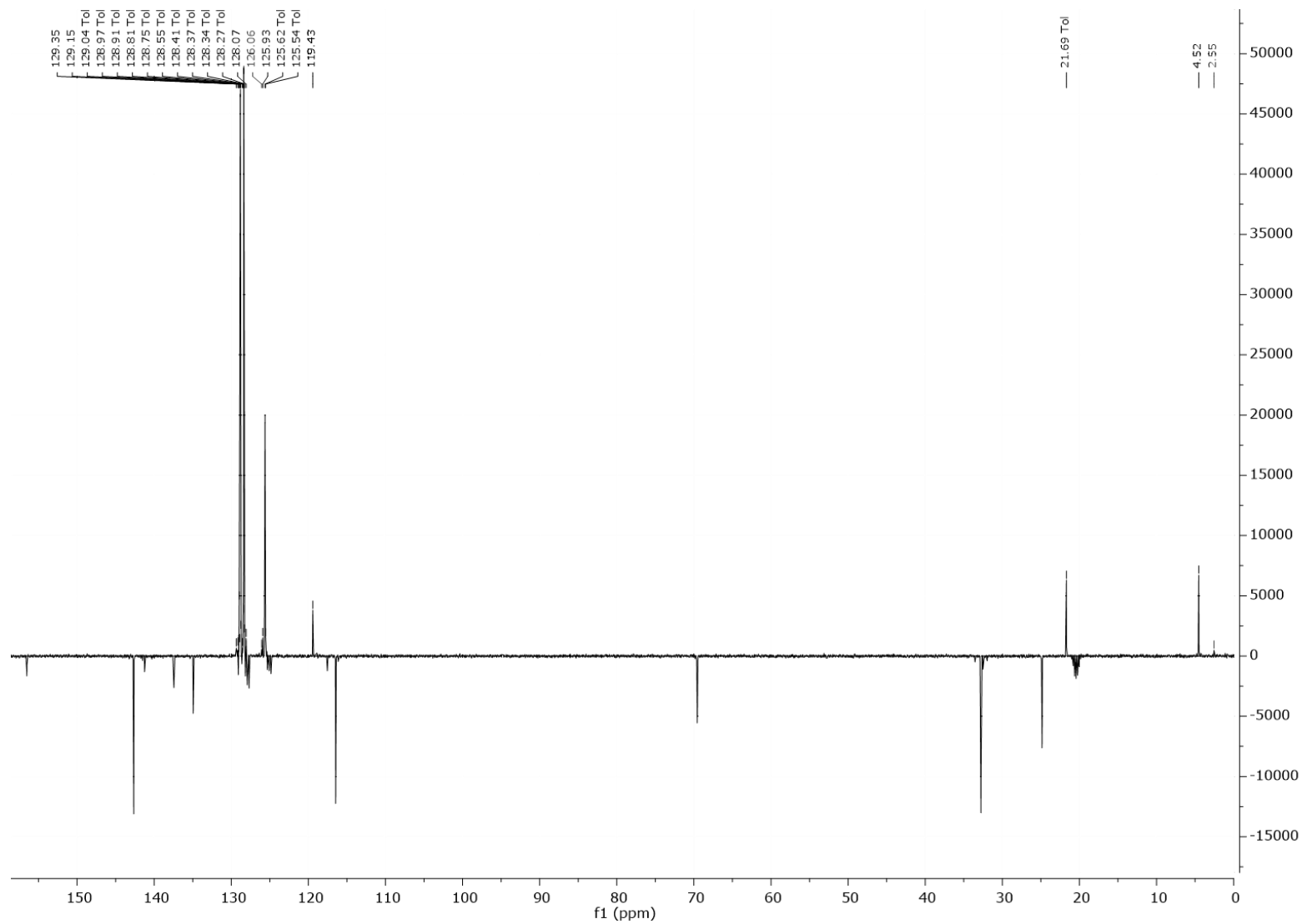
Figure 61. ^{13}C NMR spectrum of $Cp^{bz}Mg(THF)NPh(CH_3)_2TMS$ recorded in tol-d_8 after 16 hours

To a stirred solution of sodium cyclopentadienyl (NaCp^{bz}(THF)$_{2.5}$) in THF was added dropwise of 2,6-dimethylphenyl-N-trimethylsilyl-bromomagnesium amido ((THF)$_2$.MgBrNPh(CH$_3$)$_2$TMS) in THF (Fig.62).
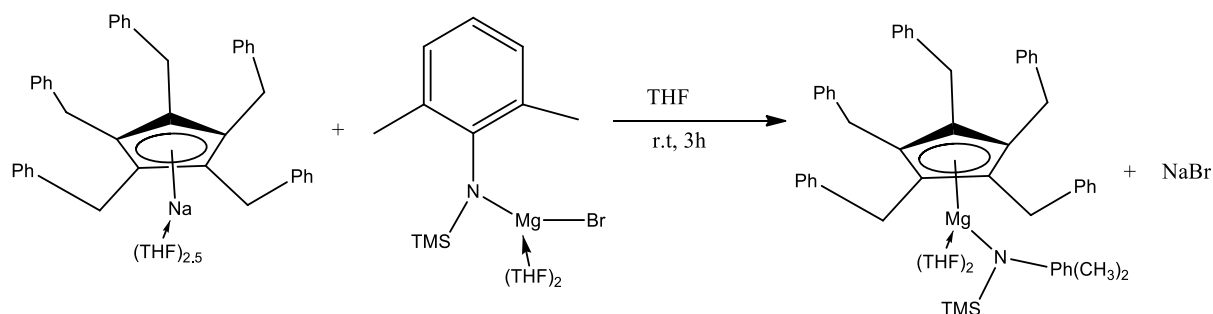
Figure 62. Synthesis of (THF)$_2$.Cp^{bz}MgNPh(CH$_3$)$_2$TMS

The reaction mixture was stirred for 3 hours at room temperature. The solvent was removed under reduced pressure. The obtained solid was dried under vacuum. The solid was dissolved in toluene. The resulting solution was filtered to remove sodium bromide (NaBr). The remaining solution was concentrated until begin to precipitate and it was kept in the freezer overnight. After that time, the solvent was removed under reduced pressure to obtain a white solid. This solid was dried under vacuum. *n*-Hexane was added and then the resulting suspension was filtered. The resulting solution was kept in the freezer and the solid was dried under vacuum.

The ^{1}H and ^{13}C NMR spectra are equal to the obtained in the first method.

2.1.6. Synthesis of 2,6-dimethylphenyl-N-trimethylsilyl-magnesium ketimide

Ketimides (R$_2$C=N$^-$) (R = alkyl, aryl or silyl groups) monoanions are important monodentate nitrogen-donor ligands used in coordination and organometallics chemistry. Negative charge is centered in the nitrogen atom and can form a covalent bond between metal and nitrogen in metal complexes. The huge differences between amidos (R$_2$N$^-$) and ketimides are related to its structure: in amidos, nitrogen hybridization is *sp²* or *sp³* and its bonded to two groups; in ketimides the nitrogen hybridization is *sp* or *sp²* and it is bonded to only one carbon atom with a N=C double bond. This fact can influence the reactivity of M-N bonds. In amidos, M-N bond is reactive and can engage in a protonolysis and insertion of unsaturated substrate. In ketimides, the M-N bond is inert and resistant to insertion or electrophilic attack, making this type of ligand the choice when it is required a stabilization of highly reactive species [52].

To a stirred solution of lithioketimine (Li-N=C(^{t}Bu$_2$)), synthetized according to [53] in toluene, at room temperature, was added a solution of 2,6-dimethylphenyl-N-trimethylsilyl-bromomagnesium amido (THF)$_2$.MgBr(CH$_3$)$_2$NTMS in the same solvent and let to react for one hour (Fig.63).
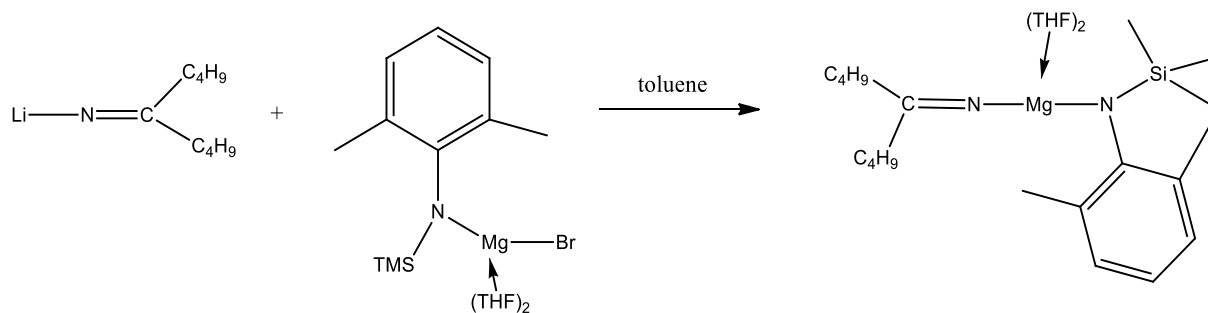
Figure 63. Synthesis of $^tBu_2C=N-Mg(THF)_2Ph(CH_3)_2N-TMS$ scheme

The yielded suspension was filtered and lithium bromide (LiBr) was rejected. The solvent from the resulting solution was removed under reduced pressure yielding a solid. This solid was dried under vacuum. Hexane was added to help the exit of toluene and the solvent was removed under reduced pressure. The yielded solid was dried under vacuum. In the next figures, it will be present the ^1H NMR (fig. 64) and ^{13}C NMR (fig.65) spectrum for the yielded product. The ^{13}C NMR spectrum was used to confirm this structure.
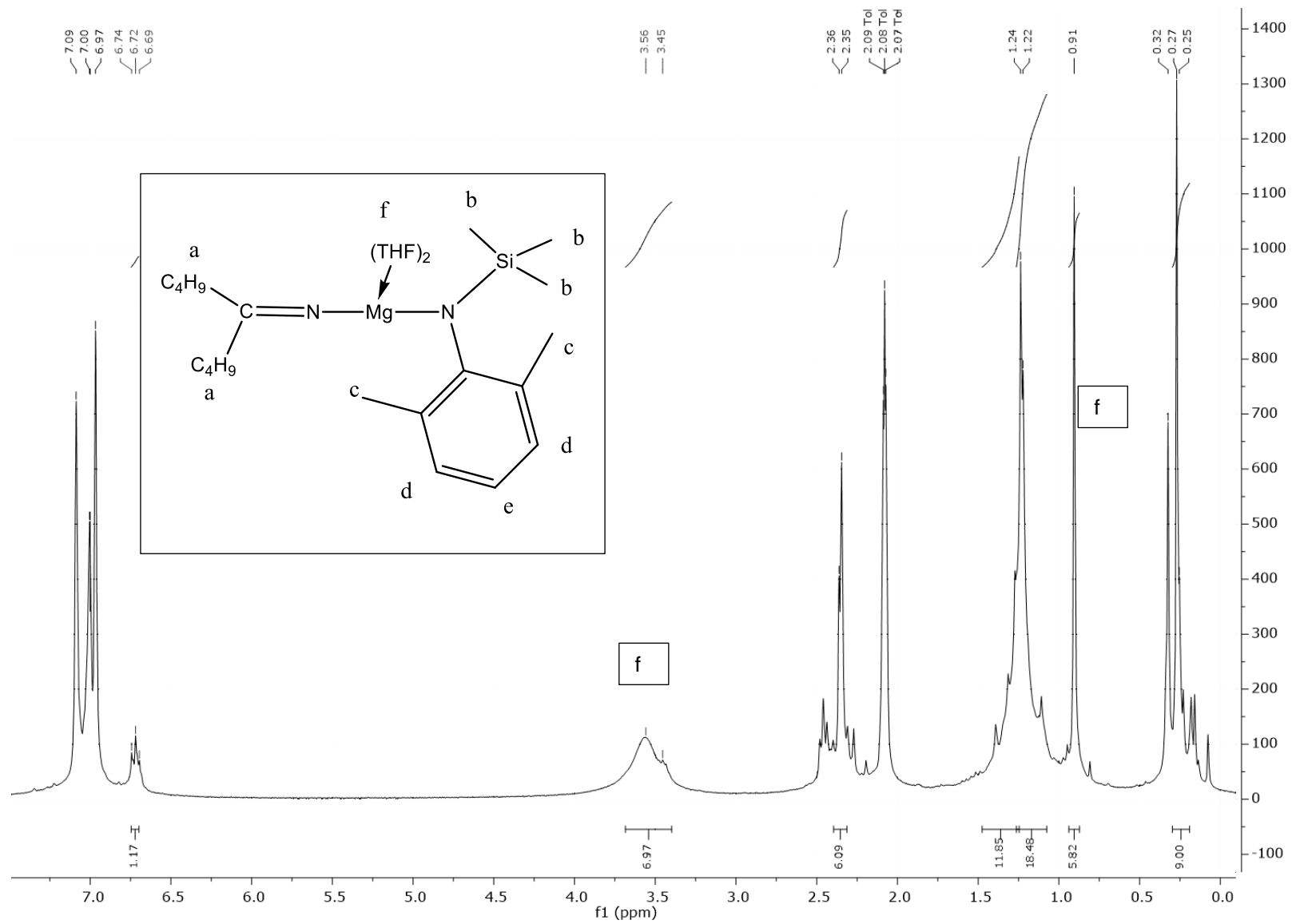
Figure 64. ^{1}H NMR spectrum of ^{t}Bu$_2$C=N-Mg(THF)$_2$Ph(CH$_3$)$_2$N-TMS recorded in tol-d$_8$
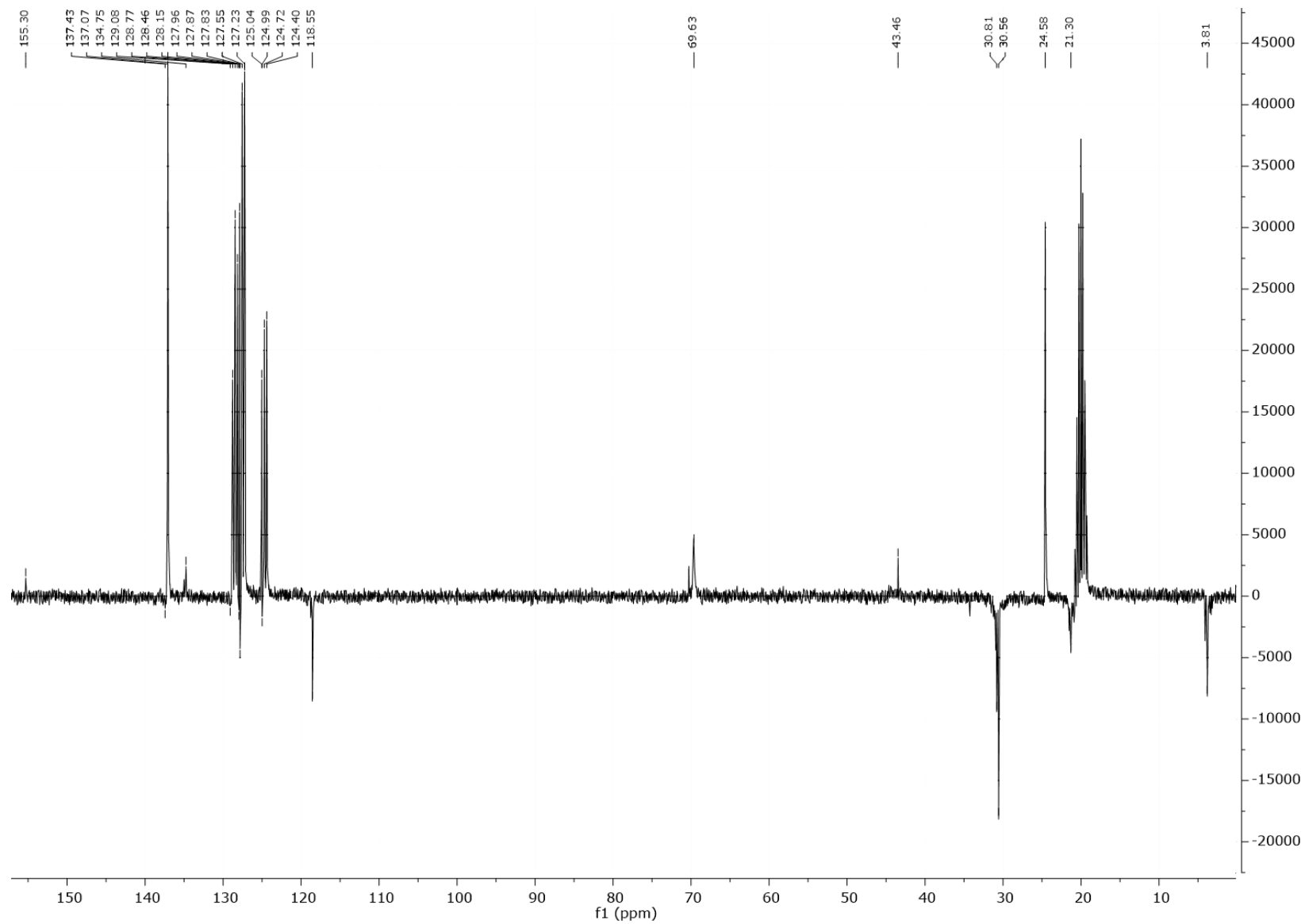
Figure 65. ^{13}C NMR spectrum of recorded $^{t}Bu_2C=N-Mg(THF)_2Ph(CH_3)_2N-TMS$ recorded in tol-d_8

2.3. Reactions with wet CO_2

2.3.1. Reaction of 2,6-diisopropylphenyl vanadium chloride

Carbon dioxide was bubbled through the solution of 2,6-diisopropylphenyl vanadium chloride for 2 hours without changes. No changes were observed. Figure 66 illustrates the IR spectrum of the crude solution. After one night, the solution changed color of violet to red with the same white solid. The solution was filtered and the solid was dried under vacuum. The solid was characterized by IR spectrum (fig.67). This remaining solution was concentrated by removing part of the solvent changing the color of red to violet again. Finished the concentration, the solution changed the color to red again and a white solid appeared. An obtained IR spectrum of the concentrated solution is shown in figure 68. The least solid was dried under vacuum and their IR spectrum is illustrated in figure 69.
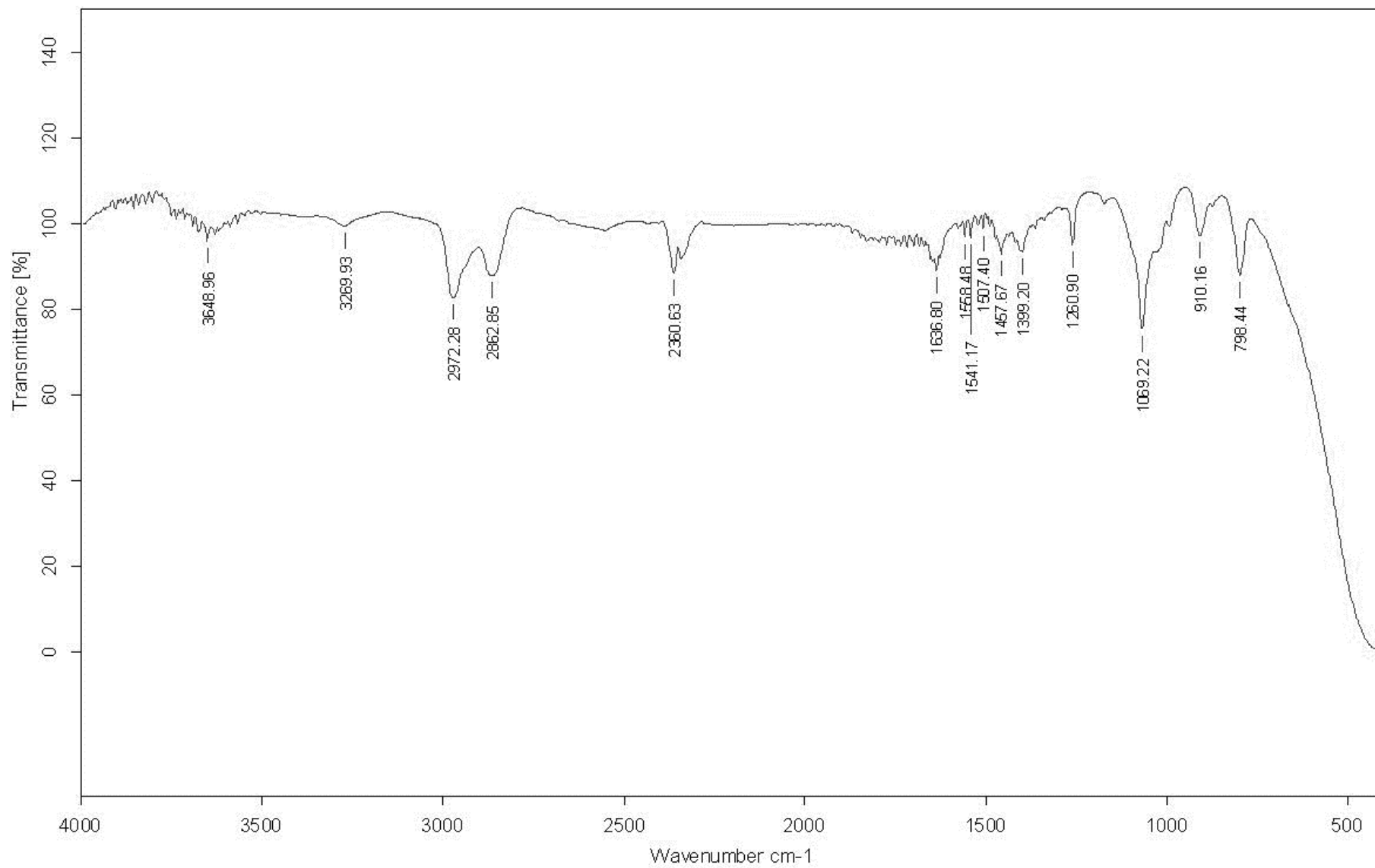
Figure 66. IR spectrum of crude solution after reaction with CO_2 in NaCl support
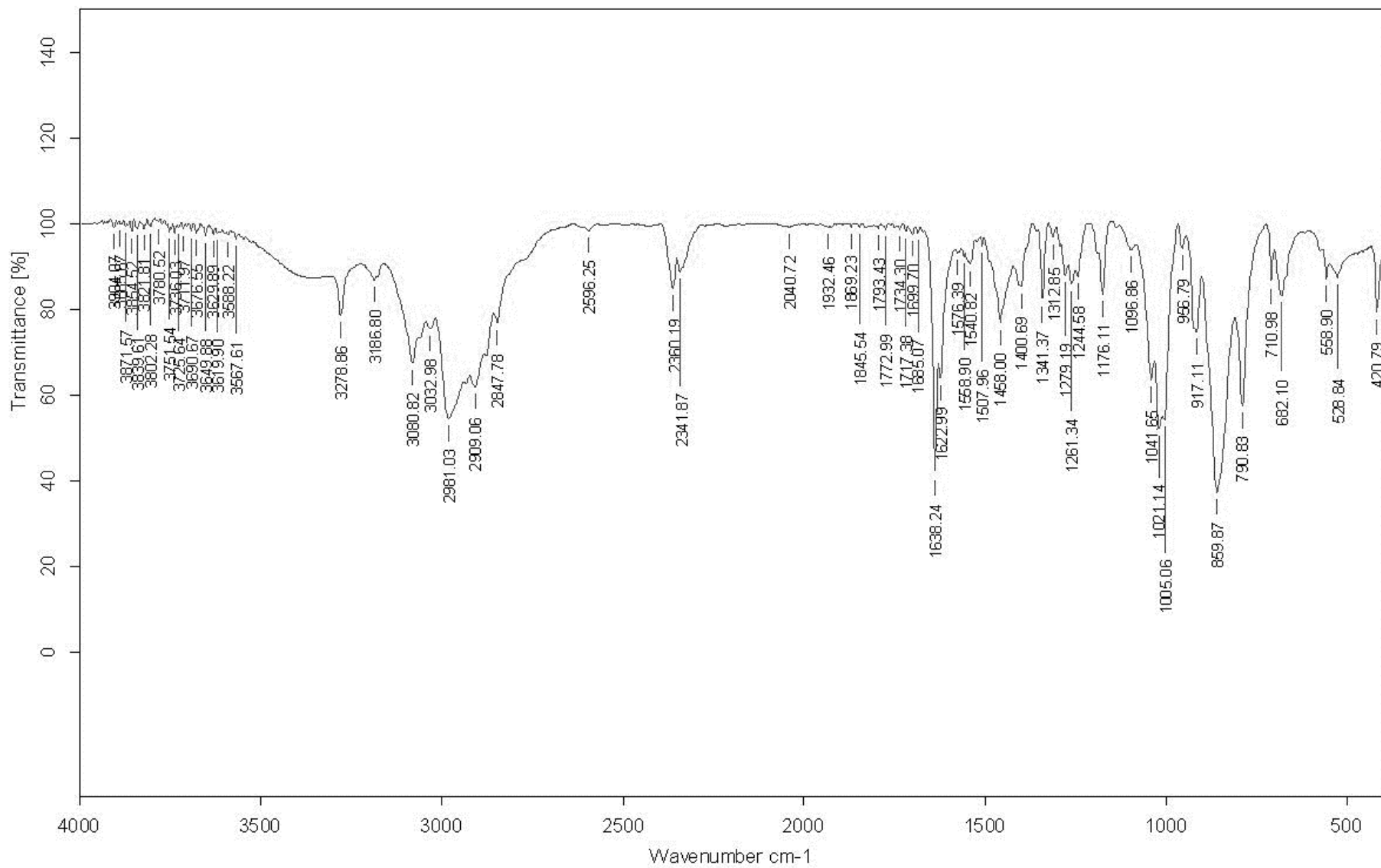
Figure 67. IR spectrum of the solid obtained after solution concentration in KBr support
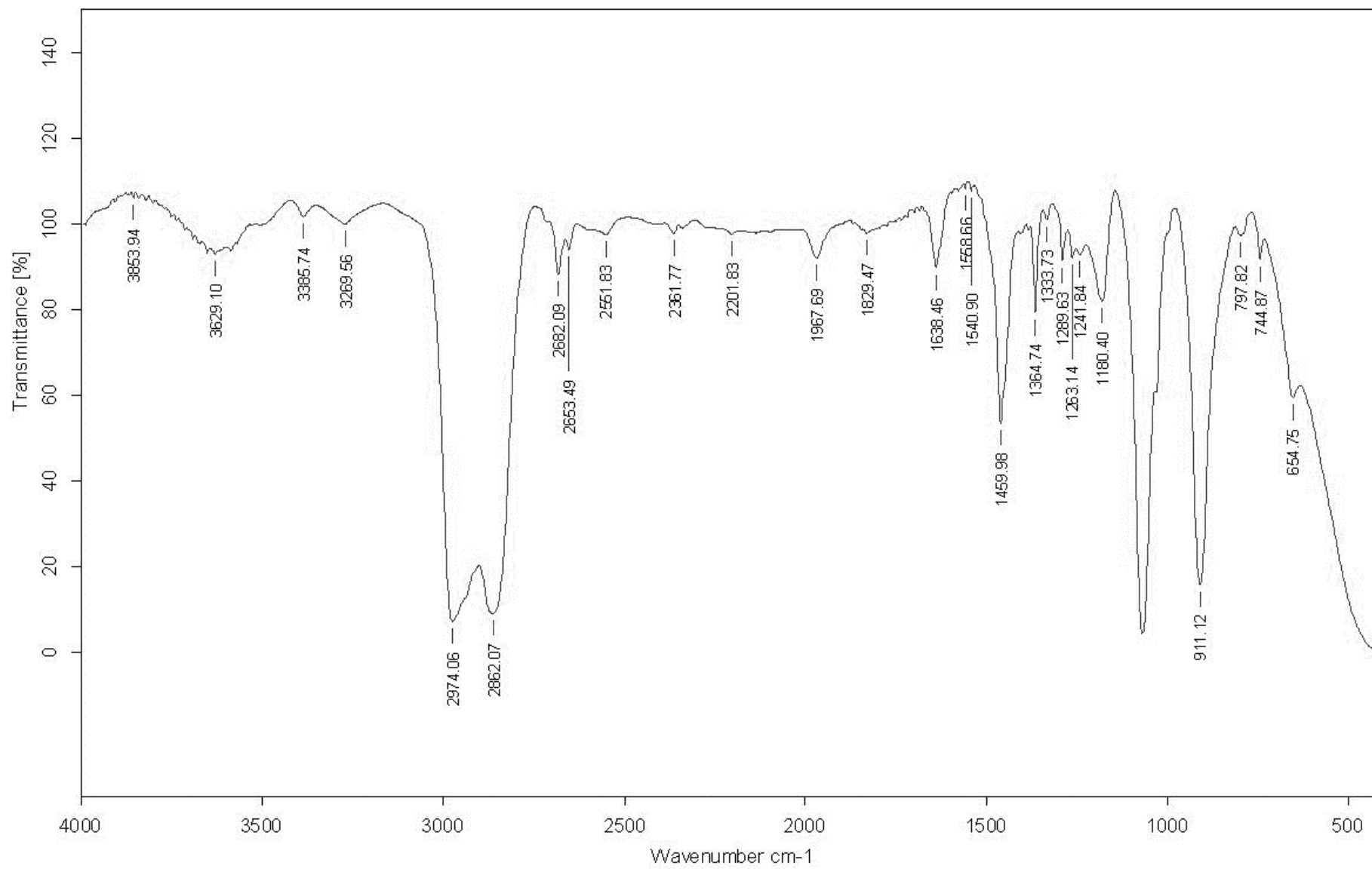
Figure 68. IR spectrum of the solution after concentration in NaCl support

59
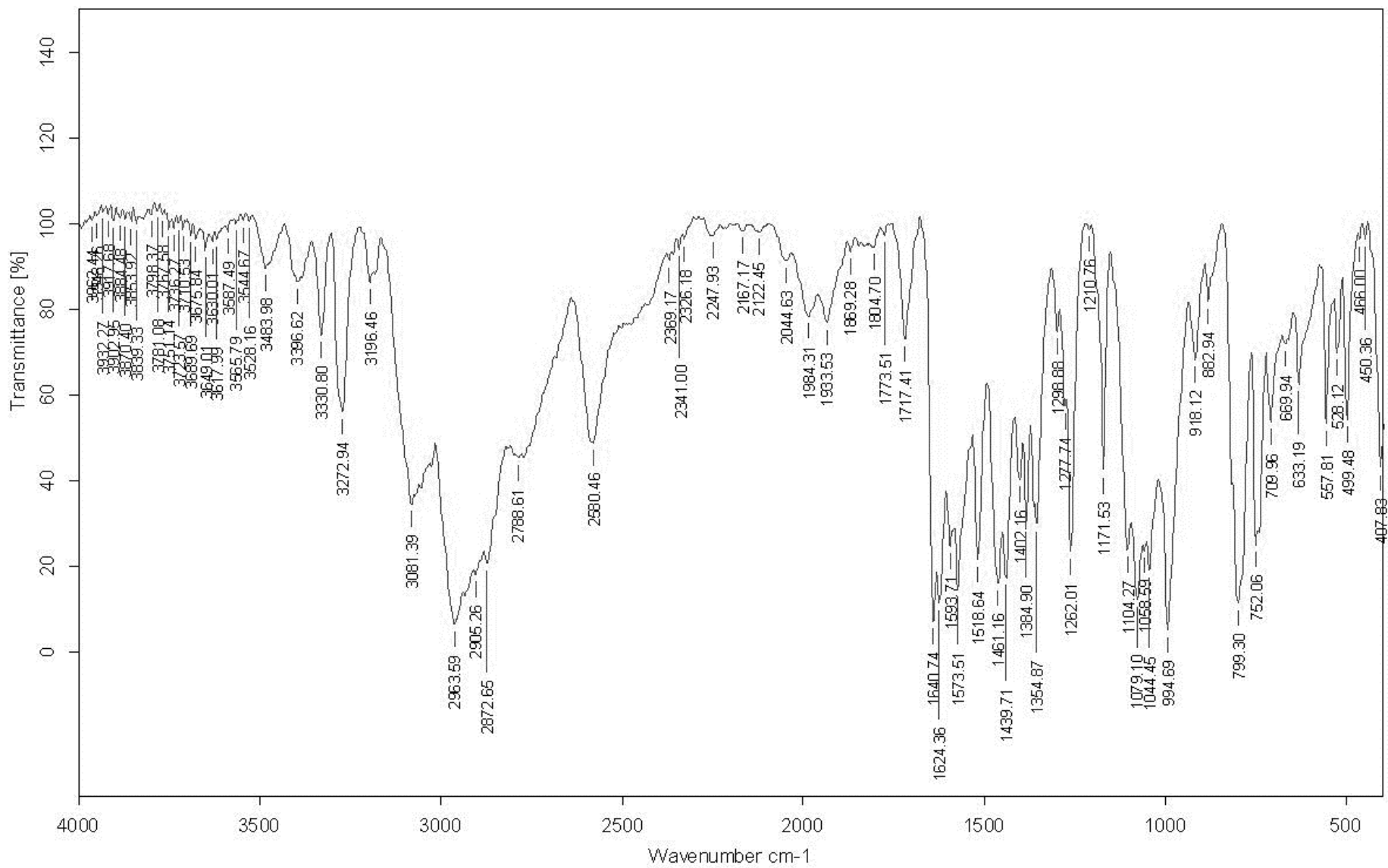
Figure 69. IR spectrum of final solution concentration in NaCl support

2.3.2. Reaction of 2,6-diisopropylphenyl-N-silyl magnesium amido

Carbon dioxide was bubbled through a crude solution of 2,6-diisopropylphenyl-N-silyl magnesium amido for 30 minutes at room temperature and 1 bar. There were no alterations of the solution.

The solvent was removed under reduced pressure. *n*-Hexane was added to the obtained residue and then the solution was filtered. Toluene was added to the previous residue and then it was filtered for the same schlenk. Solvents were removed under reduced pressure and the solid and the oil residue were dried under vacuum. The last was characterized by ^{1}H NMR (Fig.70), ^{13}C NMR (Fig.71) and by IR spectroscopy in KBr support (Fig.72).
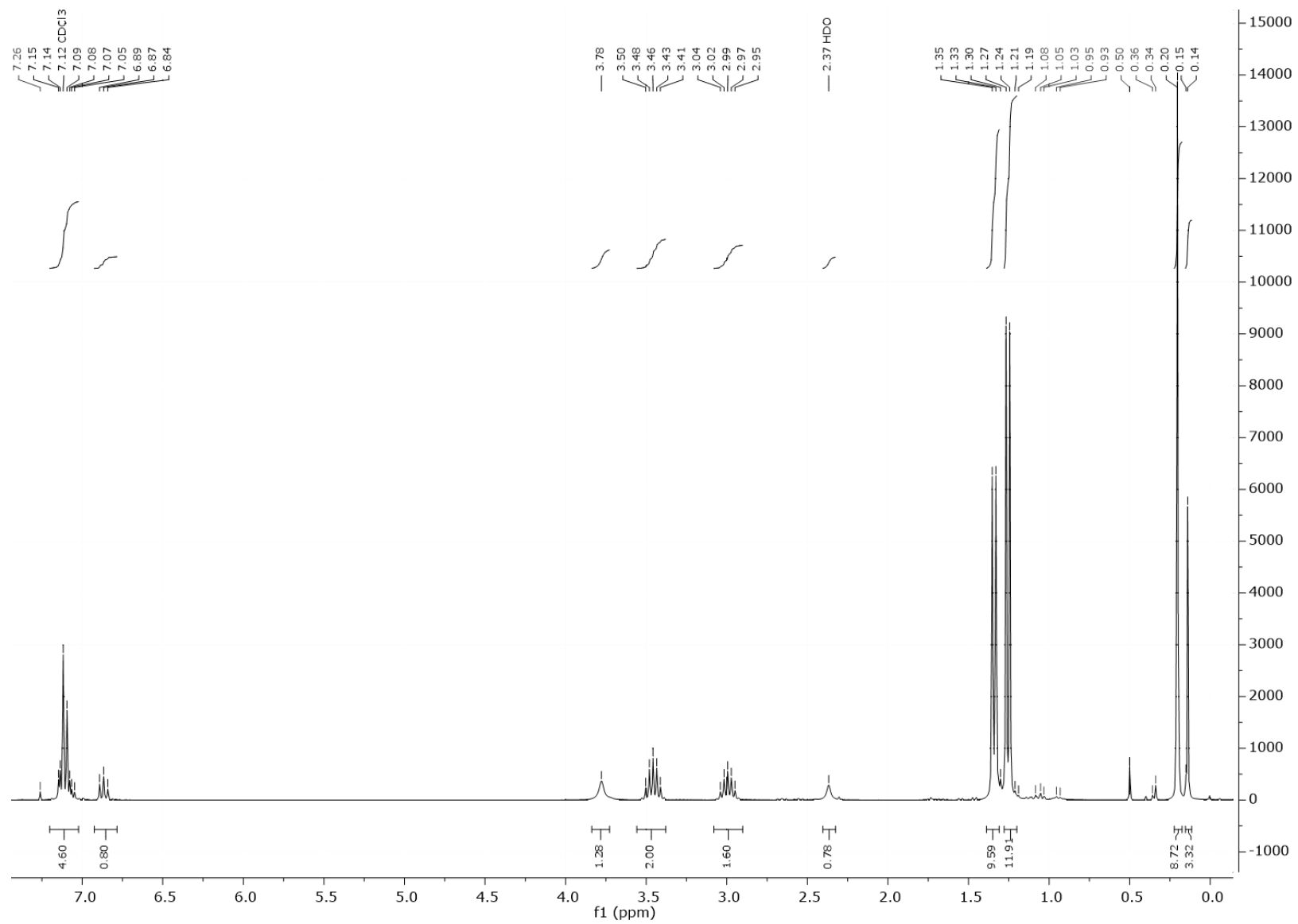
Figure 70. ^{1}H NMR spectrum of oil residue recorded in CDCl$_3$
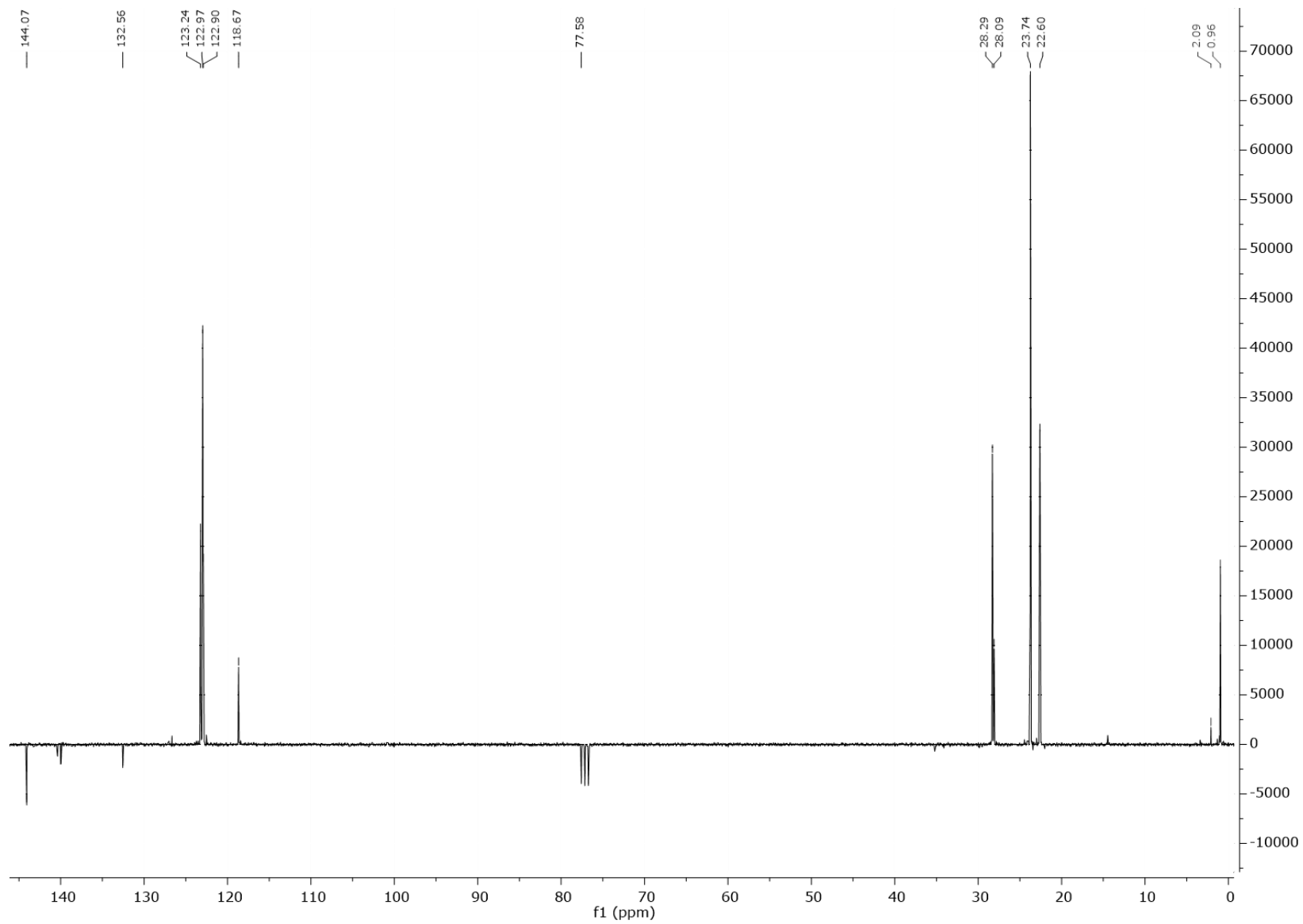
Figure 71. ^{13}C NMR spectrum of oil residue recorded in CDCl$_3$
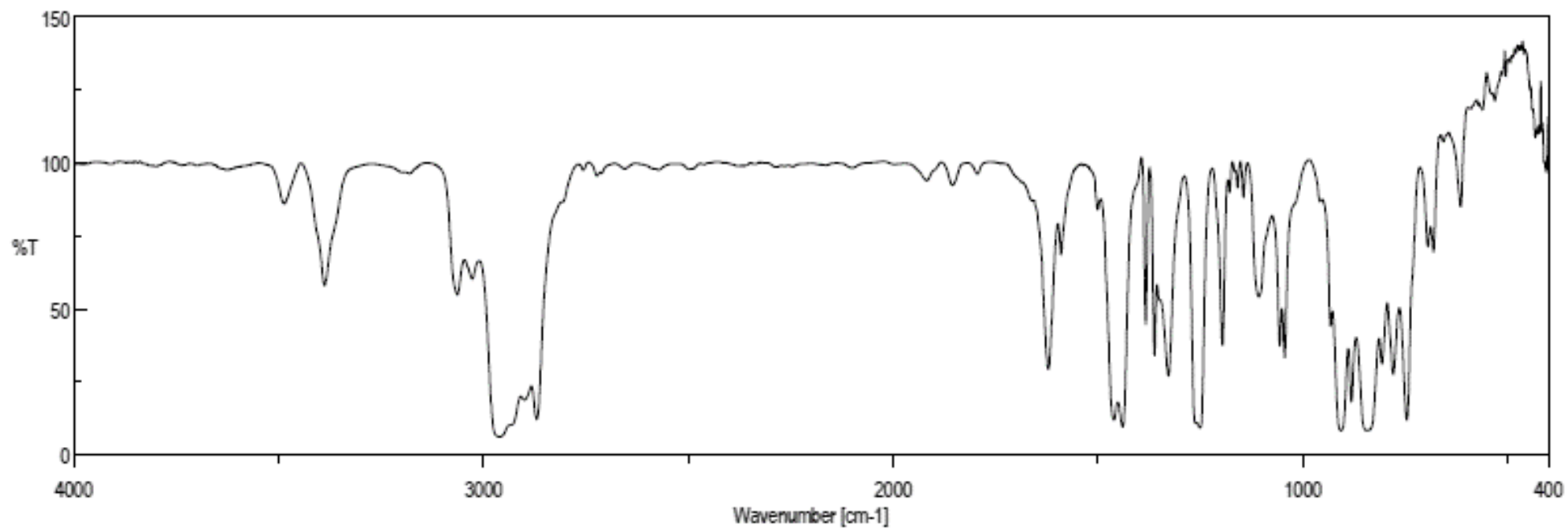
Figure 72. IR spectrum for CO$_2$ reaction in KBr support

2.3.3. Reaction of 2,6-dimethylphenyl-N-trimethylsilyl-magnesium amido

Carbon dioxide was bubbled through a crude solution of $Ph(CH_3)_2(TMS)N-Mg$ for 30 minutes at room temperature and 1 bar. The remaining solvent was removed under reduced pressure. In the next figure is possible to illustrate the ^1H NMR (Fig. 73) and ^{13}C NMR (Fig. 74) for the yielded product. The ^{13}C NMR spectrum is used to confirm the ^1H NMR spectrum. n-Hexane was added at -25°C. The solution was filtered and the obtained solid was dried under vacuum. The solvent of the remaining solution was removed under reduced pressure.
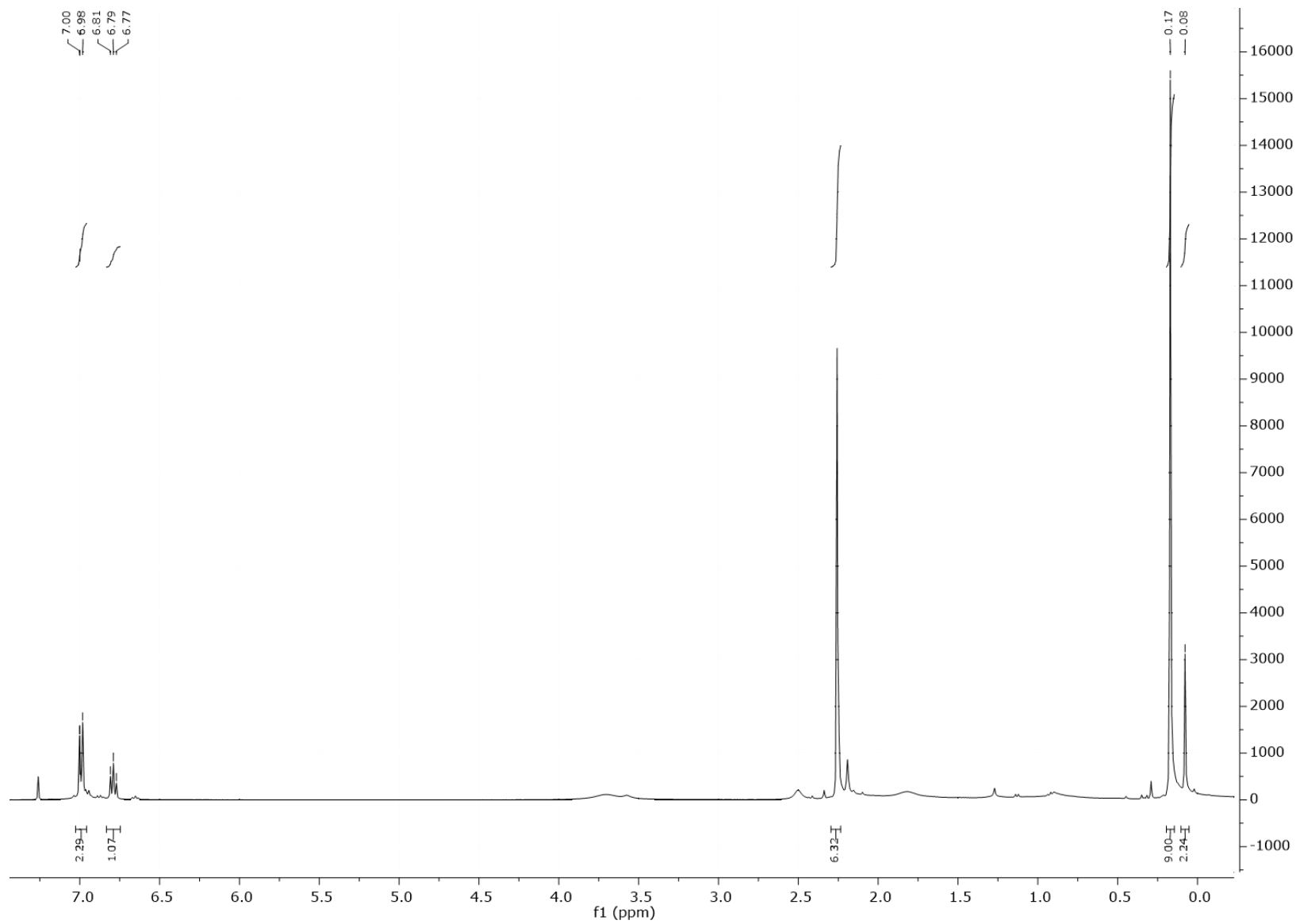
Figure 73. ^{1}H NMR spectrum for CO_2 reaction recorded in $CDCl_3$
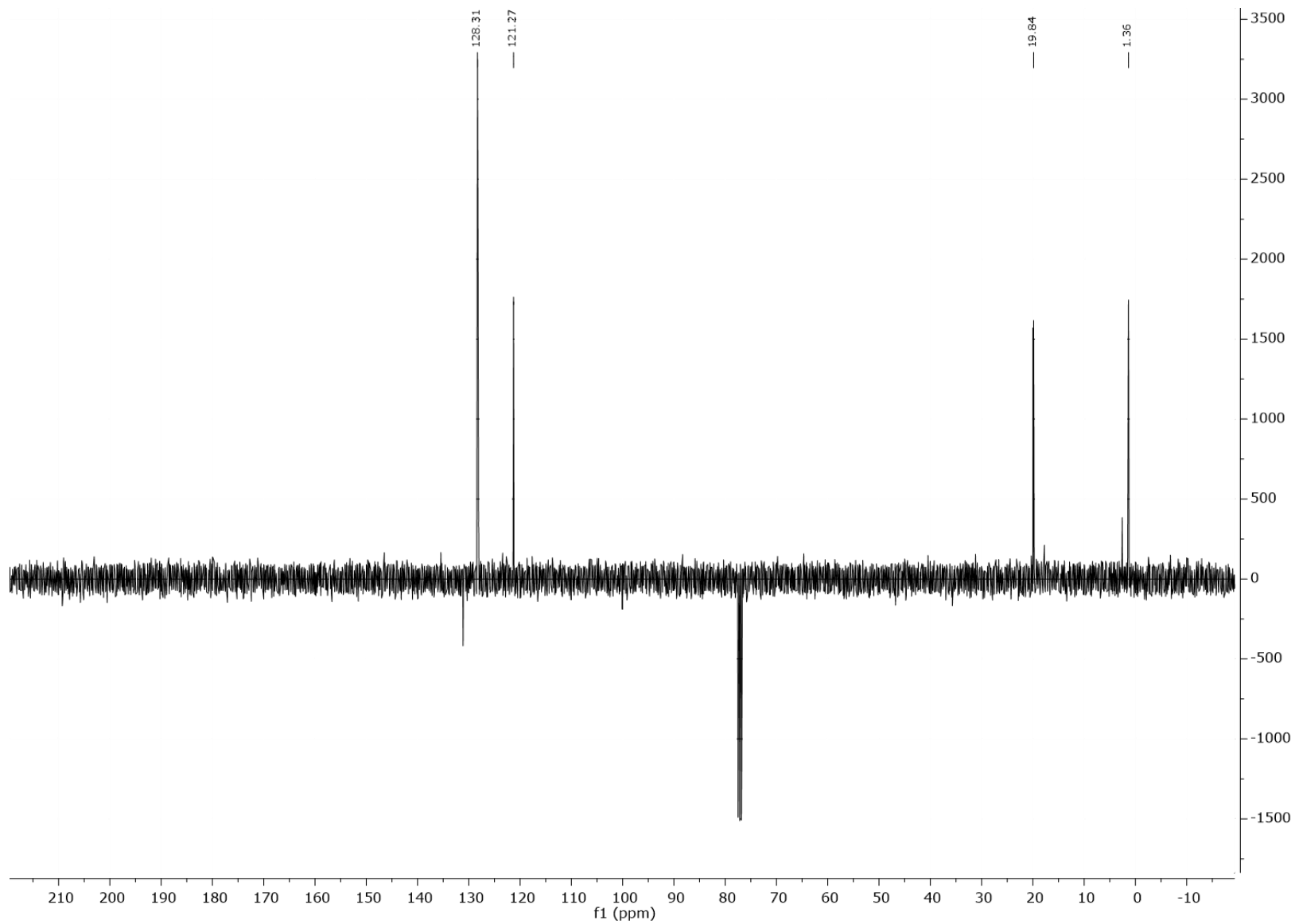
Figure 74. ^{13}C NMR spectrum for CO$_2$ reaction recorded in CDCl$_3$

2.3.4. Reaction of 2,6-dimethylphenyl-ciclopentadienyl-N-trimethylsilyl-magnesium amido

One equivalent of carbon dioxide was bubbled through a crude solution of $Cp^{bz}Mg(THF)NPh(CH_3)_2TMS$ at room temperature and 0.5 bar. The yielded solution had a yellow color. The next figure illustrates the ^{1}H NMR spectrum for the reaction of a solution of $Cp^{bz}Mg(THF)NPh(CH_3)_2TMS$ with carbon dioxide. Figure 76 illustrates the ^{13}C NMR spectrum of the yielded mixture.
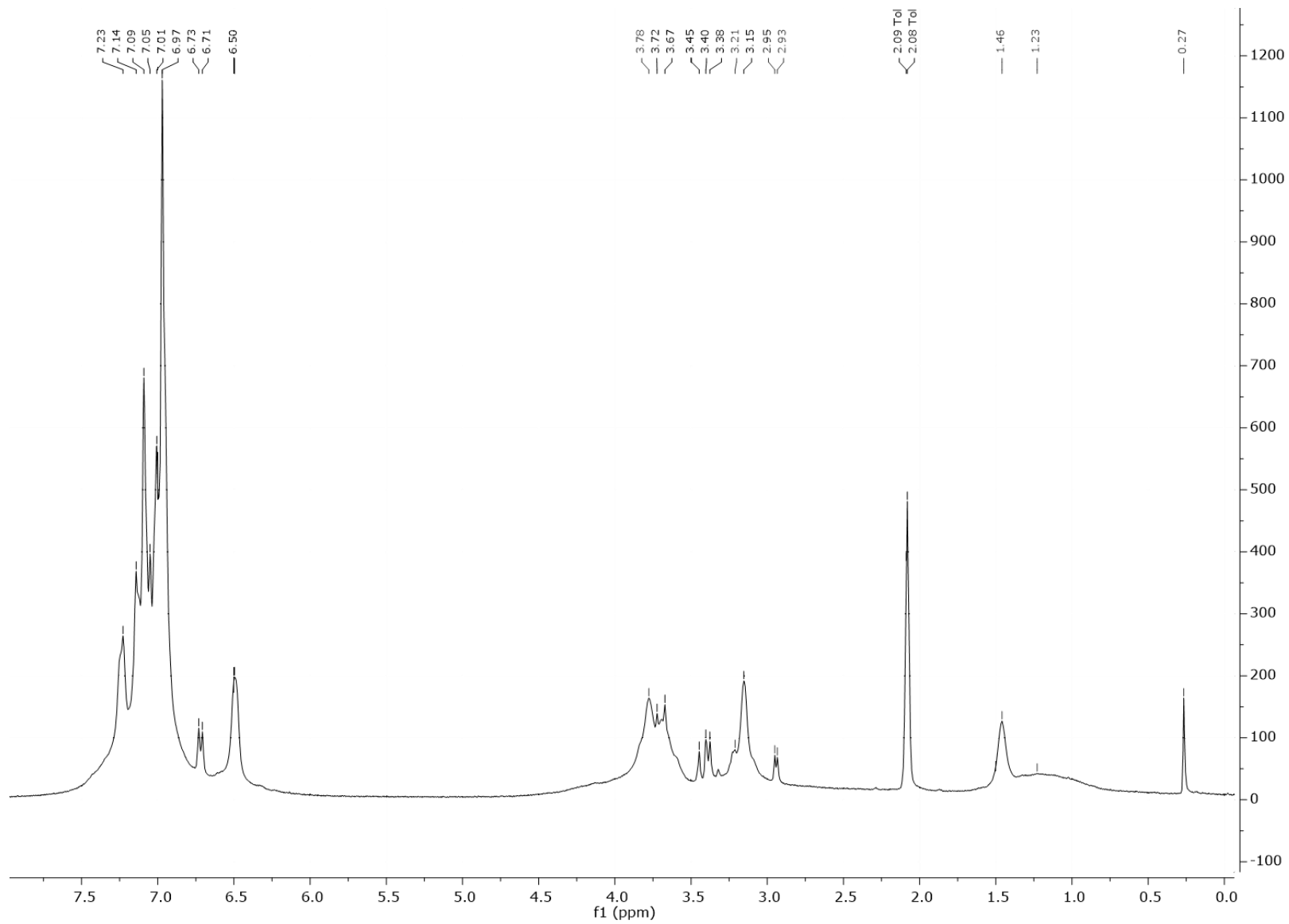
Figure 75. ^{1}H NMR spectrum for CO_2 reaction recorded in deuterated benzene
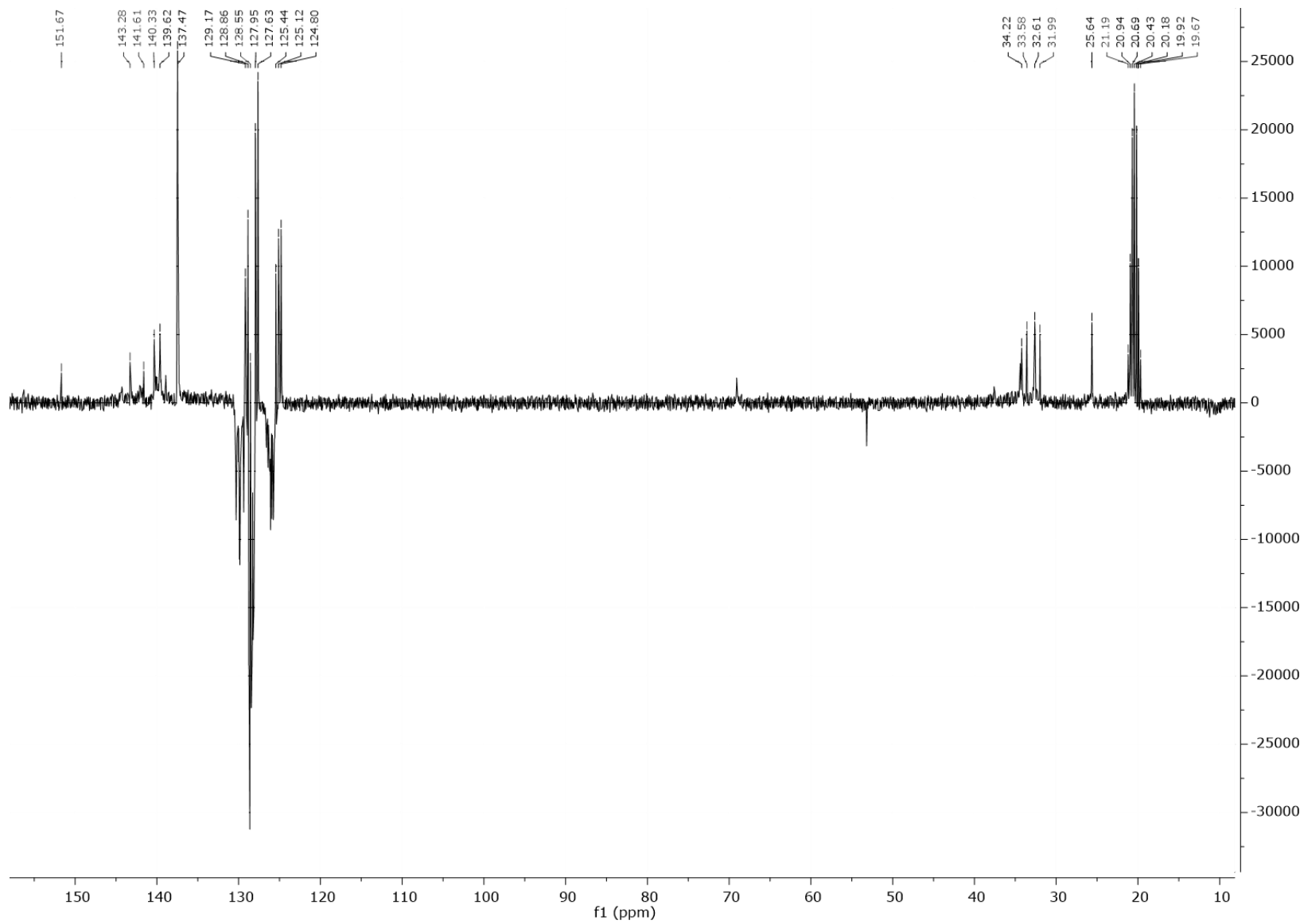
Figure 76. ^{13}C NMR spectrum for CO$_2$ reaction recorded in deuterated benzene

2.3.5. Reaction of 2,6-dimethylphenyl-trimethylsilyl-bromomagnesium amido

Carbon dioxide was bubbled through a crude solution of $(THF)_2.MgBrNPh(CH_3)_2TMS$ for 5 minutes at room temperature and 0.5 bar. In the next figure is possible to see ^1H NMR spectrum of the reaction product. Figure 78 illustrates the ^{13}C NMR spectrum for the product reaction. The solvent was removed under reduced pressure. The remaining mixture was dried under vacuum and a IR spectrum analysis was made (Fig.79).
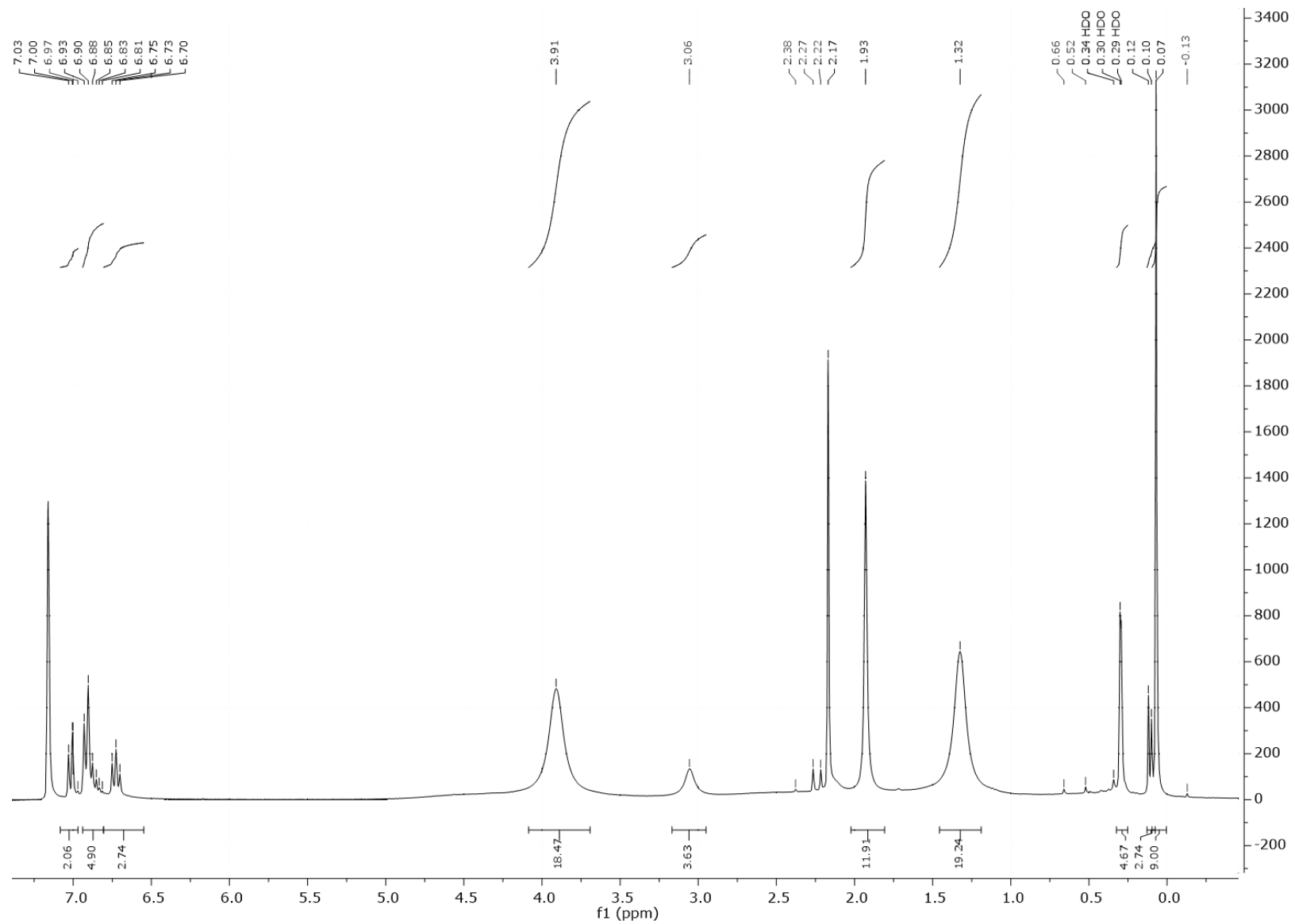
Figure 77. ^{1}H NMR spectrum for CO_2 reaction recorded in tol-d$_8$
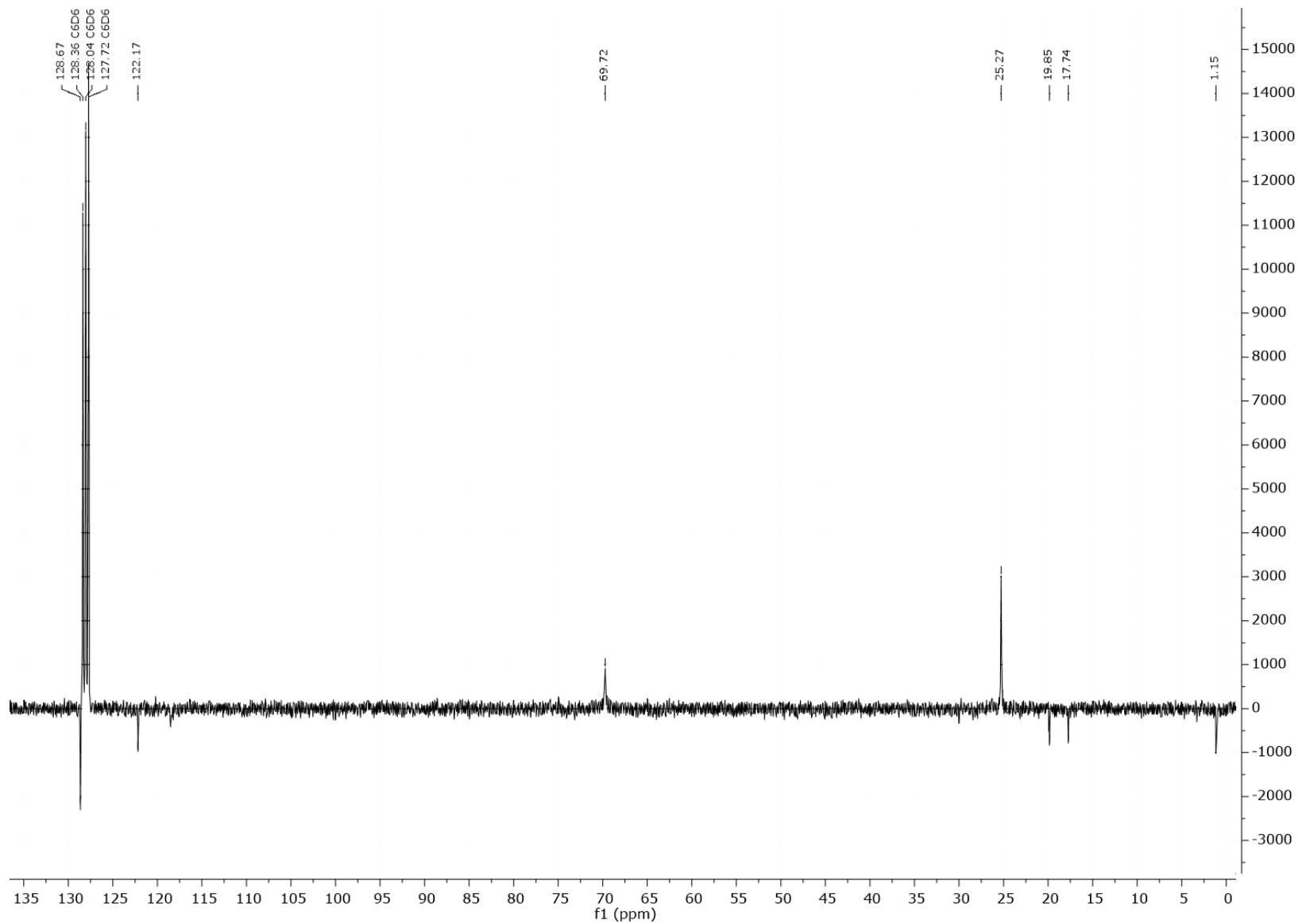
Figure 78. ^{13}C NMR spectrum for CO_2 reaction recorded in tol-d_8
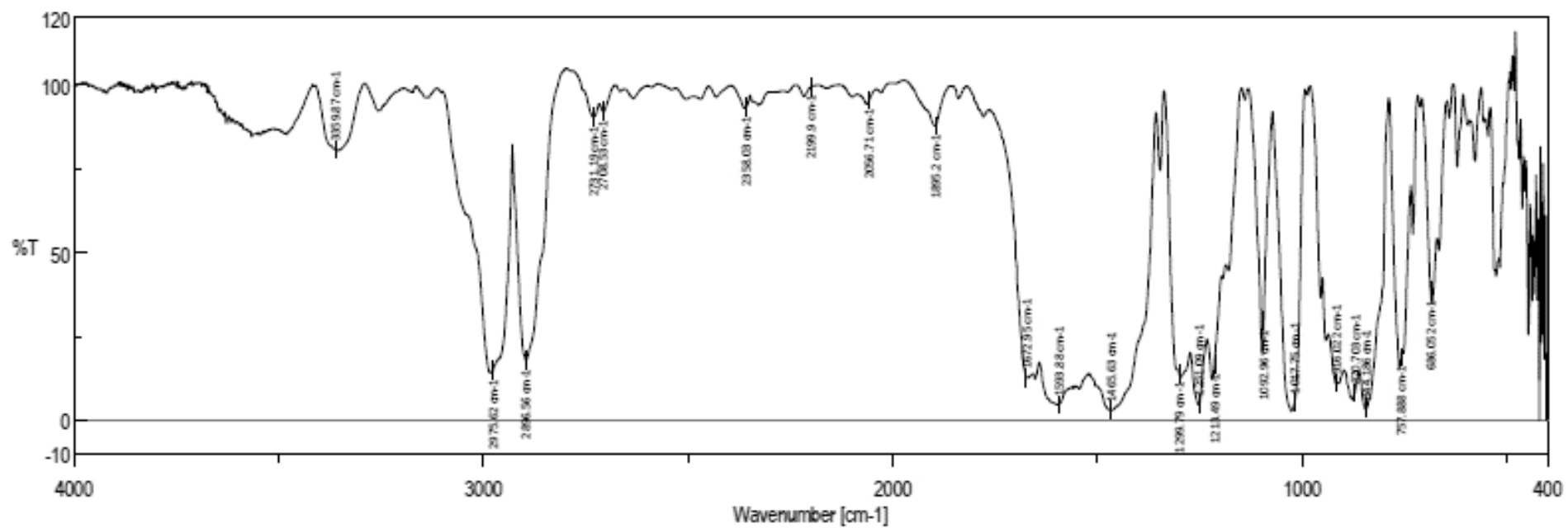
Figure 79. IR spectrum for the solid fraction in KBr support

2.3.6. Reaction of 2,6-dimethylphenyl-N-trimethylsilyl-bromomagnesium amido

Carbon dioxide was pressurized through a crude solution of $(THF)_2.MgBrNPh(CH_3)_2TMS$ for 40 minutes at room temperature and 0.5 bar. The ^1H NMR spectrum for the yielded solution is presented forward. Figure 81 illustrates the ^{13}C NMR spectrum for the yielded product. The solvent was removed under reduced pressure. The remaining solid was dried under vacuum and washed with *n*-hexane. The obtained suspension was filtered and the remaining solid was dried under vacuum. An IR spectroscopic (Fig. 82) and an elemental analysis (table 5) were made.
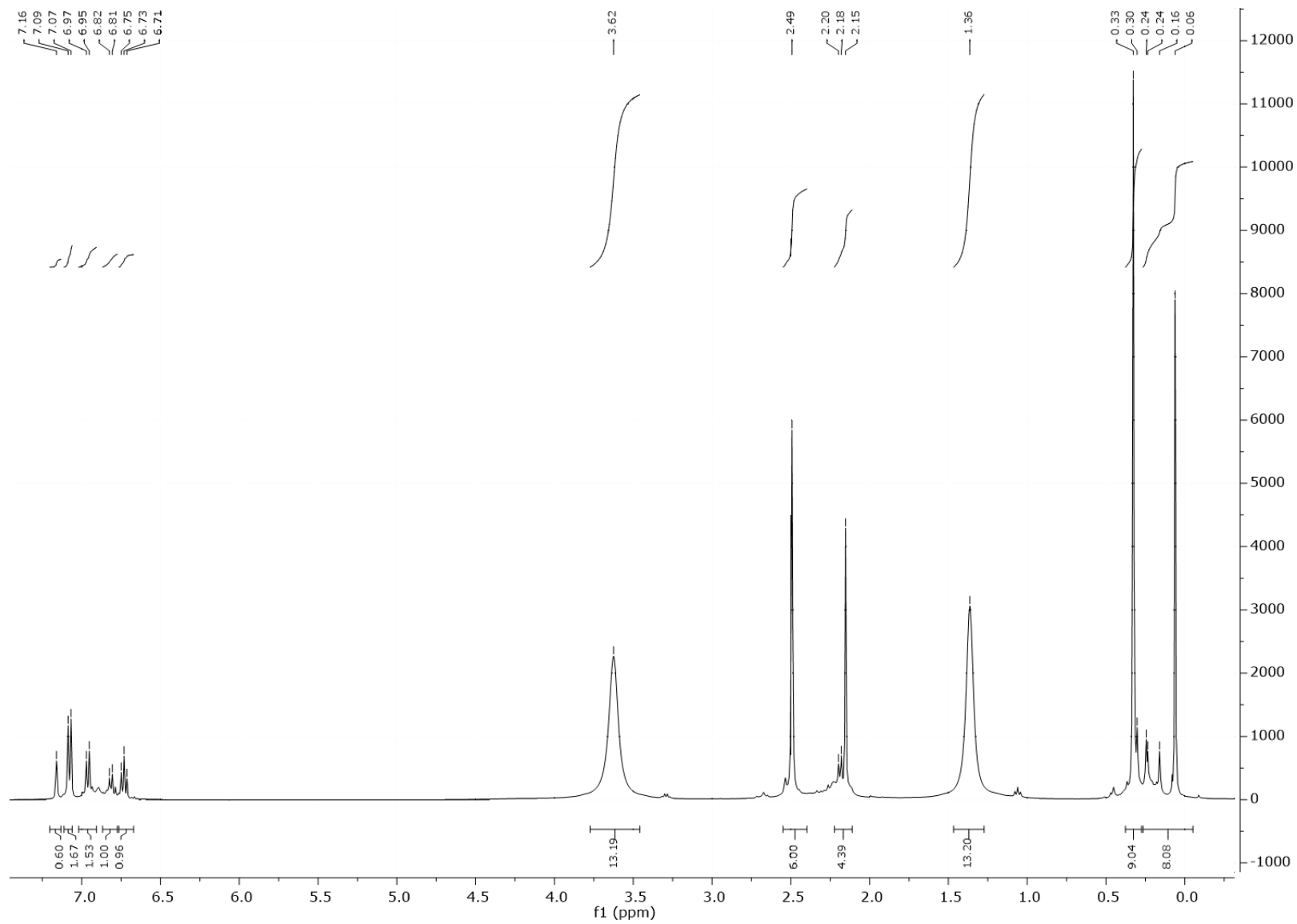
Figure 80. ^{1}H NMR spectrum for CO_2 reaction recorded in C_6D_6
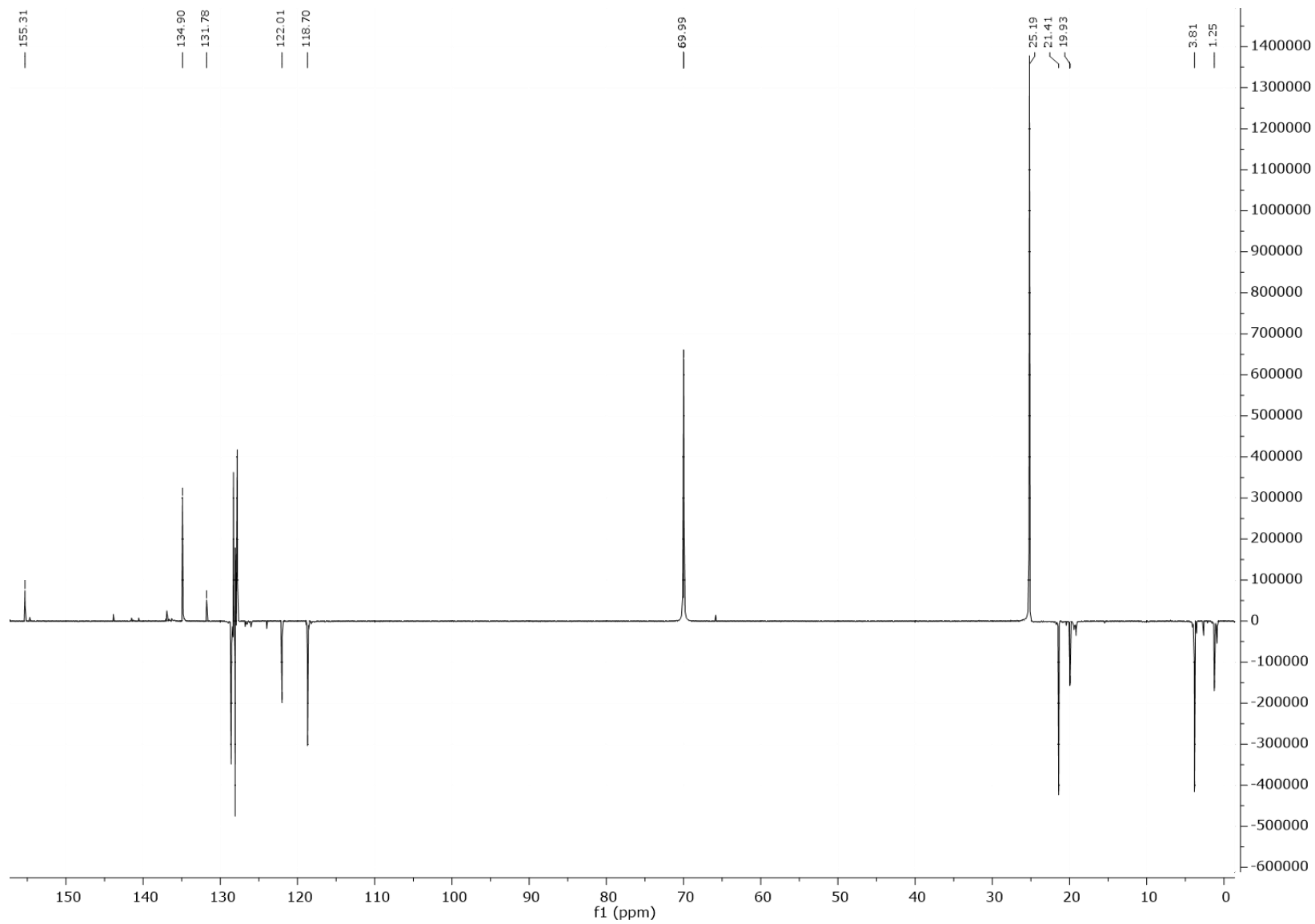
Figure 81. ^{13}C NMR spectrum for CO_2 reaction recorded in C_6D_6
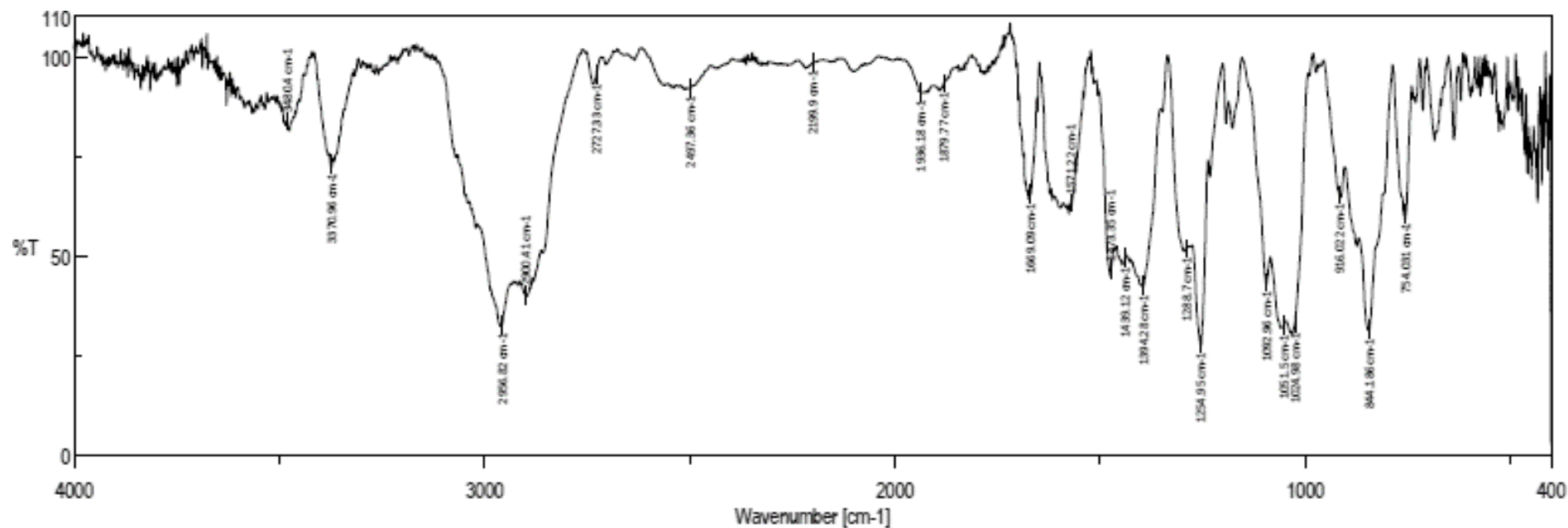
Figure 82. IR spectrum for the solid fraction

Table 5. Results for the elemental analysis

Element	Result (%)
Nitrogen	2.43 – 2.49
Carbon	31.12 – 33.09
Hydrogen	5.00 – 5.04

2.4. Reactions with dry CO_2

2.4.1. Experimental conditions

In order to avoid the hydrolysis reaction, a column filled with a gas dryer agent and molecular sieves was added to the experimental installation. The characteristics of the gas dryer agent and molecular sives used are summarized in tables 6 and 7.

Table 6. Sicapent® Characteristics
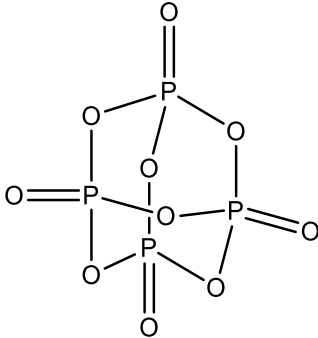
Compound	Sicapent®
Ref.	54
Molecular Formula	P_2O_5
Molecular Structure	
Molecular Weight (g/mol)	141.94

Table 7. Molecular Sieves Characteristics

Compound	Molecular Sieves
Ref.	55
Type	4A
Porous Diameter (Argstrom)	4
Bulk Density (lb/ft^3)	45
% Moisture	1.5
Eq'm H2O capacity (theory)	23
pH (5% slurry)	10.5
Regeneration Temperature (ºC)	200-315
Maximum ΔH_{ads} (BTU/lb H_2O)	1800

In the next figure, it is possible to see the experimental installation that was used (Fig. 83):
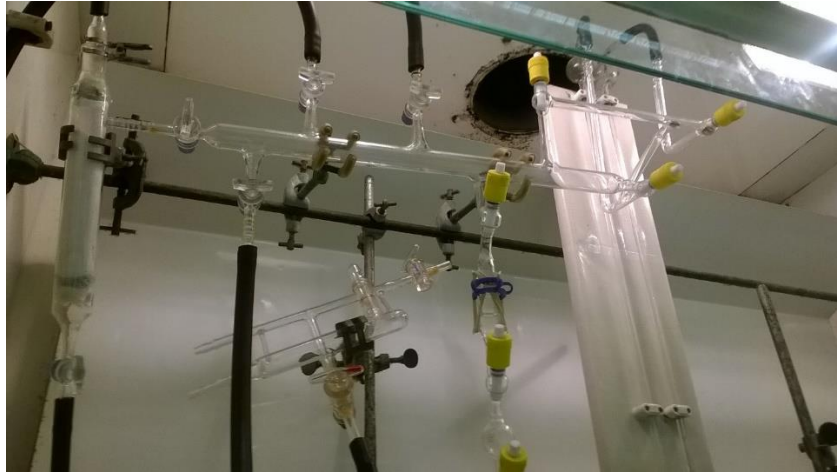
Figure 83. Experimental set-up

2.4.1. Reaction of 2,6-dimethylphenyl-N-trimethylsilyl-bromomagnesium amido in a NMR tube

In a NMR tube, one equivalent of CO_2 was pressurized to a solution of $(THF)_2.MgBrPh(CH_3)_2NTMS$, in deuterated toluene, for some minutes. The tube was frozen in a liquid nitrogen bath and allowed to warm at room temperature. No changes were observed. The yielded solution was characterized by ^{1}H NMR (fig.84). After this characterization, the NMR tube was heated at 50ºC overnight. A white powder was obtained and the solution was characterized by ^{1}H NMR (fig.85). The NMR tube was heated at 50ºC one more day. Afterwards the solution was characterized by [1]H (fig.86) and ^{13}C NMR (fig.87).
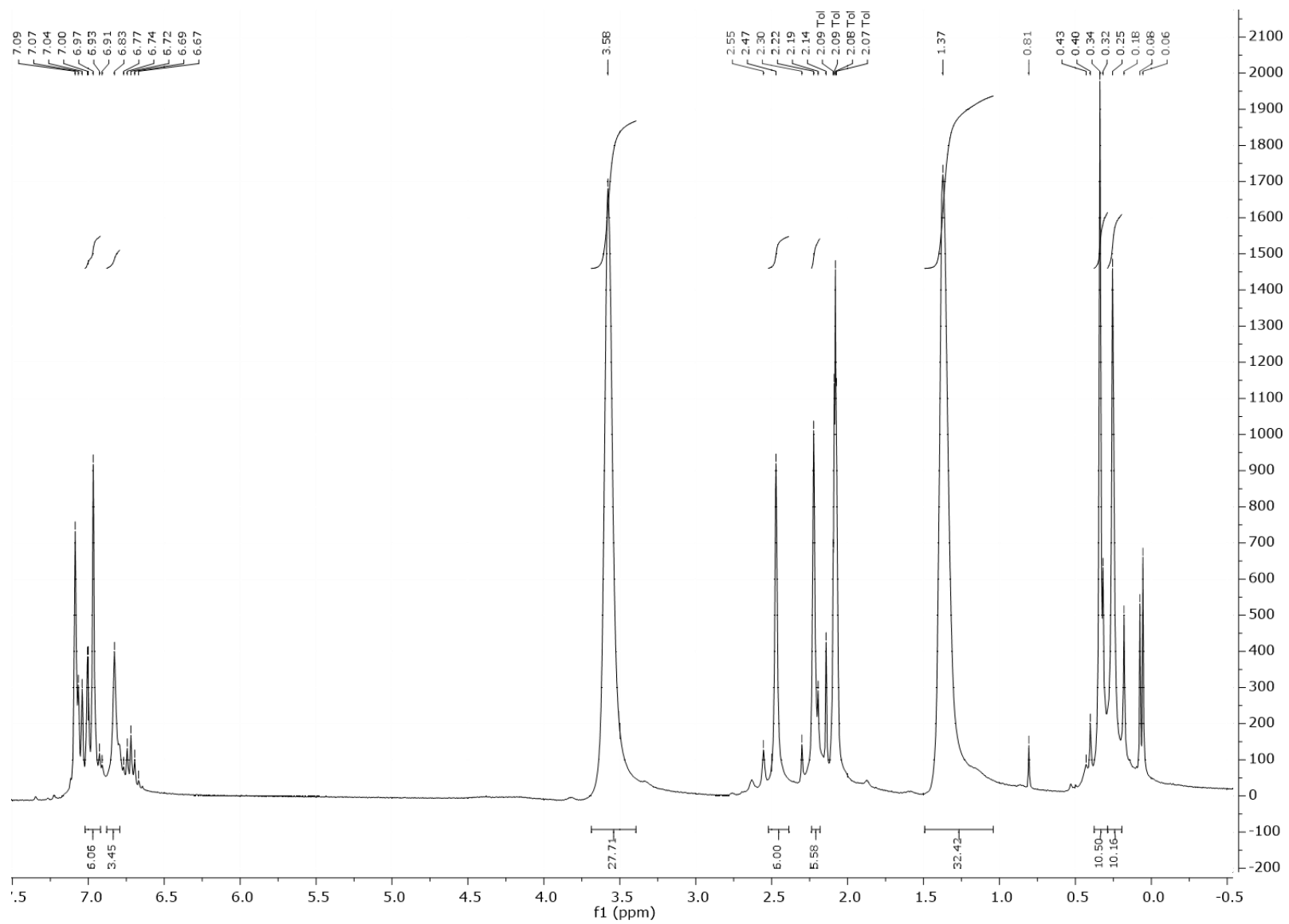
Figure 84. ^1H NMR spectrum for CO_2 reaction recorded in tol-d_8
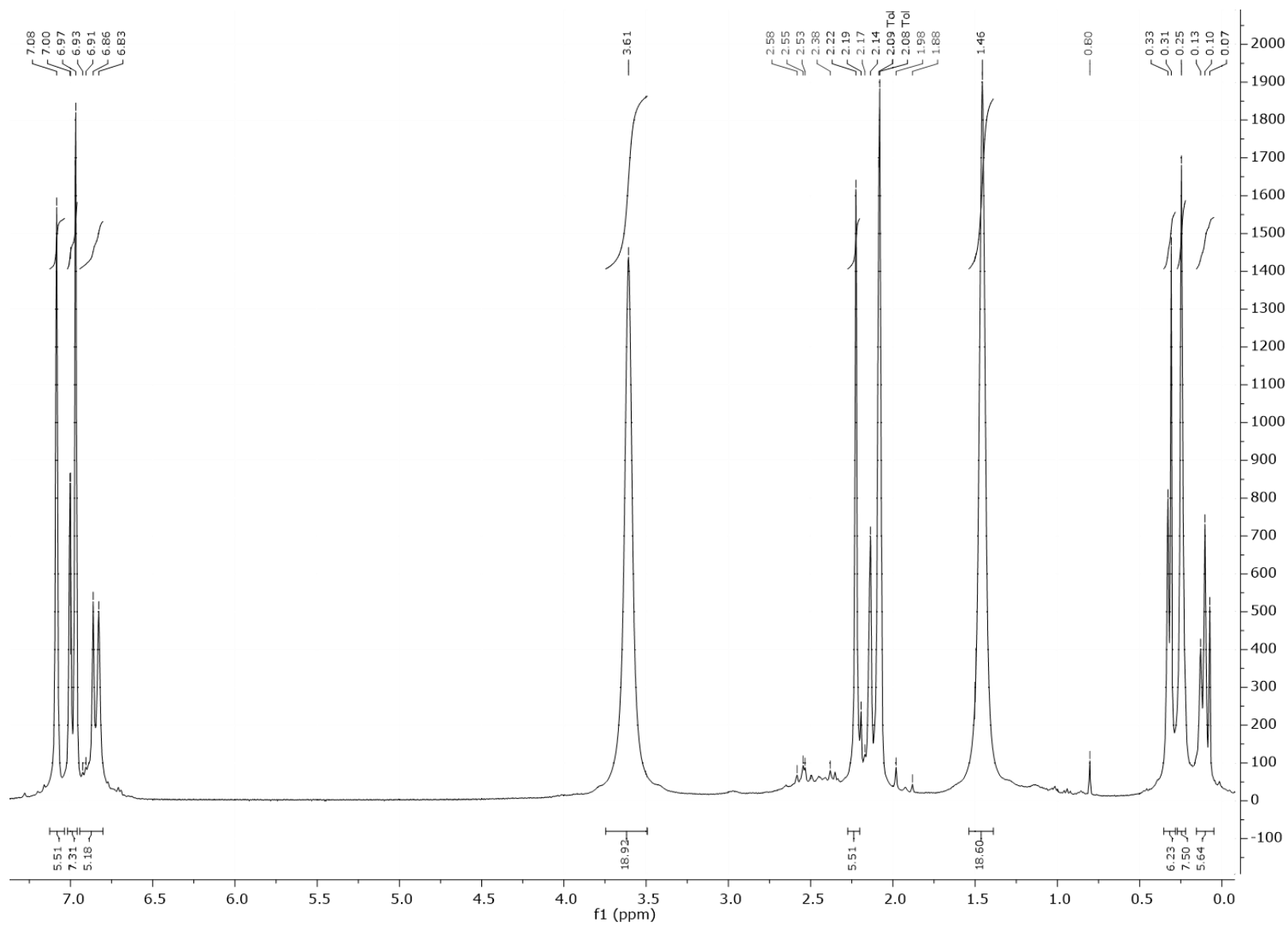
Figure 85. ^1H NMR spectrum for CO_2 reaction recorded in tol-d_8 after overnight heating at 50ºC
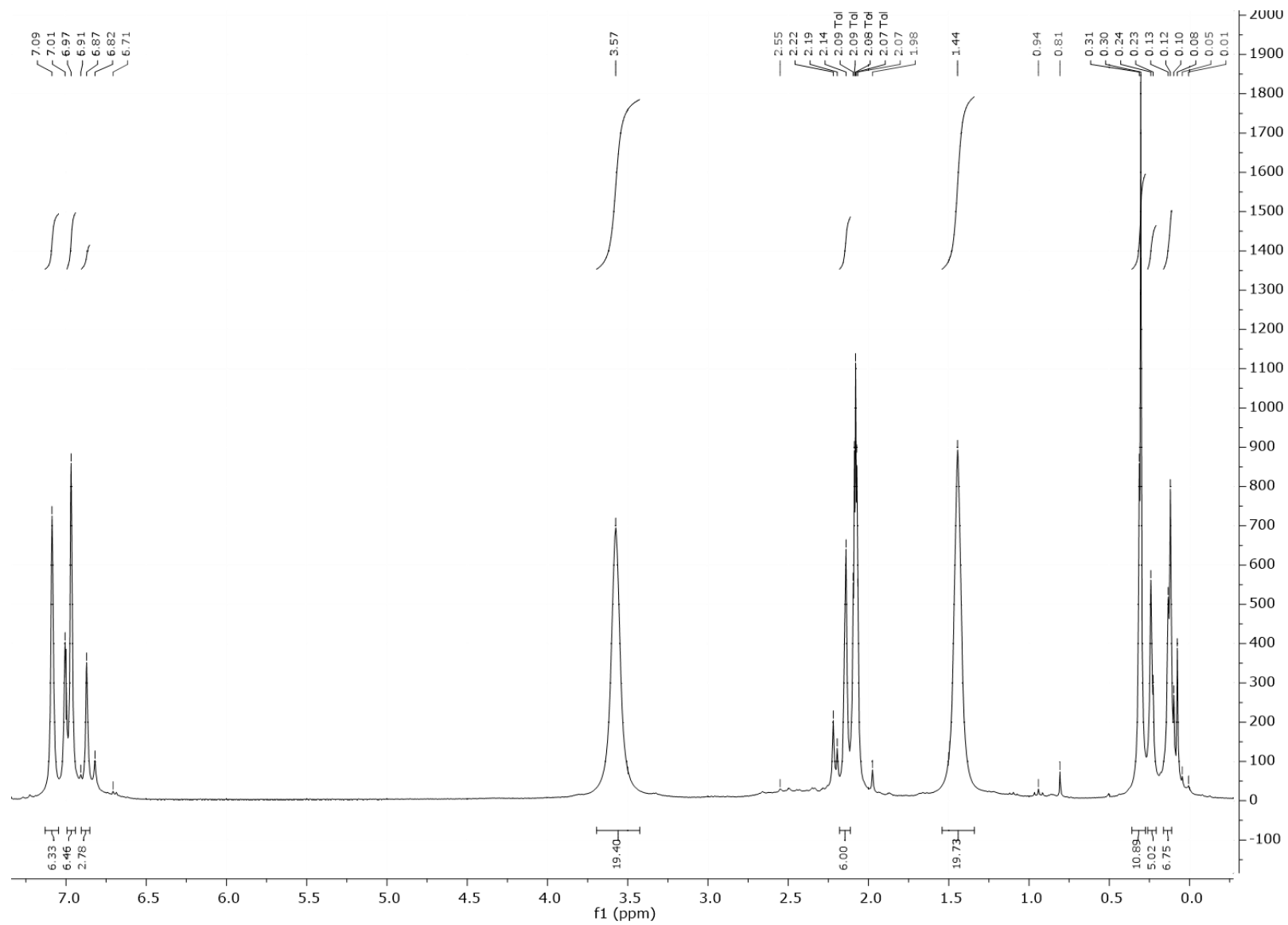
Figure 86. ^1H NMR spectrum for CO_2 reaction recorded in tol-d_8 after two days heating at 50°C
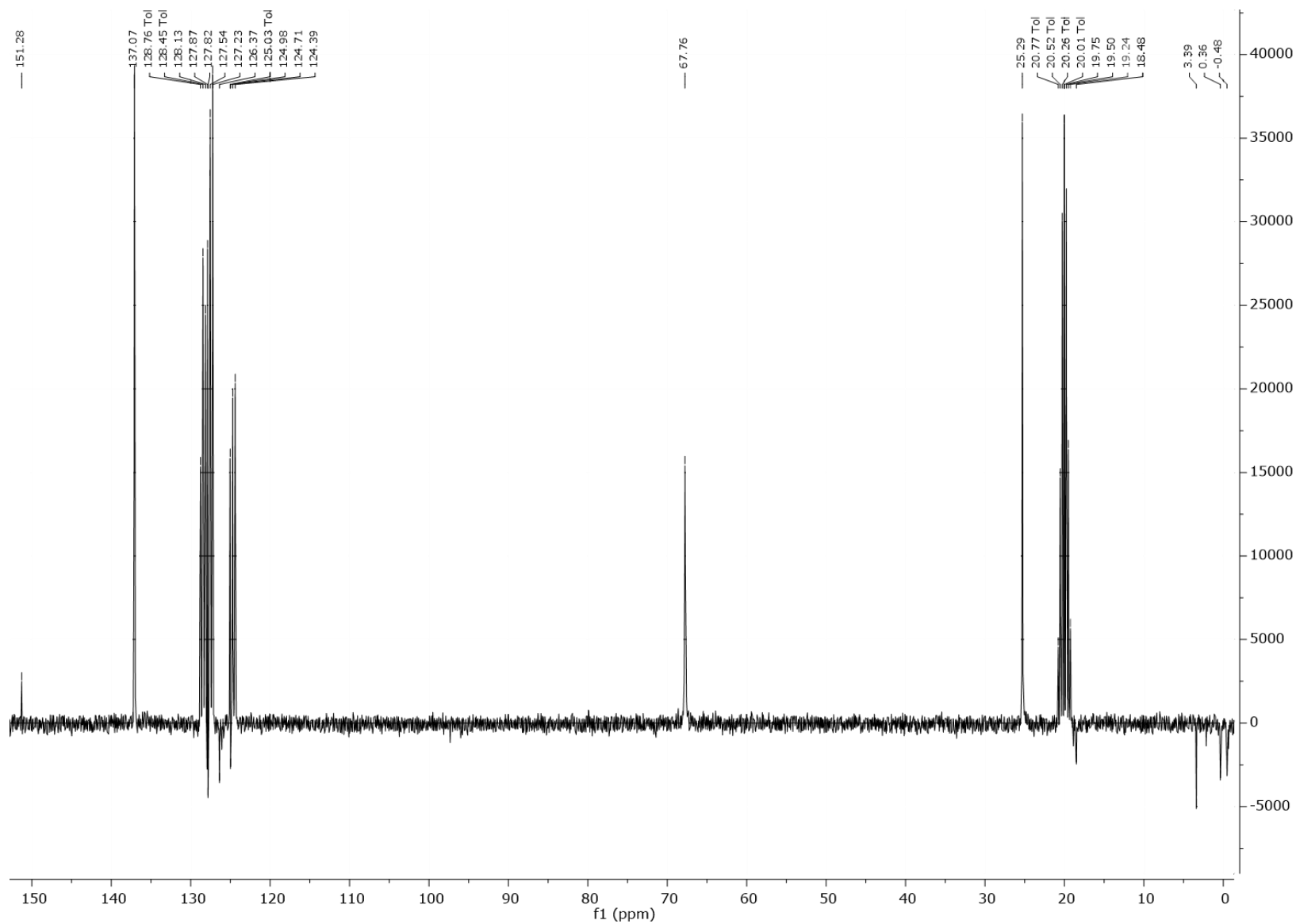
Figure 87. ^{13}C NMR spectrum for CO$_2$ reaction recorded in tol-d$_8$ after two days heating at 50ºC

2.3.2. Reaction of 2,6-dimethylphenyl-N-trimethylsilyl-bromomagnesium amido in a shlenck

In a shlenck, one equivalent of CO_2 was pressurized to a solution of $(THF)_2.MgBrPh(CH_3)_2N$-TMS (1.82 mmol, 0.54 g), in toluene, for some minutes. The shlenck was frozen in a liquid nitrogen bath and allowed to warm at room temperature. Next, the solution was heated at 50ºC, for two days, yielding a white suspension. The suspension was filtered and the solid was dried under vacuum. The solvent from the solution was removed under vacuum yielding a white solid residue. This solid was characterized by IR spectrum, ^{1}H NMR (Fig. 89) and elemental analysis (table 8).

In the next figure is presented the IR spectrum for the yielded solid.
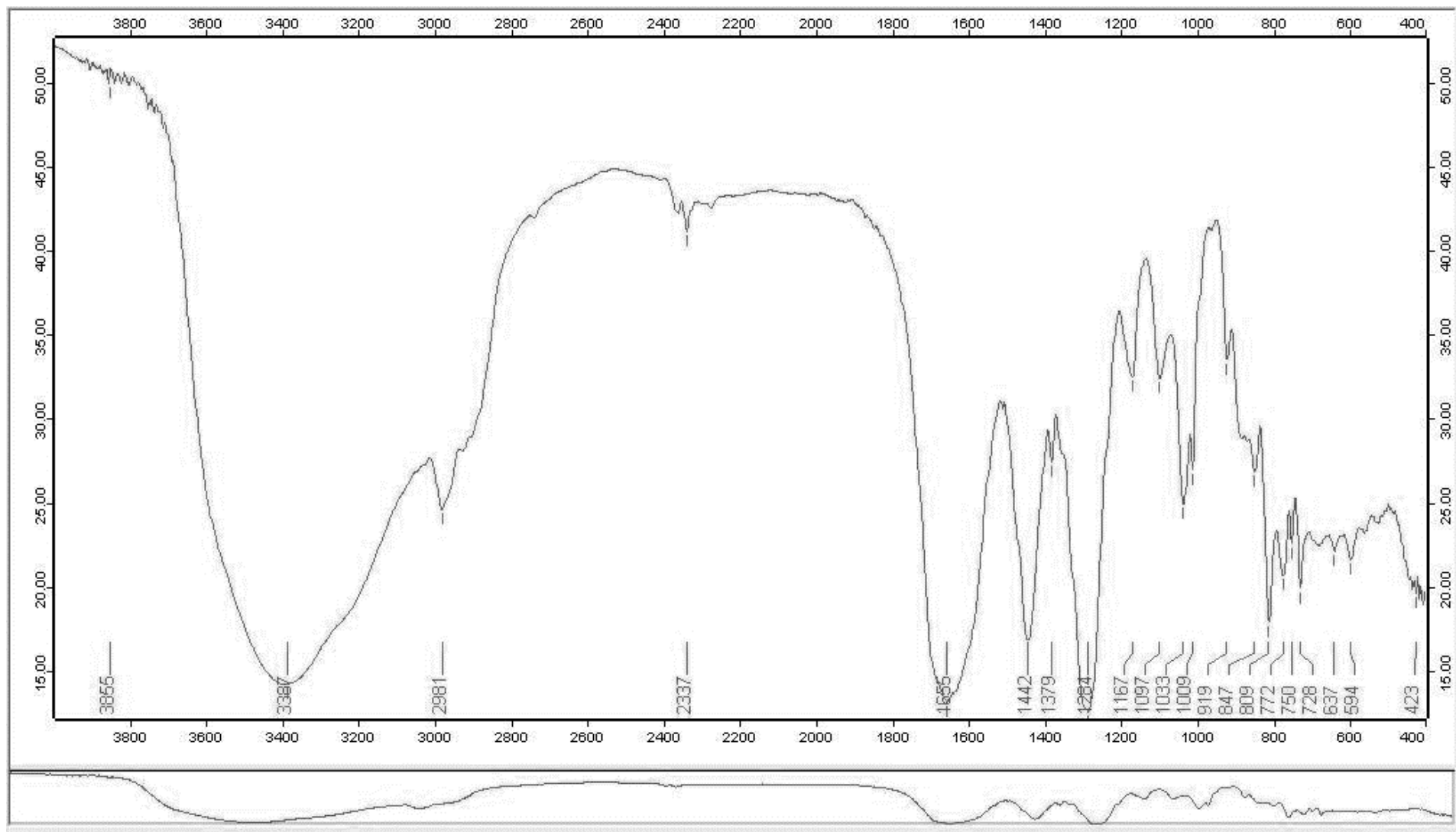
Figure 88. IR spectrum for the yielded solid in KBr support

The results for the elemental analysis are:

Table 8. Results for the elemental analysis

Element	Results (%)
Nitrogen	2.18 – 2.36
Carbon	25.83 – 32.98
Hydrogen	4.03 – 4.58

In figure 89 can be seen the ^{1}H NMR for the white solid recorded in CD_2Cl_2. It was tried to recrystallize the obtained solid by dissolving it in dichloromethane and put it the freezer, but no crystals were observed.
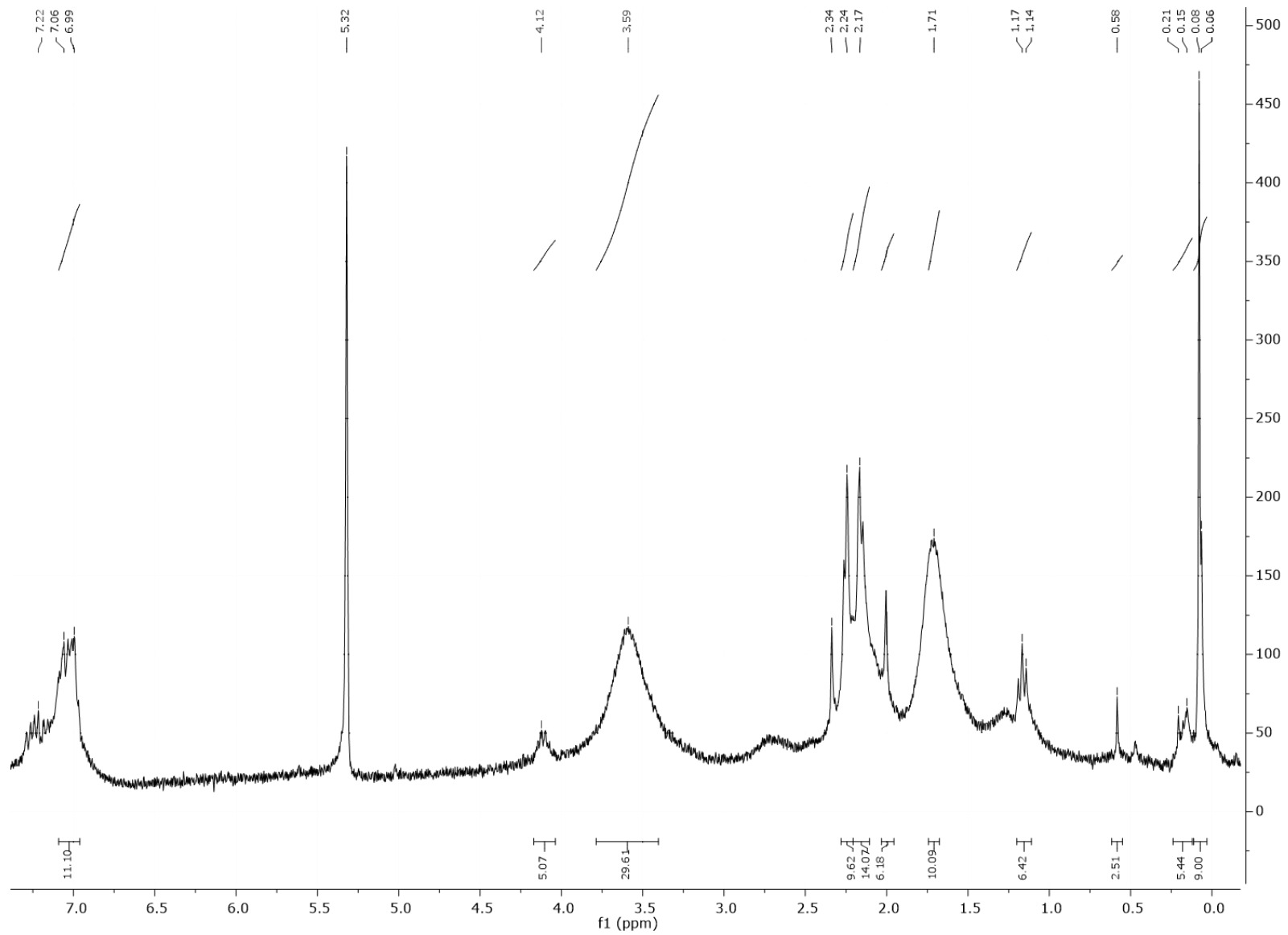
Figure 89. ¹H NMR for the yielded solid recorded in CD₂Cl₂

2.3.3. Reaction of 2,6-dimethylphenyl-N-trimethylsilyl-magnesium ketimide in a NMR tube

In a NMR tube, one equivalent of CO_2 was pressurized to a solution of ${}^tBu_2C=N-Mg-N-Ph(CH_3)_2TMS$, in deuterated toluene, for some minutes. The tube was frozen in a liquid nitrogen bath and allowed to warm at room temperature. No changes are seen. After that, the NMR tube was heated at 50ºC overnight. The yielded solution was characterized by ${}^1H$ NMR (fig. 90) and ${}^{13}C$ NMR (fig.91).
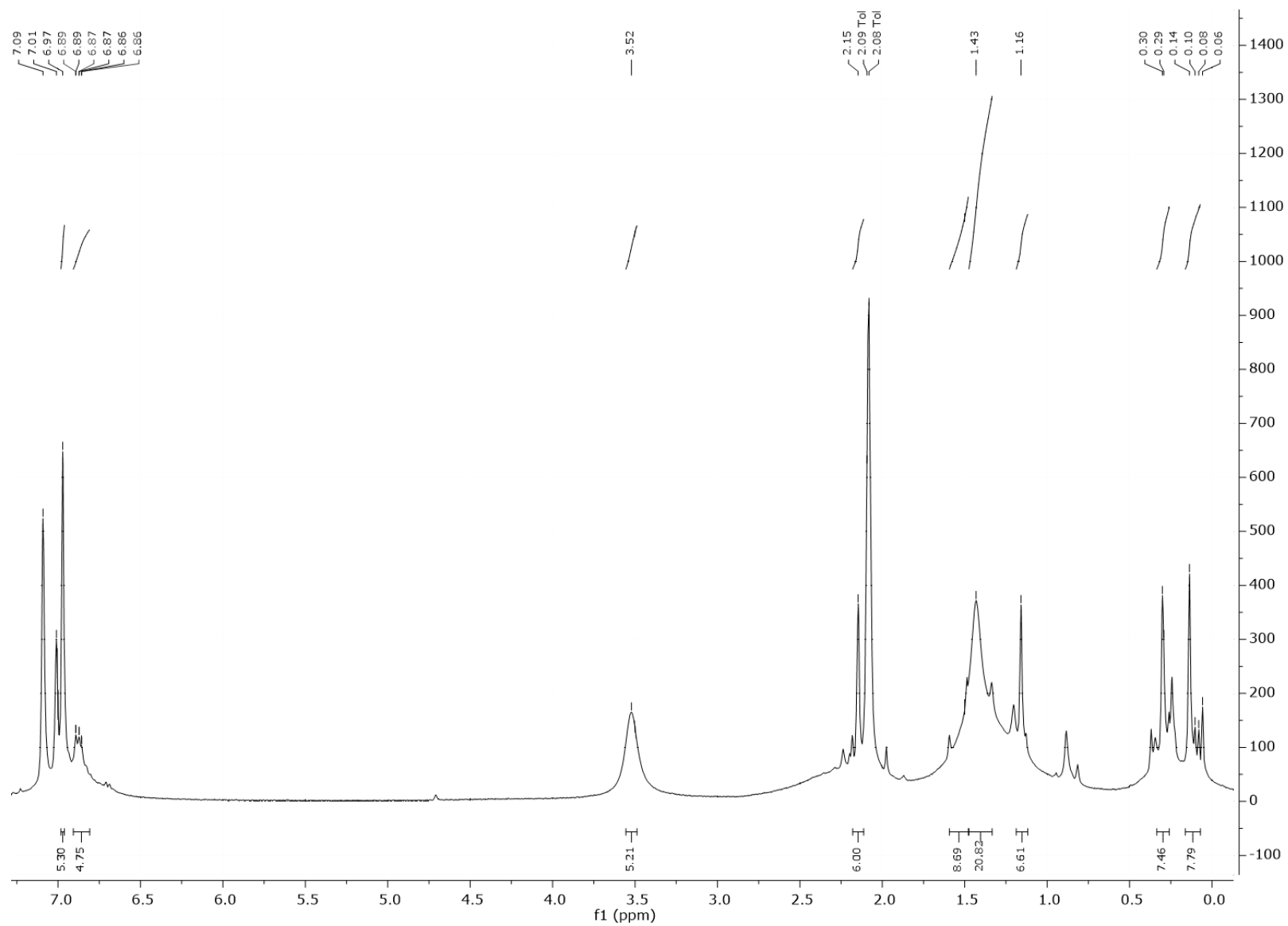
Figure 90. ^{1}H NMR spectrum for CO_2 reaction recorded in tol-d_8 after two days heating at 50°C
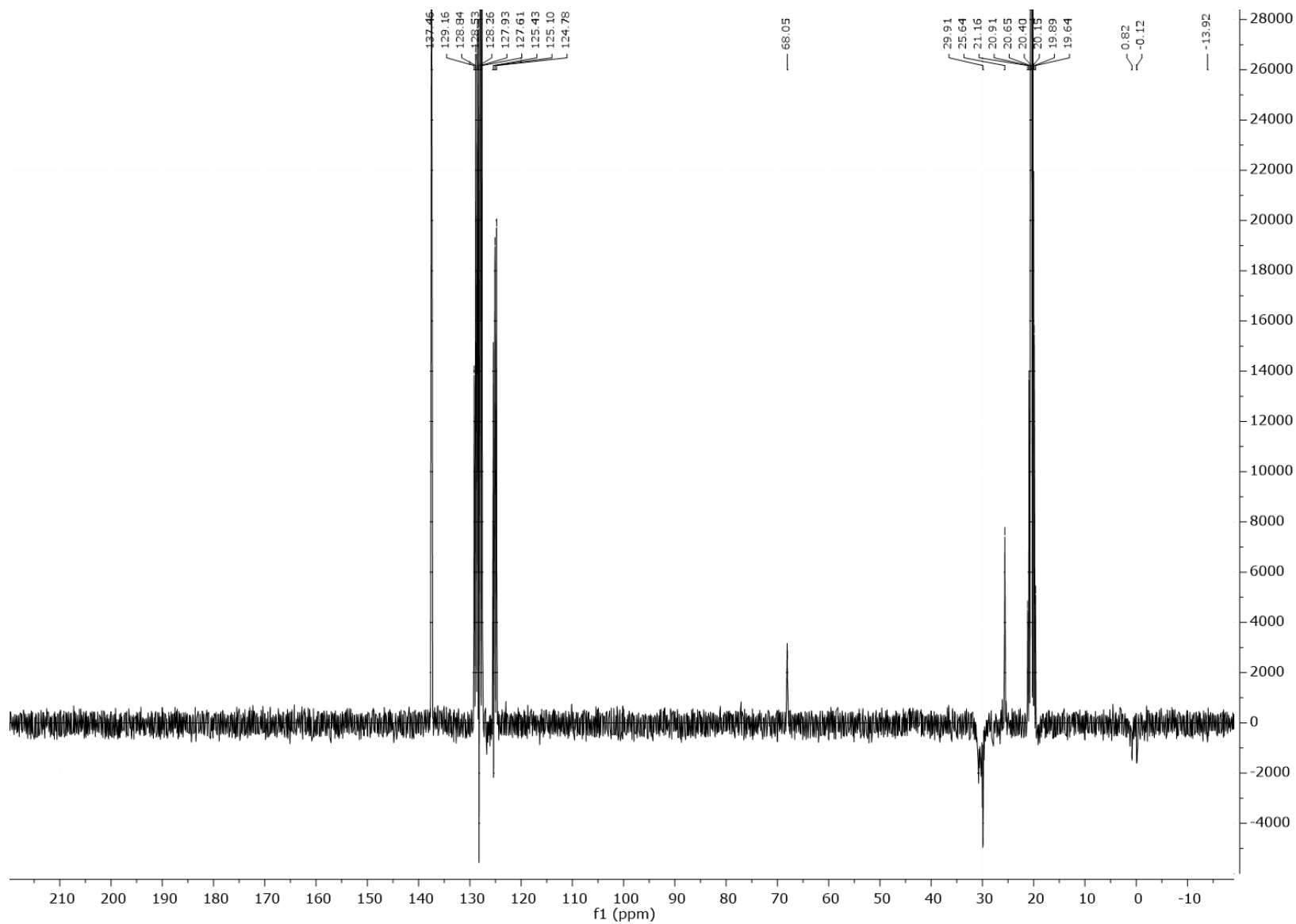
Figure 91. ^{13}C NMR spectrum for CO_2 reaction recorded in tol-d_8 after two days heating at 50ºC

2.4. Mitsunobu Reaction

The purpose of this section was to corroborate the results obtained in [21].

2.4.1. Mitsunobu Reaction with Benzilamine

This reaction can be divided in two steps. A stirred solution of benzilamine in dichloromethane was prepared and cooled between -5 and -10°C. Carbon dioxide was bubbled through this solution for 45 minutes. The Mitsunobu zwitterion was prepared by addition of diisopropyl azodicarboxylate (DIAD) to a solution of triphenylphospine in dichloromethane at -20°C. Both solutions were cooled to -78°C and the zwitterion solution was cannulated into the carbamate containing solution. More carbon dioxide was passed into the solution after addition and the reaction mixture allowed to warm to ambient temperature and to stand to react overnight. Figure 92 illustrates the IR spectrum of the final solution.
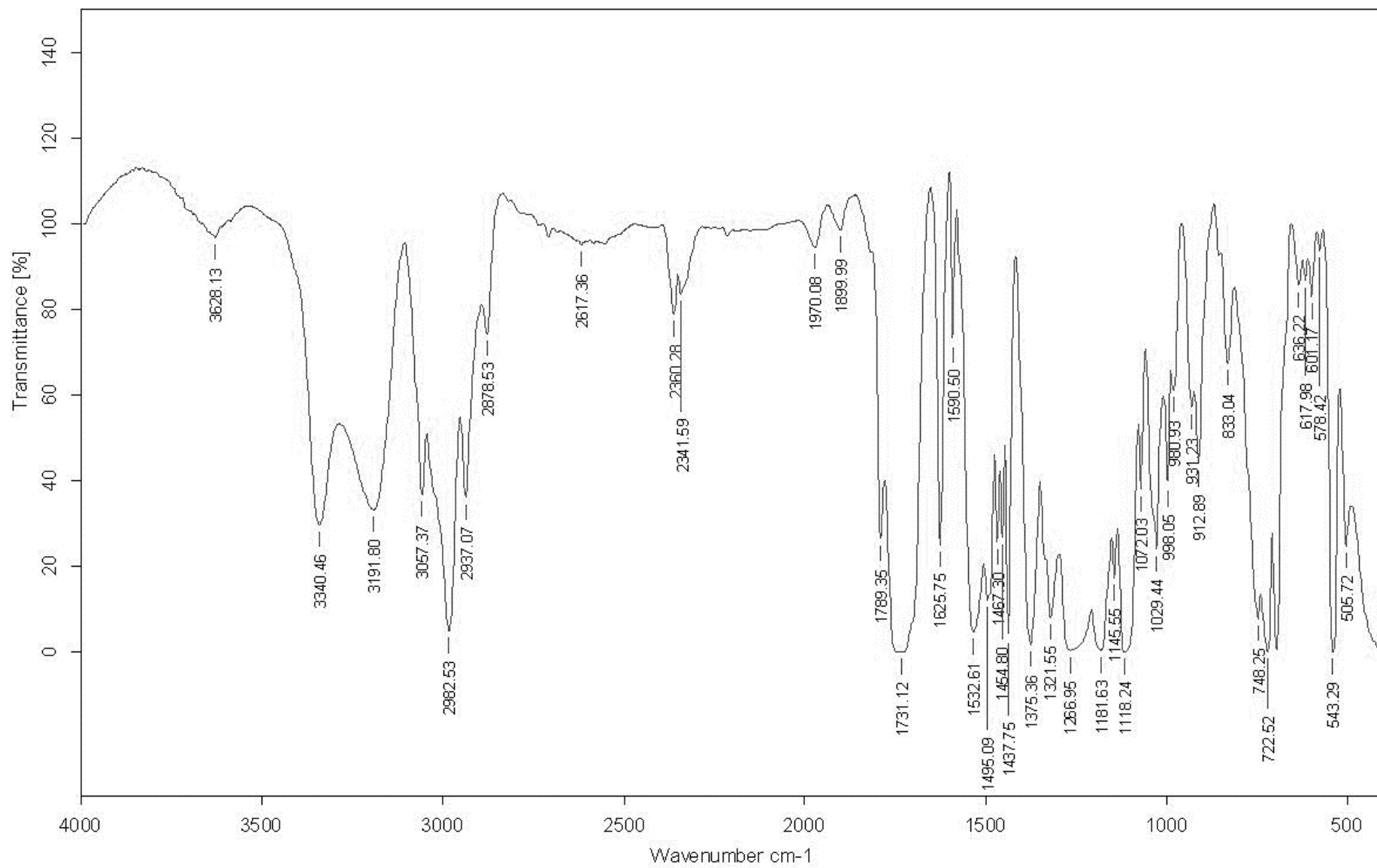
Figure 92. IR spectrum for CO₂ reaction in NaCl support

2.4.2. Mitsunobu Reaction with Isopropylamine

Carbon dioxide was bubbled through a stirred solution between -5 and -10°C of isopropylamine in dichloromethane for 45 minutes. The Mitsunobu zwitterion was prepared by addition of diisopropyl azodicarboxylate (DIAD) to a solution of triphenylphospine in dichloromethane at -20°C. Both solutions were cooled to -78°C and the zwitterion solution was cannulated into the carbamate containing solution. More carbon dioxide was passed into the solution after addition and the reaction mixture allowed to warm to ambient temperature and to stand overnight. The next figure illustrates the IR spectrum for the yielded solution.
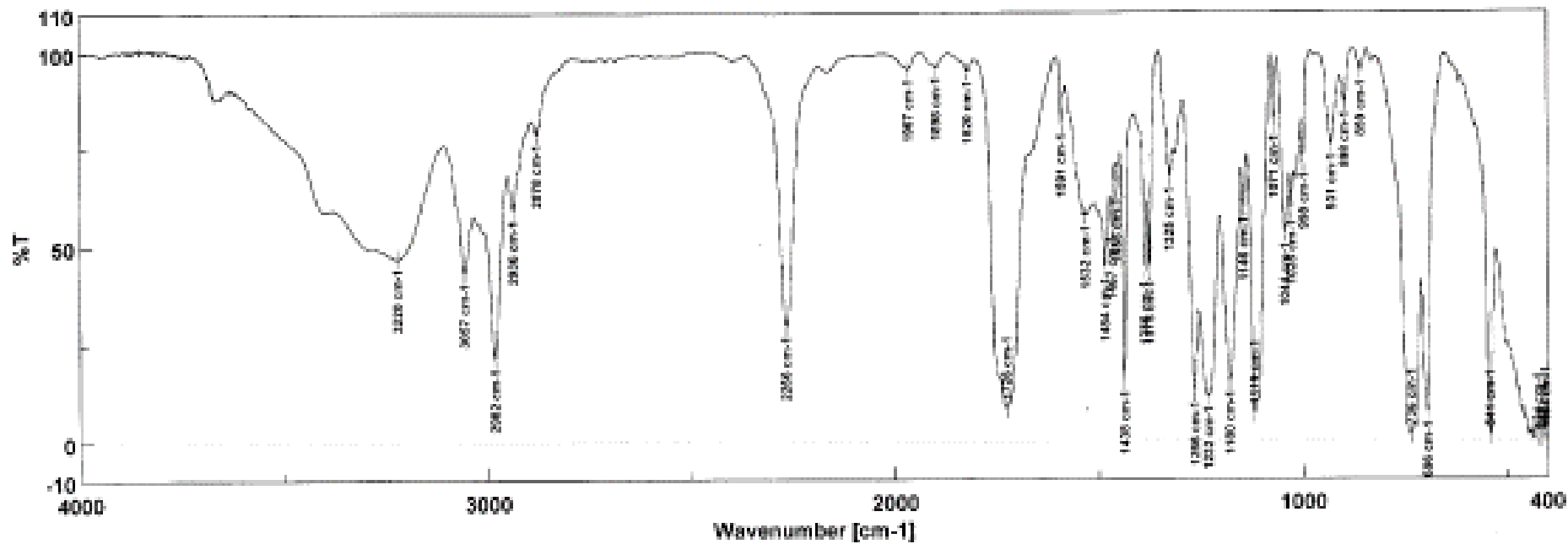
Figure 93. IR spectrum for CO$_2$ reaction with isopropylamine in NaCl support

3 Discussion of Results

3.1 Preliminary Work

The ^{1}H NMR ligand (fig. 37) presents one singlet less intense for OH group protons, two duplets for aromatic protons, one singlet for CH_3 protons group of NCH_2Ar, one multiplet for the C_2 chain ($NCH_2CH_2NMe_2$), one singlet for NMe_2 group and two different singlets for *tert*-butyl groups of the aromatic rings, which is in accordance with that is described in the literature [46].

In IR spectrum of the yielded product (Fig.40) it is possible to found evidences that can justify the existence of a Mo (V) complex compound. According to [56,57] the presence of a very strong band observed in the region of 948-942 cm^{-1} (marked with (a) in table 3) corresponds to Mo=O stretching frequency. According to [58-60] it is also possible to conclude that the peak assigned with (b) in table 3, is related to the possibility of the coordination of the metal by the phenolic oxygen, justified by the absence of a band in the region between 3200 to 3550 cm^{-1} corresponding to OH group. Other regions of the IR spectrum can be assigned to the C-H bond of the aromatics rings present in the complex structure (3100 – 3000 cm^{-1}) and the region between 3000 to 2850 cm^{-1} to the C-H bond of the *tert*-butyl substituents of the aromatic ring. The C-N bond of the aromatic amine are present between 1335 to 1250 cm^{-1} and the C=C bond are present in the region between 1600 and 1500 cm^{-1}.

Analyzing the results for the elemental analysis expressed in table 4 it is possible to observe that the percentage errors obtained for the experimental and the predict results for the same compound without oxygen exposure are higher than 5%, which makes them a valid bit. Comparing the experimental values with the values obtained for atmospheric oxygen exposure obtained with *ChemDraw*, it is possible to observe that the percentage error between these values is around or less 5%. In this segment, it can be stated that there was some kind of exposure of the sample to atmospheric oxygen, probably due to the poor sealing of the ampoule or during manipulation.

3.2 Synthesis

3.2.1. Synthesis of 2,6-diisopropylphenyl vanadium chloride

By the analysis of the IR spectrum presented in figure 43 it is possible to take some conclusions: the existence of two bands between 3650 to 3200 cm^{-1} can be assigned to the N-H bond of the free 2,6-diisopropylamine, which normally are presented with two peaks. The peak at around 1640 cm^{-1} corresponds to the C=N bond of the lutidine used. The very low peak intensities that can be observed are related to the high dilution of the crude solution. The V-Cl bond was not exhibit due to the scale of the IR spectrum. Normally, this bond is presented around 390 cm^{-1} [61]. In order to obtain a better resolution of this spectrum a previous concentration by solvent evaporation should be performed.

3.2.2. Synthesis of 2,6-diisopropylphenyl silyl magnesium amido

Through peak integration and identification was possible to take some conclusions from the ^{1}H NMR spectrum presented in figure 47. The presence of the desired silyl amine was identified by a peak as a singlet at around 0.6 ppm corresponding to -Si-CH$_3$ group. However, it is also possible to conclude that this reaction was not complete. Comparing this spectrum with the spectrum of 2,6-diisopropylaniline (fig.48) and the corresponding integration of the peaks, the obtained ratio of integrations results in 2:1 (2 2,6-diisopropylaniline: 1 diisopropylphenyl silyl aniline).

At this time of the project the characterization of the yielded Mg complex is not a required task. It was admitted that the last step of the described reaction was quantitative. The next step was the reaction *in situ* of this complex with carbon dioxide.

3.2.3. Synthesis of 2,6-dimethylphenyl-N-trimethylsilyl-magnesium amido

As in section 3.2.2 the complex characterization was not a required task. It was admitted that the last step of the described reaction was quantitative. The following step was the reaction *in situ* of the Mg complex with carbon dioxide but no proper product was possible to isolate and characterize.

3.2.4. Synthesis of 2,6-dimethylphenyl-trimethylsilyl-bromomagnesium amido

Figure 52 can illustrate the ^{1}H NMR spectrum for 2,6-dimethylphenyl-trimethylsilyl-bromomagnesium amido ((THF)$_2$.MgBrPh(CH$_3$)$_2$TMS). The protons of the TMS groups is shown by a singlet at 0.41 ppm. The protons of the methyl substituents of the aromatic ring appears as a singlet at 2.53 ppm. The two molecules of THF can be found at 1.13 and 3.49 ppm. The two protons in *meta* position appears as a duplet between 7.12 and 7.15 ppm and the proton in *para* position appears as a triplet between 6.78 and 6.83 ppm.

Analyzing the ^{13}C NMR spectrum presented in figure 53 for the yielded product it is possible to assign the peak that appears at 3.77 ppm corresponds to the Si-CH$_3$ carbon group. At 21.39 ppm, it is possible to attribute that peak to the CH$_3$ bonded to the aromatic ring. The carbons present in the two THF molecules appears at 24.98 and 69.99 ppm. The *para* position appears at 118.92 ppm and the carbon in the *meta* position appears at 128.20 ppm. The quaternary carbon bonded to the CH$_3$ groups appears at 134.80 ppm.

3.2.5. Synthesis of 2,6-dimethylphenyl-ciclopentadienyl-trimethylsilyl-magnesium amido

Figures 56 and 57 presents the ^{1}H NMR and ^{13}C NMR spectrum of 2,6-dimethyl-N-trimethylsilylaniline.

From the first, it is possible to affirm that the –Si-CH$_3$ group protons (nine in total) appears as an intense singlet at 0.06 ppm. The peak resulting from the N-H proton of the amine group is present near 1.87 ppm and the peaks of the two methyl substituents of the aromatic ring (six in total) appear near 2.15 ppm. The proton in *para* position is near 6.81 ppm and the two protons in *meta* position between 7.01 and 7.09 ppm. Analyzing now figure 57 it is possible to make an attribution of each peak and confirm the specie structure. The peak at 1.12 ppm corresponds to carbon of the methyl substituents of silane group. At 19.57 ppm it is possible to view the peak associated with the carbon of the methyl groups attached to the aromatic ring. The carbon in *para* position can be found at 121.94 ppm and the carbons

in *meta* positions can be found at 128.37 ppm. The carbon bonded to the nitrogen atom is at 131.61 ppm and the aromatic carbons attached to methyl substituents are at 131.19 ppm.

Figure 58 illustrates the ^{1}H NMR spectrum of Cp^{bz}Mg(THF)NPh(CH$_3$)$_2$Si(CH$_3$)$_3$ synthesis. It is possible to take some conclusion from the spectrum analysis: the presence of the desired molecule at an initial state of the reaction and the release of ethane. It is possible to determine these conclusions through peak identification and integration. Attention should be paid to the proton peak corresponding to the different groups that exist in the molecule: the phenyl proton (25 in total) of Cp^{bz} corresponds to a multiplet that appears at 7.06 ppm; the C-CH$_2$ protons (10 in total) corresponds to a singlet that should appear between that should appear near 3.89 ppm. The evidence of the release of ethane can be comproved by the existence of a singlet peak near 0.31 ppm. The two methyl substituent groups of aniline are present near 2.14 ppm. The presence of one THF molecule can be seen at two singlet peaks at around 2.64 ppm and 0.95 ppm. The –N-H proton appears near 1.87 ppm. The –Si-CH$_3$ group appears as a singlet group near 0.06 ppm.

Analyzing the spectrum shown in figure 59, it is possible to see the decreasing of the intensity of the aromatic peaks, one molecule of THF and the peak respects to ethane release. The proton of N-H group of the amine disappeared.

By the analysis of figure 60 it is possible to conclude, that the reaction is complete by the well-established peaks for the Si-(CH$_3$)$_3$ group at 0.32 ppm, the ten protons of C-CH$_2$ groups present at 3.87 ppm. Methyl substituents of the aromatic ring from the amine are present at 2.37 ppm and the protons of one molecule of THF present at 1.06 and 2.74 ppm. However, there was not a disappearance of the peak assigned to ethane given that this gas it is in equilibrium with the solution.

By the interpretation of the ^{13}C NMR spectrum, presented in figure 61 it is possible to confirm the purposed structure for the Cp^{bz} magnesium amido. The peak present at 4.52 ppm corresponds to the carbon atoms present in the -Si-CH$_3$ group. The carbons of the two methyl substituents groups are present at 21.69 ppm. The CH2-Ph carbons are shown at 32.3 ppm. The THF molecule could be identified at 69.57 ppm. The peak at 116.45 ppm can be attributed to the five carbons of the cyclopentadienyl ring. At 119.43 ppm is present the peak for the carbon in *meta* positions prevenient from the amine. At 125.62 ppm is shown a peak that can be attributed to the carbon in the *para* position in the phenyl substituents of the of the cyclopentadienyl ring. At 128.37 is shown the peak for the carbon in *para* position prevenient from the amine. At 128.81 ppm is shown the peak for the carbon in *meta* position prevenient from the phenyl substituents of the of the cyclopentadienyl ring. The carbon attached to the methyl substituents of the aromatic ring prevenient form the amine is present at 134.94 ppm. The *ipso* position of the phenyl carbons from the cyclopentadienyl ring are at 142.64 ppm and the carbon bonded to nitrogen atom are present at 156.42 ppm.

3.2.6. Synthesis of 2,6-dimethylphenyl-N-trimethylsilyl-magnesium ketimide

By the analysis of the ^{1}H NMR spectrum presented in figure 64 it is possible to assign some peaks to the pretended product. Although, it is important to point out the existence of impurities and trace of solvents, probably prevenient from the starting materials that was used as obtained, which somehow hinder the proper peaks integration and attribution. In a general form, the singlet present at 0.27 ppm

can be assigned to the Si(CH$_3$)$_3$ protons, one peak as a singlet for the *tert*-butyl groups, two peaks for the THF molecules and a singlet for the protons of the two methyl substituents.

3.3 Reactions with wet CO$_2$

3.3.1. Reaction of 2,6-diisopropylphenyl vanadium chloride

The proposed mechanism for the reaction of 2,6-diisopropylphenyl vanadium chloride with carbon dioxide can be [39]:
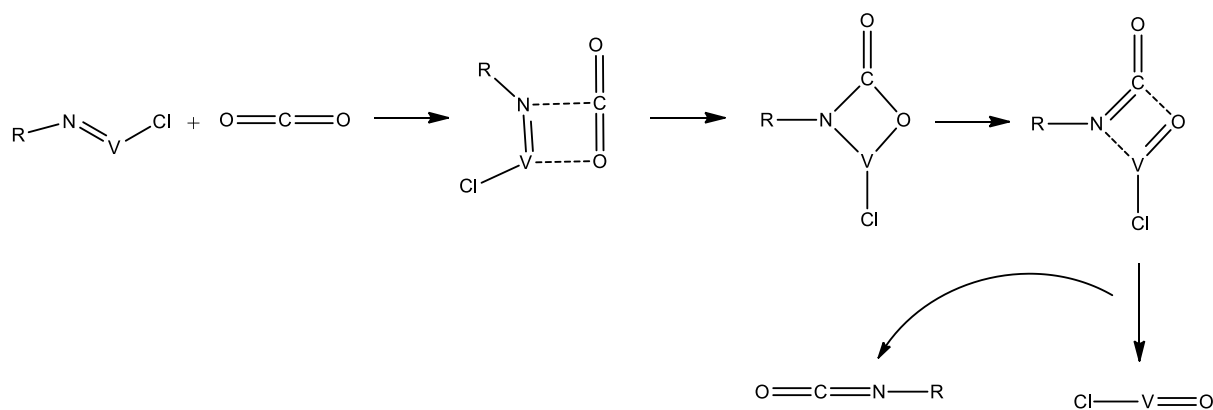
Figure 94. Proposed mechanism for the reaction of 2,6-diisopropylphenyl vanadium chloride with carbon dioxide [39]

Attending to the IR spectrum in figure 66 the first conclusion that can be taken is related to the high dilution of the crude solution, resulting in a low intensity of the peaks. Although, it is possible to make an identification of some bands presented in the spectrum. At around 3650 cm^{-1}, is exhibited the peak corresponding to free 2,6-diisopropylaniline in solution (N-H stretch). The C-H bonds of alkyl substituents are present around 2960 cm^{-1} and the C=C bond of aromatic structure can be assigned to 1541 cm^{-1} stretch. At 1070 cm^{-1}, it is possible to identify the N-C bond of 2,6-diisopropylaniline and at 1639 cm^{-1} the N=C bond of lutidine. At 910 cm^{-1}, is present a band which may be characteristic of V=O bond, which normally appears between 900 and 960 cm^{-1}.

Isocyanates have a very characteristic intensity region located between 2100 and 2270 cm^{-1} in IR spectrum. It is possible to see in this figure that there is no intense band located in this region leading to believe that there was no formation of the desired product.

Regarding the spectrum present in figure 67, the first thing to note is the increase intensity of some peaks. Comparing this spectrum with the one present in previous figure it is possible to mark the existence of same peaks at around 1640 cm^{-1} (C=N stretch) and the alkyl and aromatic structures. Although, it is important to point out the disappearance of N-C stretch from 2,6-diisopropylaniline and the band present at 910 cm^{-1}. However, is still not possible to identify a sign of isocyanate formation because there is no peak around the characteristic region of N=C=O functional group.

In figure 68, is presented the IR spectrum of the remaining solution after filtration and concentration by reduced pressure. Comparing this spectrum with the one present in figure 69 it is possible to affirm that they have the same aspect and the existence of an intense peak at around 910 cm^{-1}.

Concerning now to the least spectra and comparing it to the one present on figure 69, it is possible to affirm that they are very similar and the only point to be noted is the increase of the intensity of the peaks.

In summary, none of the spectra exhibits the clear formation of the pretended isocyanate. Still, the existence of an intense peak at 910 cm^{-1} can lead to conclude that it was some interaction between carbon dioxide and vanadium compound, forming some specie with V=O bond, which cannot be defined only with this IR spectroscopic analysis.

3.3.2. Reaction of 2,6-diisopropylphenyl silyl magnesium amido

By analysis of ^1H NMR spectrum in figure 70, it is possible to see the existence of two species coexisting in the oil residue in the proportion 2:1. The magnesium compound characterization was not a required task at this point of the project, so it is not possible to conclude which peaks present in this spectra can correspond to the compound in the initial state. However, comparing the obtained spectra with the one in figure 48, it is possible to assign some peaks to free 2,6-diisopropylaniline in solution, suggesting an hydrolysis reaction, probably due to the existence of some moisture in the experimental installation and/or in carbon dioxide used.

By the analysis of the ^{13}C NMR spectrum in figure 71 it is possible to identify the following peaks: the peak at 0.96 ppm corresponds to the Si-Me_3 group. Between 22.59 and 28.29 ppm there are the CH$(Me)_2$ groups for the two identified species. At around 75 ppm, the present peaks correspond to CDCl$_3$ and between 118.68 and 123.2 ppm there are the aromatic carbons. Without more information of the starting material and the amine used it is impossible to assign the presented peaks to this structures.

Relatively to the IR spectra (Fig.72), it is possible to confirm the existence of free 2,6-diisopropylaniline in solution due to the existence of a strong band at around 3000 cm^{-1} compatibles with the characteristic value for N-H bond. It is also possible to confirm the existence of the hydrolysis reaction from the band present in the area of 3500 cm^{-1}, a value characteristic for the O-H bond from the water.

3.3.3. Reaction of 2,6-dimethylphenyl-N-trimethylsilyl-magnesium amido

Figure 73 illustrates the ^1H NMR for the yielded product with the reaction of 2,6-dimethylphenyl-N-trimethylsilyl-magnesium amido with carbon dioxide. It is possible to conclude the existence of free amine comparing this spectrum with the spectrum of the corresponding amine present in figure 56. However, as in section 3.3.2, no proper isolation of the starting material was made, so it is not possible to know if the peak at 0.17 ppm are related to the magnesium compound or result of the reaction.

Analyzing the ^{13}C NMR spectrum, in figure 74, it is possible to identify the following peaks: the peak at 1.36 ppm corresponds to the Si-Me_3 group. At 19.84 ppm there are the CH$(Me)_2$ group for the specie. At around 75 ppm, the present peaks correspond to CDCl$_3$ and between 118.68 and 123.2 ppm there are the aromatic carbons. Once again, without more information of the starting material and the amine used it is impossible to assign the presented peaks to this structures.

3.3.4. Reaction of 2,6-dimethylphenyl-ciclopentadienyl-trimethylsilyl-magnesium amido

By the analysis of the ^{1}H NMR spectra presented in figure 75 for the reaction of 2,6-dimethylphenyl-ciclopentadienyl-trimethylsilyl-magnesium amido with carbon dioxide it is possible to conclude that the region between 3.0 and 4.0 ppm corresponds to the protonated form of cyclopentadienyl compound. Once more, during the reaction hydrolysis occurred and there's no formation of the desired product.

In figure 76, it is shown the ^{13}C NMR spectra for this reaction. The existence of overlapping peaks does not allow a correct attribution to the starting materials structures.

3.3.5. Reaction of 2,6-dimethylphenyl-N-trimethylsilyl-bromomagnesium amido

By the spectrum analysis for the reaction of 2,6-dimethylphenyl-N-trimethylsilyl-bromomagnesium amido solution with bubbled carbon dioxide, in figure 77, and peak integration and comparation with the spectrum of the starting material and the spectrum of the free amine is possible to conclude that it corresponds to a mixture of bromo magnesium amido starting material and free amine which leads to the conclusion that, once more, could be occurred a hydrolysis reaction. Relatively to ^{13}C NMR spectra, in figure 78, this confirm the previous conclusion. The peak at 17.74 ppm belongs to 2,6-dimethyl-N-trimethylsilylaniline and the peak at 25.27 ppm can be assigned to the bromo magnesium starting material, which are coincident with the chemical shift where determined in *Synteshis Section*.

Figure 79 shows an IR spectrum for the yielded mixture from the reaction of the magnesium amido with carbon dioxide. It is possible to confirm the existence of free amine by the presence of a broad band corresponding to the –N-H bond at around 3300 cm^{-1}. However, the existence of a band at around 1670 cm^{-1} can be assigned to the existence of a specie with a C=O bond [62-64]. Even so, there is no formation of the pretended isocyanate, by absence of a band in the characteristic region of N=C=O bond.

Now by the analysis of the ^{1}H and ^{13}C NMR spectra (Fig.80 and Fig.81, respectively), for the reaction of 2,6-dimethylphenyl-N-trimethylsilyl-bromomagnesium amido solution with pressurized carbon dioxide, the reaction product corresponds to a mixture of free amine and bromo magnesium starting material.

The IR spectra of the yielded solid (Fig.82) shows the existence of some 2,6-dimethyl-N-trimethylsilylaniline by the presence of a broad band corresponding to the –N-H bond at around 3300 cm^{-1}. Also shows the existence of a band in the region around 1670 cm^{-1}, which leads to the conclusion that there is specie with a C=O bond [62-64. Once more, there is no formation of the pretended isocyanate, by absence of a band in the characteristic region of N=C=O bond.

The results of the elemental analysis (table 9) of the solid were compared with the predict results using *ChemDraw* software for the following species:
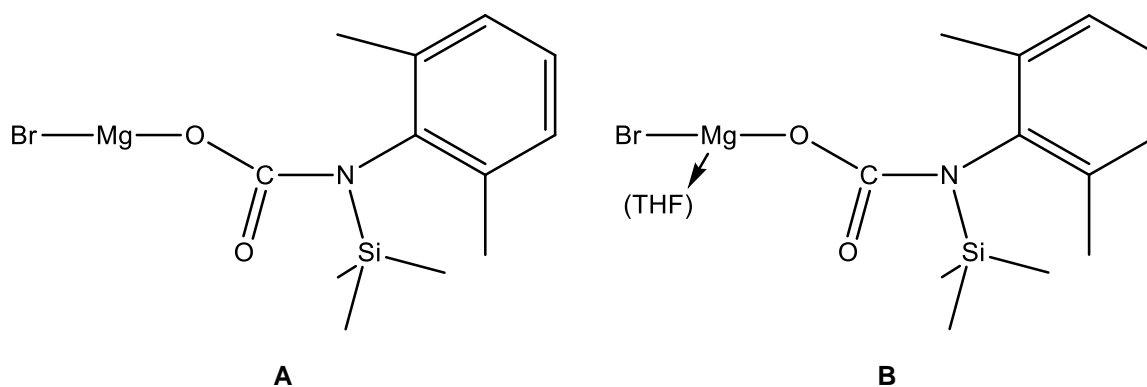
Figure 95. Predicted stuctures for the yielded product

For the elemental analysis, the obtained results are expressed in the next table:

Table 9. Elemental analysis for the predicted structures

	Specie	
Element	**A (%)**	**B (%)**
Nitrogen	4.11	3.40
Carbon	42.32	46.68
Hydrogen	5.33	6.12

The elemental analysis for yielded product of the reaction of the magnesium amido with carbon dioxide was different for the elemental analysis for the predicted structures and cannot be determined only by this way. The yielded product can be a mixture of a structure with a C=O bond with starting material and formed by-products which were nod determined in this study. To obtain more clear results and more suggestive of the structures of the yielded products a recrystallization should be made and if there exist suitable crystals, an X-Ray analysis could be done.

3.4 Reactions with dry CO_2

3.4.1. Reaction of 2,6-dimethylphenyl-N-trimethylsilyl-bromomagnesium amido in a NMR tube

By the analysis of the spectrum presented in figure 84 is possible to conclude that are some peaks that can be attributed to the existence of free amine in solution, but in a small quantity. There are also two peaks that can be assigned to two silicium groups (0.255 ppm and 0.338 ppm). None of them can be identified as a peak of the starting material or free amine. At 1.37 ppm and 3.58 ppm it is possible to see the existence of two THF molecules. However, none of the integration for these peaks corresponds to the coordination of these molecules to the compound, but as if the molecules were free in solution. At 2.22 ppm and 2.47 ppm it is possible to conclude that are two peaks that corresponds to the methyl groups, but again none of them can be assigned to the starting materials or free amine. In the aromatic region, the attribution is more difficult to do because of its large split.

Figure 85 shows the ^{1}H NMR spectrum for the yielded solution of the reaction with carbon dioxide after overnight heating at 50°C. Comparing this spectrum with the one in figure 84 it is possible to appoint some differences. First, the inversion of the two new groups of silicium groups (0.246 ppm and 0.307 ppm). The first one increases it intensity while the second peak was decreased. The methyl protons at 2.136 ppm had decreased its intensity while the peak at 2.226 ppm was increased. It is possible to see a better resolution of the aromatic protons. The peak at 6.828 ppm can be assigned to the protons in *para* position and the peak at 7.084 ppm can be attributed to the protons in *meta* position.

Analyzing the ^{1}H NMR spectrum, in figure 86, it is possible to appoint some diferences to the spectrum illustrated in figure 85. At 0.304 ppm, the peak from silicium group increased it intensity and the peak at 0.204 ppm decreased. The peak present at 2.226 ppm, from the protons of one methyl group disappeared as well the peak from a proton at *para* position, at 6.871 ppm.

Comparing this results with [62-64] it is possible to assume that a new specie with a -OSiMe$_3$ is formed by the reaction of the magnesium amido with carbon dioxide, as a silylcarbamate.

By the analysis of this spectrum it is possible to confirm the existence of a carbamate specie due to the existence of peaks with a negative chemical shift (-0.48 ppm) and the existence of a peak that can be assigned to the C=O at around 150 ppm [62-64].

3.4.2. Reaction of 2,6-dimethylphenyl-N-trimethylsilyl-bromomagnesium amido in a shlenck

By the analysis of the figure 88 it is possible to point some typical stretches as the C-H aromatic bonds and N-H bonds between 3300 and 3500 cm^{-1}. Si-CH$_3$ bonds appears around 1250 cm^{-1}, and C-N bonds appears around 1080 and 1360 cm^{-1}. The aromatic C=C bonds appears between 1500 cm^{-1} and 1700 cm^{-1}. At 1655 cm^{-1} it is possible to notice the presence of an intense peak. Comparing this value to the described in the literature from IR spectroscopy analysis and for other carbamate structures [62-64] it is coincident with the values for the carbamate group.

By the previous results it is possible to predict some structures that can exist in the solid matrix (Fig.96):
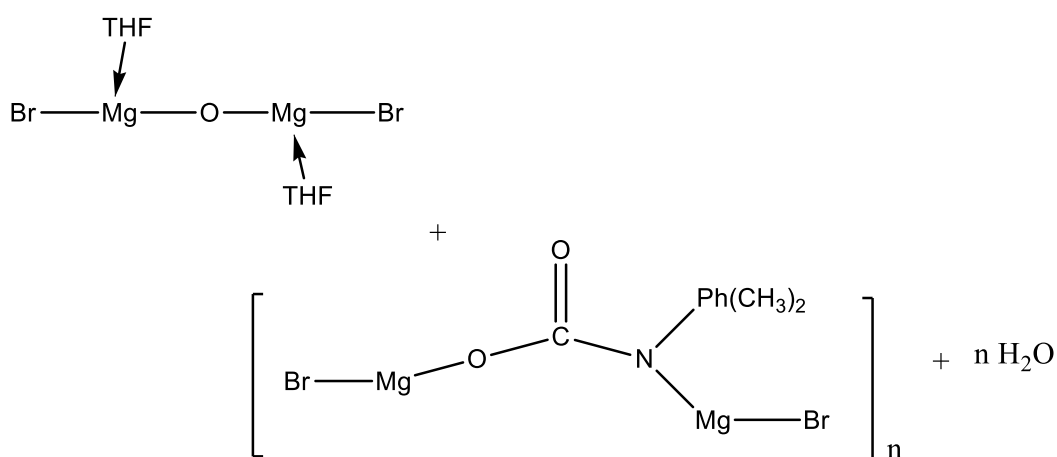
Figure 96. Predict structures that can exist in the solid matrix

Analyzing the spectrum in figure 89 and comparing it with the spectrums for the starting materials (figures 52 and 56) it is possible to conclude that in this mixture there are present some free amine,

toluene and two THF molecules. Between 2.00 ppm and 2.26 ppm, due to existence of a broad peak and to the low concentration of the sample it is difficult to do the correct integration of all the peaks and attribute them to proton groups.

3.4.3. Reaction of 2,6-dimethylphenyl-N-trimethylsilyl-magnesium ketimide in a NMR tube

By the analysis of the spectrum in figure 90 is possible to conclude that are some peaks that can be assigned to the existence of free amine in solution, but in small quantity (0.06 ppm). Between 0.10 ppm and 0.30 ppm there are some peaks that can be attributed to the protons of Si-CH$_3$ groups. Due to large split of region between 1.16 ppm and 1.43 ppm it is difficult to do the integration of *t*-butyl and one of the THF molecules, but by the chemical shifts there are present in this region. The other THF molecule are present at 3.52 ppm. The protons of the methyl groups are present around 1.16 ppm and 2.15 ppm. In the aromatic region it is possible to indicate the existence of protons in *para* position at around 6.86 ppm and the protons in *meta* position at 6.97 ppm.

The ^{13}C NMR spectrum (Fig.91) exhibits a peak at -0.12 ppm that as concluded in the previous section is coincident with the formation of -OSiMe$_3$ of a silylcarbamate specie [62-64]. Due to the dilution of the solution the carbon of C=O bond is not present. The yielded product can have the following structure:
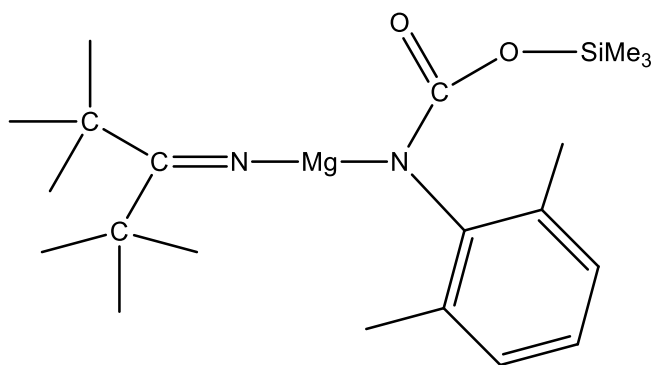
Figure 97. Possible structure for the yielded product

3.5 Mitsunobu Reaction

3.5.1. Mitsunobu Reaction with Benzilamine

By the analysis of the IR spectrum presented in figure 92 and comparing it with [21] it is possible to take some conclusions. First, the existence of a band that can be assigned to O-H bond, caused for the presence of moisture in the sample (3628 cm^{-1}). Between 3191 cm^{-1} and 3340 cm^{-1}, the two peaks presented can be attributed to N-H bond of benzilamine. Lastly, it is possible to conclude that no isocyanate was formed by the absence of a band in the characteristic region of N=C=O region.

3.5.2. Mitsunobu Reaction with Isopropyl amine

By the analysis of the IR spectrum presented in figure 93 and comparing it with [21] it is possible to take some conclusions. First, between 3067 cm^{-1} and 3220 cm^{-1}, the two peaks presented can be attributed to N-H bond of isopropyl amine. Lastly, it is possible to conclude that there was some isocyanate formation by the existence of a band in the characteristic region of N=C=O region (2240 cm^{-1}).

3.6 Discussion Summary

Figure 98 illustrates all the reactions with carbon dioxide studied in this work.
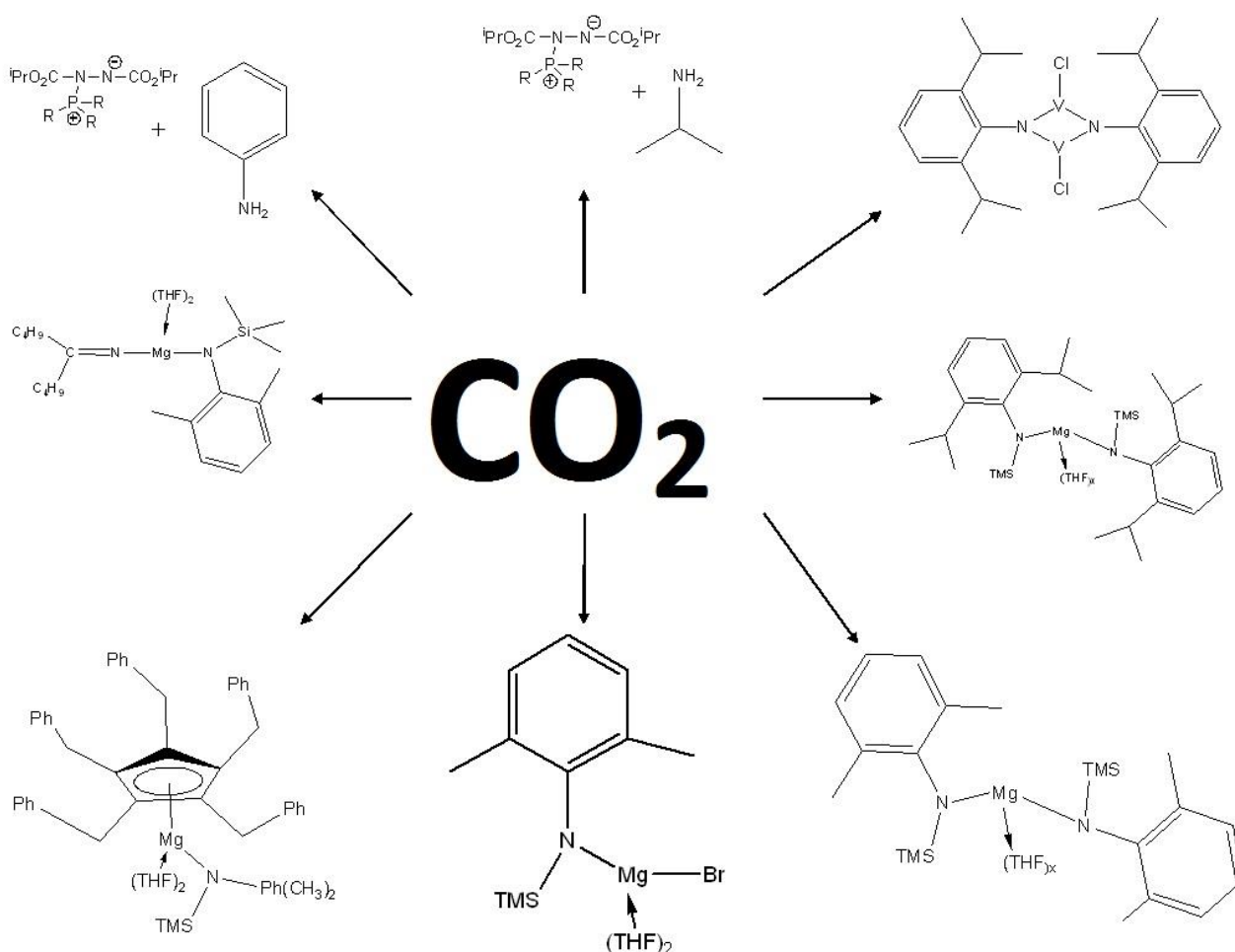
Figure 98. Studied reactions resume

In order to complete the discussion section some consideration can be done from the previous figure. Only the Mitsunobu reaction with isopropyl amine proved to be efficient to isocyanate synthesis. The same reaction with benzilamine did not gave the pretended product due to atmospheric air exposure of the reactional system.

Relatively to the reactions with the magnesium amido compounds the experiences shows the existence of a carbamate compound by the IR analysis and interpretation and the existence of $OSiMe_3$ structures. However, in order to be able to determine what are the products and what their structures, is necessary to do a suitable recrystallization of the solid material obtained in each reaction.

Although one of the objectives of this work was to synthetize aromatic isocyanates, the study of the same type of starting materials with alkylic substituents should be made so that it is possible to compare the yielded products in this reactions with the yielded products during this work.

4 Conclusions and Perspectives

Isocyanates are important intermediate compounds to produce PU systems. Although, the actual production processes carry huge environmental problems due to high toxicity of starting materials and formed byproducts.

Carbon dioxide is one of the major greenhouse gases, but it is possible to consider it as an important carbon source to produce several types of chemicals, although carbon dioxide utilization struggles several obstacles due to its thermodynamics and kinetics characteristics.

The aim of this project was the search for a sustainable route for isocyanates production using carbon dioxide and amines.

Along the time, there were some attempts to synthetize isocyanates using amines and carbon dioxide. Thus, due to the environmental problems related with isocyanates production and the possibility of CO_2 valorization is possible to affirm that new synthesis processes are needed.

The Mitsunobu reaction was prepared for two examples of amines: isopropylamine, an aliphatic amine, and benzilamine, an aromatic amine. As it was possible to verify, the first reaction was more efficient than the second. As it was described the utilization of DIAD with an aromatic amine gave lower yields of isocyanate.

In other section of this project, it was an attempt of isocyanates synthesis using magnesium amido compounds. The study of these reactions was made by NMR and IR spectroscopy which allows verify that occurred a decomposition of the used starting materials with wet carbon dioxide. When was used a high purity carbon dioxide it is possible to assume the formation of a carbamate specie. Although none of these reactions were successful to synthetize isocyanates.

Industrially, the application of such synthesis techniques may require a deep analysis of both technical aspects, due to the high sensitive type of compounds that was used, as well as economical aspects in order to compare with the existing technology and realize if a process of this type could be implemented and lucrative.

Organometallics synthesis can be a way to develop a new process for isocyanate synthesis and carbon dioxide valorization. Some work in this area have been made but it necessary more study to achieve an efficient technique for CO_2 activation and insertion reaction due to several limitations of this specie.

5 Experimental Section

5.1. General Procedures

Unless stated otherwise, all manipulations were perfomed under an atmosphere of dry-oxygen-free nitrogen by means of standard Shlenck and glovebox techniques. Solvents were pre-dried using 4 A molecular sieves and collected by distillation under an atmosphere of nitrogen. Deuterated solvents were dried with a 4 A molecular sieves and freeze-pump-thaw degassed prior to use. All other reagents were commercial grade and used without further purification. Carbon dioxide were purchased from Air Liquide and used as received. NMR spectra were recorded in a Brucker AVANCE II 300 MHz and 400 MHz spectrometers, at 296 K unless stated otherwise, reference internally to residual proton-solvent (^{1}H) or solvent (^{13}C) resonances, and reported relative to tetramethylsilane (0 ppm). 2D NMR experiments such as ^{1}H-^{13}C{^{1}H} HSQC, ^{1}H-^{1}H NOESY, ^{1}H-^{13}C{^{1}H} HMBC were performed to make all the assignments. FT-IR spectra were recorded in KBr using a *JASCO FT/IR-430* spectrometer. Elemental analysis was obtained from Laboratório de Análises do IST, Lisbon, Portugal.

5.2. Preliminary Work

5.2.1. Synthesis of Mo (V) complex

To a stirred solution of NaH (4.5 mmol, 0.11 g) in anhydrous THF was added dropwise a diamine bis(phenolate) ligand solution (2.25 mmol, 1.18 g) in anhydrous THF. The reaction mixture was kept at 50°C for 2 hours. After this time, the reaction mixture was added over a Mo compound (2 mmol, 0.725g) in cold THF. The reaction mixture was stirred overnight allowing warming up to room temperature. The solvent was removed under reduced pressure. The crude product was dissolved in Et$_2$O and then filtered to remove some solids. The filtered solution was concentrated and kept in the freezer allowing recrystallizing. After four months, the crude product was filtered. The obtained solution was kept in the freezer and the obtained solid was dried under vacuum.

5.3. Synthesis

5.3.1. Synthesis of 2,6-diisopropylphenyl vanadium chloride

To a stirred solution of VCl$_3$(THF)$_3$ (1 mmol, 0.3784 g) in anhydrous THF (30 - 40 mL) was added dropwise a solution of 2,6-diisopropylaniline (1 mmol, 0.19 mL) and lutidine (1.1 mmol, 0.13 mL). The reaction mixture was allowed to react at room temperature for 2 hours. After this time, the solvent was removed under reduced pressure and the crude product was kept in the freezer overnight. More THF was added and then the crude solution was filtered. The obtained solid was washed with more THF. *n*-Hexane is added to the filtered solution to create a new layer and stored in the freezer.

5.3.2. Synthesis of 2,6-diisopropylphenyl silyl magnesium amido

To a stirred solution of 2,6-diisopropylaniline (3.7 mmol, 0.7 mL) in anhydrous THF was added dropwise a solution of *n*-butyllithium (4.07 mmol, 0.383 mL) in THF. The reaction mixture was stirred for 2 hours

at 50°C. After that time, TMSCl (4.07 mmol, 0.516 mL) was added to the crude product and the resulting solution was stirred overnight at room temperature. Then *n*-dibutylmagnesium (1.8 mL) was added to the cold previous solution at it was kept overnight allowing warming up to room temperature.

5.3.3. Synthesis of 2,6-dimethylphenyl-N-trimethylsilyl-magnesium amido

To a stirred solution of 2,6-dimethyl-N-trimethylsilylaniline (3.65 mmol, 0.64 mL) in anhydrous THF was added dropwise a solution of n-dibutylmagnesium (1.8 mL) in THF. The reaction mixture was stirred overnight at room temperature.

5.3.4. Synthesis of 2,6-dimethylphenyl-ciclopentadienyl-trimethylsilyl-magnesium amido

In a first synthesis route, in a NMR tube, $Cp^{bz}MgEt(THF)_2$ (0.05 mmol, 0.03 g) was dissolved in deuterated toluene. 2,6-dimethyl-N-trimethylsilylaniline (0.05 mmol, 0.01 mL) was added to the previous mixture that was kept at 50°C overnight.

In a second way, to a stirred solution of $NaCp^{bz}$ (2 mmol, 1.30 g) in THF was added dropwise $(THF)_2.MgBrNPh(CH_3)_2TMS$ (2 mmol, 0.92 g) in anhydrous THF. The reaction mixture was stirred for 3 hours at room temperature. The solvent was removed under reduced pressure. The obtained solid was dried under vacuum. The solid was dissolved in toluene. The resulting solution was filtered to remove NaBr. The remaining solution was concentrated until begin to precipitate and it was kept in the freezer overnight. After that time, the solvent was removed under reduced pressure to obtain a white solid. This solid was dried under vacuum. *n*-Hexane was added and then the resulting suspension was filtered. The resulting solution was kept in the freezer and the solid was dried under vacuum.

5.3.5. Synthesis of 2,6-dimethylphenyl-N-trimethylsilyl-bromomagnesium amido

To a stirred cold solution of EtMgBr (10 mmol, 3.34 mL) in THF was added dropwise $Ph(CH_3)_2NHTMS$ (10 mmol, 2.04 mL). The reaction mixture was stirred overnight allowing warming up to room temperature. Solvent was removed under reduced pressure and the resulting solid was dried under vacuum.

5.3.6. Synthesis of lithium ketimide

To a frozen solution of *t*-butyl cyanide (40 mmol, 4.44 mL) at -196ºC, in *n*-hexane, was added a solution of *t*-butyl-lithium in pentane (40 mmol, 1.5 mol/dm^3 in pentane, 26.68 mL) and let to react for one hour. Subsequent warming to room temperature affords a pale yellow-green solution of $Li(N=C^tBu_2)$. The solvent was removed by reduced pressure and the yielded solid was dried under vacuum. *n*-Hexane was added and then the resulting suspension was filtered and the remaining solid was rejected. The solvent from the filtered solution was removed under reduced pressure yielding a solid. This solid was dissolved in pentane and the solution was kept in the freezer overnight to allow the solid recrystallization. The yielded mixture was filtered and the solid was dried under vacuum.

5.3.7. Synthesis of 2,6-dimethylphenyl-N-trimethylsilyl-magnesium ketimide

To a stirred solution of $Li-N=C(^tBu_2)$ (6 mmol, 0.90 g) in toluene, at room temperature, was added a solution of $(THF)_2.MgBr(CH_3)_2N-TMS$ (6 mmol, 1.78 g) in the same solvent and let to react for one hour. The yielded suspension was filtered and the solid part was rejected (LiBr). The solvent from the resulting

solution was removed under reduced pressure yielding a solid. This solid was dried under vacuum. *n*-Hexane was added to help the exit of toluene and the solvent was removed under reduced pressure. The yielded solid was dried under vacuum.

5.4. Reactions with wet CO_2

5.4.1. Reaction of 2,6-diisopropylphenyl vanadium chloride
A crude solution of ClV=N-(2,6-diisopropyl) was reacted with CO_2 for 2 hours at room temperature and 1 bar. After this time the solution was filtered and the solid was dried under vacuum. The resulting solution was concentrated. The solid and the concentrated solution was kept in the freezer.

5.4.2. Reaction of 2,6-diisopropylphenyl silyl magnesium amido
Carbon dioxide was bubbled through a crude solution of $RNMgBu_2$ for 30 minutes at room temperature and 1 bar. The solvent was removed under reduced pressure *n*-Hexane was added to the obtained residue and then the solution was filtered. Toluene was added to the previous residue and then it was filtered for the same schlenk. Solvents were removed under reduced pressure and the solid was dried under vacuum.

5.4.3. Reaction of 2,6-dimethylphenyl-N-trimethylsilyl-magnesium amido
Carbon dioxide was bubbled through a crude solution of $RNMgBu_2$ for 30 minutes at room temperature and 1 bar. The remaining solvent was removed under reduced pressure. *n*-Hexane was added at -25°C. The solution was filtered and the obtained solid was dried under vacuum. The solvent of the remaining solution was removed under reduced pressure.

5.4.4. Reaction of 2,6-dimethylphenyl-ciclopentadienyl-trimethylsilyl-magnesium amido
One equivalent of carbon dioxide (0.05 mmol) was bubbled through a crude solution of $Cp^{bz}Mg(THF)NPh(CH_3)_2TMS$ at room temperature and 0.5 bar for some minutes.

5.4.5. Reaction of 2,6-dimethylphenyl-N-trimethylsilyl-bromomagnesium amido
In a first route, carbon dioxide was bubbled through a crude solution of $(THF)_2.MgBrPh(CH_3)_2N\text{-}TMS$ for 5 minutes at room temperature and 0.5 bar. The solvent was removed under reduced pressure. The remaining mixture was dried under vacuum.

In a second way, carbon dioxide was pressurized through a crude solution of $(THF)_2.NMgBrPh(CH_3)$ TMS for 40 minutes at room temperature and 0.5 bar. The solvent was removed under reduced pressure. The remaining solid was dried under vacuum and washed with *n*-hexane. The obtained suspension was filtered and the remaining solid was dried under vacuum.

5.5. Reactions with dry CO_2

5.5.1. Reaction of 2,6-dimethylphenyl-N-trimethylsilyl-bromomagnesium amido in a NMR tube
One equivalent of carbon dioxide (0.05 mmol) was pressurized through a frozen solution of one equivalent of $(THF)_2.MgBrNPh(CH_3)_2TMS$ (0.05 mmol, 0.015 g) in deuterated toluene for some minutes.

After this, the solution was let too warm to room temperature. Another NMR tube with the same quantity of reactant was heated for two days at 50ºC.

5.5.2. Reaction of 2,6-dimethylphenyl-N-trimethylsilyl-bromomagnesium amido in a shlenck

One equivalent of carbon dioxide (1.80 mmol) was pressurized through a frozen solution of one equivalent of $(THF)_2.MgBrNPh(CH_3)_2TMS$ (1.80 mmol, 0.54 g) in toluene for some minutes. After this, the solution was let too warm to room temperature and then the shlenck was heated for two days at 50ºC.

5.5.3. Reaction of 2,6-dimethylphenyl-N-trimethylsilyl-magnesium ketimide

One equivalent of carbon dioxide (0.05 mmol) was pressurized through a frozen solution of one equivalent of $^tBu_2C=N-MgBrPh(CH_3)_2N-TMS$ (0.05 mmol, 0.017 g) in deuterated toluene for some minutes. After this, the solution was let too warm to room temperature.

5.6. Mitsunobu Reaction

5.6.1. Mitsunobu Reaction with Benzilamine

Carbon dioxide was bubbled through a stirred solution at -5 to -10°C of benzilamine (5 mmol, 0.55 mL) in dichloromethane for 45 minutes. The Mitsunobu zwitterion was prepared by addition of diisopropyl azodicarboxylate (DIAD) (6 mmol, 1.2 mL) to a solution of triphenylphospine (6 mmol, 1.8282 g) in dichloromethane at -20°C. Both solutions were cooled to -78°C and the zwitterion solution was cannulated into the carbamate containing solution. More carbon dioxide was passed into the solution after addition and the reaction mixture allowed to warm to ambient temperature and to stand overnight.

5.6.2. Mitsunobu Reaction with Isopropylamine

Carbon dioxide was bubbled through a stirred solution at -5 to -10°C of isopropylamine (17.6 mmol, 1.5 mL) in dichloromethane for 45 minutes. The Mitsunobu zwitterion was prepared by addition of diisopropyl azodicarboxylate (DIAD) (21.3 mmol, 4.2 mL) to a solution of triphenylphospine (22.5 mmol, 5.54 g) in dichloromethane at -20°C. Both solutions were cooled to -78°C and the zwitterion solution was cannulated into the carbamate containing solution. More carbon dioxide was passed into the solution after addition and the reaction mixture allowed to warm to ambient temperature and to stand overnight.

References

[1] H. Ulrich, *The chemistry and technology of Isocyanates*. United Kingdom: John Wiley & Sons, 1996.

[2] "WorkSafeBC," 2016. [Online]. Available: http://www.worksafebc.com/. Accessed: May 20, 2016.

[3] P. N. A. LLC, "PR newswire: Press release distribution, targeting, monitoring and marketing," 2016. [Online]. Available: http://www.prnewswire.com/. Accessed: May 20, 2016.

[4] S. 2016, "Search 55, 789 technical Datasheets, contact suppliers, get samples," 2016. [Online]. Available: http://coatings.specialchem.com/. Accessed: May 20, 2016.

[5] CDC, "CDC works 24/7," CDC, 2016. [Online]. Available: http://www.cdc.gov/. Accessed: May 20, 2016.

[6] S. Map, "Tri-iso Tryline, LLC is a western U.S. Distributor of specialty chemical raw materials," 2016. [Online]. Available: http://www.tri-iso.com/. Accessed: May 20, 2016.

[7] "Eco-profiles of the European Plastics Industry," I Boustead, 2005. [Online]. Available: http://www.polyurethanes.org/uploads/documents/eco_tdi.pdf. Accessed: May 20, 2016.

[8] A. Goossens, T. Detienne, and M. Bruze, "Occupational allergic contact dermatitis caused by isocyanates," *Contact Dermatitis*, vol. 47, no. 5, pp. 304–308, Nov. 2002.

[9] "Online press release distribution service," PRWeb, 2015. [Online]. Available: http://www.prweb.com/. Accessed: May 20, 2016.

[10] The Editors of Encyclopædia Britannica, "Britannica.com," in *Encyclopædia Britannica*, Encyclopædia Britannica, 2010. [Online]. Available: http://www.britannica.com/. Accessed: May 20, 2016.

[11] "Emergency preparedness and response," 2016. [Online]. Available: http://emergency.cdc.gov/. Accessed: May 20, 2016.

[12] "New World Encyclopedia,". [Online]. Available: http://www.newworldencyclopedia.org/entry/Info:Main_Page. Accessed: May 20, 2016.

[13] "General Introduction," in *Towards a Sustainable Synthesis of Aromatic Isocyanates*. 2011. [Online]. Available: https://openaccess.leidenuniv.nl/bitstream/handle/1887/18270/01.pdf?sequence=12. Accessed: May 20, 2016.

[14] O. Meth-Cohn and C. W. Rees, *Comprehensive organic functional group Transformations*, A. R. Katritzky, Ed. Netherlands: A Pergamon Title, 1995.

[15] A.-H. Liu, Y.-N. Li, and L.-N. He, "Organic synthesis using carbon dioxide as phosgene-free carbonyl reagent," *Pure and Applied Chemistry*, vol. 84, no. 3, Jan. 2011.

[16] O. Kreye, H. Mutlu, and M. A. R. Meier, "Sustainable routes to polyurethane precursors," *Green Chemistry*, vol. 15, no. 6, p. 1431, 2013.

[17] "Thieme Connect,". [Online]. Available: https://www.thieme.de/en/thieme-connect/home-3939.htm. Accessed: May 20, 2016.

[18] "Curtius rearrangement,". [Online]. Available: http://www.name-reaction.com/curtius-rearrangement. Accessed: May 22, 2016.

[19] "Hofmann rearrangement,". [Online]. Available: http://www.name-reaction.com/hofmann-rearrangement. Accessed: May 22, 2016.

[20] "What is lossen rearrangement and its mechanism?,". [Online]. Available: https://www.quora.com/What-is-lossen-rearrangement-and-its-mechanism. Accessed: May 22, 2016.

[21] D. Saylik, M. J. Horvath, P. S. Elmes, W. R. Jackson, C. G. Lovel, and K. Moody, "Preparation of Isocyanates from primary amines and carbon dioxide using Mitsunobu chemistry 1," *The Journal of Organic Chemistry*, vol. 64, no. 11, pp. 3940–3946, May 1999.

[22] T. Sakakura, J.-C. Choi, and H. Yasuda, "Transformation of carbon dioxide," *ChemInform*, vol. 38, no. 36, Sep. 2007.

[23] M. Abla, J.-C. Choi, and T. Sakakura, "Halogen-free process for the conversion of carbon dioxide to urethanes by homogeneous Catalysis," *ChemInform*, vol. 33, no. 9, p. no–no, May 2010.

[24] Q. Liu, L. Wu, R. Jackstell, and M. Beller, "Using carbon dioxide as a building block in organic synthesis," *Nature Communications*, vol. 6, p. 5933, Jan. 2015.

[25] "Down to earth climate change,". [Online]. Available: http://globalclimate.ucr.edu/. Accessed: May 22, 2016.

[26] "The statistics portal," Statista, 2015. [Online]. Available: http://www.statista.com/. Accessed: May 22, 2016.

[27] S. B. Halligudi, R. V. Chaudhari, and L. K. Doraiswamy, "Carbonylation of nitrobenzene to phenyl isocyanate using palladium complex catalysts. Screening of catalysts and kinetic study," *Industrial*

& Engineering Chemistry Process Design and Development, vol. 23, no. 4, pp. 794–801, Oct. 1984.

[28] E. W. Stern and M. L. Spector, "Carbonylation of amines in the presence of palladium(II) chloride. A new route to Isocyanates," *The Journal of Organic Chemistry*, vol. 31, no. 2, pp. 596–597, Feb. 1966.

[29] T. E. Waldman and W. D. McGhee, "Isocyanates from primary amines and carbon dioxide: 'Dehydration' of carbamate anions," *J. Chem. Soc., Chem. Commun.*, no. 8, pp. 957–958, 1994.

[30] Z. W. Wicks, F. N. Jones, and S. P. Pappas, *Organic coatings: Science and technology*, 3rd ed. United Kingdom: Wiley-Blackwell (an imprint of John Wiley & Sons Ltd), 2007.

[31] A. Lapprand, F. Boisson, F. Delolme, F. Méchin, and J. . Pascault, "Reactivity of isocyanates with urethanes: Conditions for allophanate formation," *Polymer Degradation and Stability*, vol. 90, no. 2, pp. 363–373, Nov. 2005.

[32] R. B. Moreno, "The design and synthesis of complexes for the activation of carbon dioxide," 2010.

[33] S. C. Bart, C. Anthon, F. W. Heinemann, E. Bill, N. M. Edelstein, and K. Meyer, "Carbon dioxide activation with Sterically pressured mid- and High-Valent uranium complexes," *Journal of the American Chemical Society*, vol. 130, no. 37, pp. 12536–12546, Sep. 2008.

[34] W. J. Evans, C. A. Seibel, and J. W. Ziller, "Organosamarium-Mediated Transformations of CO 2 and COS: Monoinsertion and Disproportionation reactions and the Reductive coupling of CO 2 to [O 2 CCO 2] 2-," *Inorganic Chemistry*, vol. 37, no. 4, pp. 770–776, Feb. 1998.

[35] W. J. Evans, D. B. Rego, J. W. Ziller, A. G. DiPasquale, and A. L. Rheingold, "Facile insertion of CO 2 into Tetra- and Pentamethylcyclopentadienyl Lanthanide Moieties to form (C 5 me 4 RCO 2) - Carboxylate ligands (R = H, me)," *Organometallics*, vol. 26, no. 19, pp. 4737–4745, Sep. 2007.

[36] W. J. Evans, K. A. Miller, and J. W. Ziller, "Synthesis of (O 2 CEPh) 1 - ligands (E = S, se) by CO 2 insertion into Lanthanide Chalcogen bonds and their utility in forming Crystallographically Characterizable Organoaluminum complexes [Me 2 al(μ-o 2 CEPh)] 2," *Inorganic Chemistry*, vol. 45, no. 1, pp. 424–429, Jan. 2006.

[37] C. Lescop, T. Arliguie, M. Lance, M. Nierlich, and M. Ephritikhine, "Bispentamethylcyclopentadienyl uranium(IV) thiolate compounds. Synthesis and reactions with CO2 and CS2," *Journal of Organometallic Chemistry*, vol. 580, no. 1, pp. 137–144, May 1999.

[38] L. P. Spencer, P. Yang, B. L. Scott, E. R. Batista, and J. M. Boncella, "Imido exchange in Bis(imido) uranium(VI) complexes with aryl Isocyanates," *Journal of the American Chemical Society*, vol. 130, no. 10, pp. 2930–2931, Mar. 2008.

[39] A. M. Felix *et al.*, "Insertion of CO2 into divalent group 2 and 12 bis(silylamidos)," *IOS Press Content Library*, pp. 11–29, 2012.

[40] L. R. Sita, J. R. Babcock, and R. Xi, "Facile Metathetical exchange between carbon dioxide and the Divalent group 14 Bisamidos M[N(SiMe 3) 2] 2 (M = Ge and Sn) J . Am . Chem . Soc . 1996 , 118 , 10912−10913," *Journal of the American Chemical Society*, vol. 119, no. 40, pp. 9588–9588, Oct. 1997.

[41] C. J. Smith, T. R. Early, A. B. Holmes, and R. E. Shute, "Palladium catalysed cross-coupling reactions of silylamines," *Chem. Commun.*, no. 17, pp. 1976–1977, 2004.

[42] Y. Tang, A. M. Felix, B. J. Boro, L. N. Zakharov, A. L. Rheingold, and R. A. Kemp, "Syntheses and x-ray crystal structures of monomeric zinc and mercury bis(silylamidos)," *Polyhedron*, vol. 24, no. 9, pp. 1093–1100, Jun. 2005.

[43] A. Yamamoto, "Organometallic chemistry. Past, present, and future," *Pure and Applied Chemistry*, vol. 73, no. 2, Jan. 2001.

[44] R. H. Crabtree, "An Organometallic future in green and energy chemistry? †," *Organometallics*, vol. 30, no. 1, pp. 17–19, Jan. 2011.

[45] E. Y. Tshuva, M. Versano, I. Goldberg, M. Kol, H. Weitman, and Z. Goldschmidt, "Titanium complexes of chelating dianionic amine bis(phenolate) ligands: An extra donor makes a big difference," *Inorganic Chemistry Communications*, vol. 2, no. 8, pp. 371–373, Aug. 1999.

[46] F. Madeira, "Complexos paramagnéticos de Ti(III) para acoplamento radicalar de substratos orgânicos Dissertação para a obtenção do Grau de Mestre em," 2010.

[47] "Elec_nuc.html,". [Online]. Available: http://www.chem.ucla.edu/~harding/tutorials/elec_nuc/elec_nuc.html. Accessed: May 22, 2016.

[48] James, "What makes A good Nucleophile?," 2016. [Online]. Available: http://www.masterorganicchemistry.com/2012/06/18/what-makes-a-good-nucleophile/. Accessed: May 22, 2016.

[49] "Chem 59-651 main group Metallocenes," *Angew. Chem. Int. Ed.* [Online]. Available: http://mutuslab.cs.uwindsor.ca/macdonald/Teaching/651-class/651-Metallocenes3.pdf. Accessed: May 22, 2016.

[50] A. D. Warren, "Synthesis and characterization of Cyclopentadienyl transition metal complexes bearing Tetrafluoropyridyl Substituents," Virginia Tech, 2001.

[51] "Complexes of π − bound ligands - Metal cyclopentadienyl complexes,". [Online]. Available: http://nptel.ac.in/courses/104101006/downloads/lecture-notes/mod9/lec3.pdf. Accessed: May 22, 2016.

[52] E. Lu, W. Lewis, A. J. Blake, and S. T. Liddle, "The Ketimide ligand is not just an inert spectator: Heteroallene insertion reactivity of an Actinide-Ketimide linkage in a Thorium Carbene amido Ketimide complex," *Angewandte Chemie*, vol. 126, no. 35, pp. 9510–9513, Jul. 2014.

[53] W. Clegg, R. Snaith, H. M. M. Shearer, K. Wade, and G. Whitehead, "Azomethine derivatives. Part 20. Crystal and molecular structures of the lithioketimine [{Li(N☐CBu t 2)} 6] and lithioguanidine [{Li[N☐C(NMe 2) 2]} 6]; electron-deficient bridging of Li 3 triangles by methyleneamino-nitrogen atoms," *J. Chem. Soc., Dalton Trans.*, no. 7, pp. 1309–1317, 1983.

[54] "Phosphorus pentoxide," 2016. [Online]. Available: http://www.sigmaaldrich.com/catalog/substance/phosphoruspentoxide14194131456311?lang=pt&region=PT. Accessed: May 22, 2016.

[55] "Molecular sieves, 4 Å," 2016. [Online]. Available: http://www.sigmaaldrich.com/catalog/product/sial/208590?lang=pt&region=PT. Accessed: May 22, 2016.

[56] S. P. Patil, V. K. Naik, and N. B. Mallur, "Synthesis, spectral and antibacterial studies of oxomolybdenum (v) and dioxomolybdenum (VI) complexes with 2-imidazolyl mercaptoaceto hydrazone," *Der Pharma Chemica*, vol. 4, no. 5, pp. 1812–1818, Jan. 2012. [Online]. Available: https://www.researchgate.net/publication/286171365_Synthesis_spectral_and_antibacterial_studies_of_oxomolybdenum_v_and_dioxomolybdenum_VI_complexes_with_2-imidazolyl_mercaptoaceto_hydrazone. Accessed: May 23, 2016.

[57] C. G. Young, "Oxomolybdenum chemistry: An experiment," *Journal of Chemical Education*, vol. 72, no. 8, p. 751, Aug. 1995.

[58] K. Dey, R. K. Maiti, and J. K. Bhar, "Oxocation complexes, part X. Oxomolybdenum(V) and dioxomolybdenum(VI) complexes with tri- and tetra-dentate Schiff bases," *Transition Metal Chemistry*, vol. 6, no. 6, pp. 346–351, Dec. 1981.

[59] A. Syamal and M. R. Maurya, "Dioxomolybdenum(VI) complexes with tridentate dibasic Schiff bases derived from various hydrazides," *Transition Metal Chemistry*, vol. 11, no. 6, pp. 235–238, Jun. 1986.

[60] A. Syamal and M. A. B. Niazi, "Molybdenum complexes of biochemical iinterest. New coordination complexes of oxomolybdenum(V) with the tridentate ONO donor schiff bases derived from salicylaldehydes and ethanolamine," *Transition Metal Chemistry*, vol. 10, no. 2, pp. 54–56, Feb. 1985.

[61] S. J. Swamy, D. A. Redd, and K. Bhaskar, "Synthesis and spectral studies of some oxovanadium(IV) and vanadium(IV) complexes," *Indian Journal of Chemistry*, vol. 40, pp. 1166–7, 2012. [Online]. Available: http://nopr.niscair.res.in/bitstream/123456789/18599/1/IJCA%2040A%2811%29%201166-1171.pdf. Accessed: May 23, 2016.

[62] "SDBS," 2016. [Online]. Available: http://sdbs.db.aist.go.jp/. Accessed: May 23, 2016.

[63] M. J. Fuchter *et al.*, "Clean and efficient synthesis of O-silylcarbamates and ureas in supercritical carbon dioxide," *Chemical Communications*, no. 18, p. 2152, 2008.

[64] S. Jana, R. Fröhlich, and N. W. Mitzel, "Organozinc Siloxide-Hydrazide aggregates [(RZn)4(NHNMe2)x(OSiMe3)(4 – x)]," *Zeitschrift für Naturforschung B*, vol. 61, no. 7, Jan. 2006.